MULTI LINEAR REGRESSION - BASED MODELING AND PERFORMANCE MONITORING OF A FLAT PLATE SOLAR COLLECTOR OUTLET TEMPERATURE IN ALICE, SOUTH AFRICA

A dissertation submitted in fulfilment of the requirements for the degree of

MASTERS OF SCIENCE

BY

NOTHANDO NDLOVU

In the Faculty of Science and Agriculture at the University of Fort Hare

Supervisor: Dr Michael Simon

December 2015

DECLARATION

I, Nothando Ndlovu, hereby declare that the work contained in this dissertation is my own original work and that I have not previously in its entirety or in part submitted it to any other university for a degree.

Signature…….Date……..

DEDICATION

To my late father FM Ndlovu, who unfortunately could not be there to see me through to the end of this Masters' degree. His belief in me right at the beginning encouraged me to take on this challenge and his presence in my heart, gave me that 'one more push' and determination to complete my studies.

ACKNOWLEDGEMENTS

First of all I would like to acknowledge the God Almighty who by His grace and strength helped me bring this thesis to completion.

To Doctor Simon, thank you for taking the time to provide me with constructive criticism and guidance, for your tolerance and patience. Your support and guidance have been instrumental in the fruition of this research. From you I learnt that a dissertation does not only test a person's intellectual capabilities, but also one's resilience to succeed despite the odds. My sincere thanks also goes Prof Meyer, for providing the necessary resources during the study period. I also acknowledge the University of Fort Hare and Eskom for provision of equipment and resources for this research.

I am grateful to Stephen Tangwe Loh for your invaluable assistance; your dedication to work and technical knowledge have always been a source of inspiration. Fort Hare is truly blessed to have you. To the maintenance and Science workshop team, your input is unforgettable.

My heartfelt gratitude goes to my mother Nokuthula, whose love and support helped me through the challenging times, and whose prayers made me stronger each day. Words cannot express the love and gratitude I feel for you. To Silindile Mlilo, my sister friend, thank you for being my voice of reason when sanity escaped me. Your support (especially emotionally) kept me going through frustrating moments which indeed where a pushing force to complete this research. Lastly, to my many friends and relatives, who in both big and small ways, were there for me through this MSc journey a very big THANK YOU.

ABSTRACT

In a period of rapidly increasing energy demand, the exploitation of abundantly available solar energy is imperative. Temperate climates like South Africa show good potential for utilizing solar-driven technologies such as solar water heaters. These systems offer an attractive alternative over conventional water geysers as a means to supply hot water for residential use. In South Africa, the solar water heater industry is growing rapidly as the government offers incentives manufactures and consumers. This necessitates the determination of performance of these systems through experimental analysis as well as performance prediction.

This study evaluated the summer and winter performance of a flat plate, thermosyphon solar water heater under climatic conditions encountered in Alice, South Africa by considering the collector outlet temperature. The performance and weather data obtained were used to develop a multi linear regression (MLR) model for each season. MLR is a simple and easily applicable modelling approach which uses a set of input and output data to determine the model coefficients of a linear relation of two or more variables. The collector outlet temperature was correlated with solar radiation, ambient temperature, relative humidity, and collector inlet temperature since these variables have a direct impact on the collector temperature rise. Results from the performance showed that the collector performs well, attaining temperatures up to 87.2^{o}C during the summer season and 70^{o}C during winter season. The summer and winter percentage mean absolute error for the whole monitoring period were 4.07 % and 6.2 % respectively which indicate that MLR can be successfully applied to predict collector outlet temperatures in both seasons.

TABLE OF CONTENTS

LIST OF TABLES

LIST OF FIGURES

LIST OF ABBREVIATIONS

SWH:	Solar water heaters
MLR:	Multi linear regression
FPC:	Flat plate collector
ETC:	Evacuated tube collector
PMAE:	Percentage mean absolute error
I:	Solar radiation [W/m^2]
Rh:	Relative humidity [%]
ANN	Artificial Neural Network
OLS	Ordinary least squares
WLS	Weighted least squares
GOP	Generic optimization program

NOMENCLATURE

		Units
T_a	Ambient temperature	^oC
T_{ci}	Measured collector inlet temperature	^oC
T_{co}	Collector outlet temperature	^oC
T_{mod}	Modelled collector outlet temperature	^oC
T_{meas}	Measured collector outlet temperature	^oC

Design parameters determined during MLR parameter estimation ;

α_0		°C
α_1		$^oC.m^2/W$
α_2		-
α_3		°C
α_4		-
R^2	Coefficient of determination	-
s_e	Standard error estimate	

CHAPTER ONE

INTRODUCTION

1.1 BACKGROUND

Over the years there has been a gradual rise in energy use worldwide due to increase in industrialization and society modernization. As human population growth increases and standard of living improves, more energy will be required per person. According to the International Energy Agency [2013], world energy consumption will increase by 56% in the years 2010 - 2040, rising from 524 quadrillion British thermal units (Btu) in 2010 to 820 quadrillion Btu in 2040 [International Energy Agency World Energy Outlook, 2013]. In emerging economies such as South Africa development is closely linked to energy demand, and the supply of energy has to be sufficient and sustainable in order to meet the growing need.

For several decades, fossil fuels have been the primary source of energy meeting global demand [International Energy Agency World Energy Outlook, 2013]. Fossil fuels range from very volatile materials like natural gas and liquid oil, to non-volatile materials such as coal. In 2011, fossil fuels accounted for 82% of the worlds' primary energy use [International Energy Agency, Monthly Review, 2011]. In most parts of the world coal dominates other fossil fuels as an energy source due to its abundant availability and relatively lower price in comparison to other fuels. On the downside however, the combustion of fossil fuels releases pollutant gases which decreases air quality posing a serious threat to human health and agricultural produce. According to the Centre for Climate and Energy Solutions coals supplies 29.7% of energy use

worldwide and is responsible for 44% of global carbon dioxide emissions [Center for Climate and Energy Solutions, 2014]. This has prompted global shift to the use of cleaner and renewable sources of energy.

In South Africa, coal mining is a major drive in the economy contributing 94% of electricity generation [International Energy Agency, World Energy Outlook, 2013]. The huge investment in coal power stations allows the South African national utility Eskom to supply approximately 45% of Africa's energy needs [Coetzee, 2009]. The energy intense industrial sector has the highest share in electricity consumption as shown in Figure 1.1.

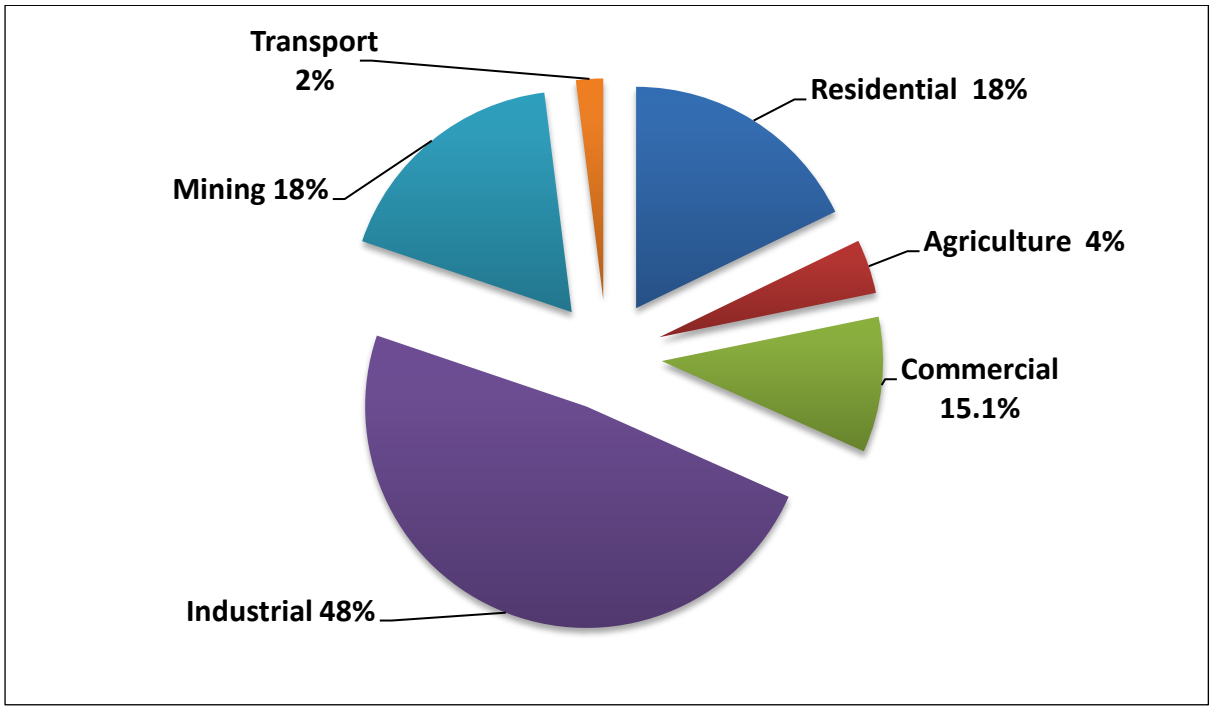

Figure 1.1: South Africa electricity market share [Eskom, 2009].

The energy demand in the residential sector can be divided into twelve sub sectors as shown in Figure 1.2. Water heating holds the largest share of total energy consumption and this is a result

of controlled and uncontrolled heating of water throughout the day. Activities such as cooking, drinking and sanitary use lead to controlled heating while uncontrolled heating is due to geyser standing losses.

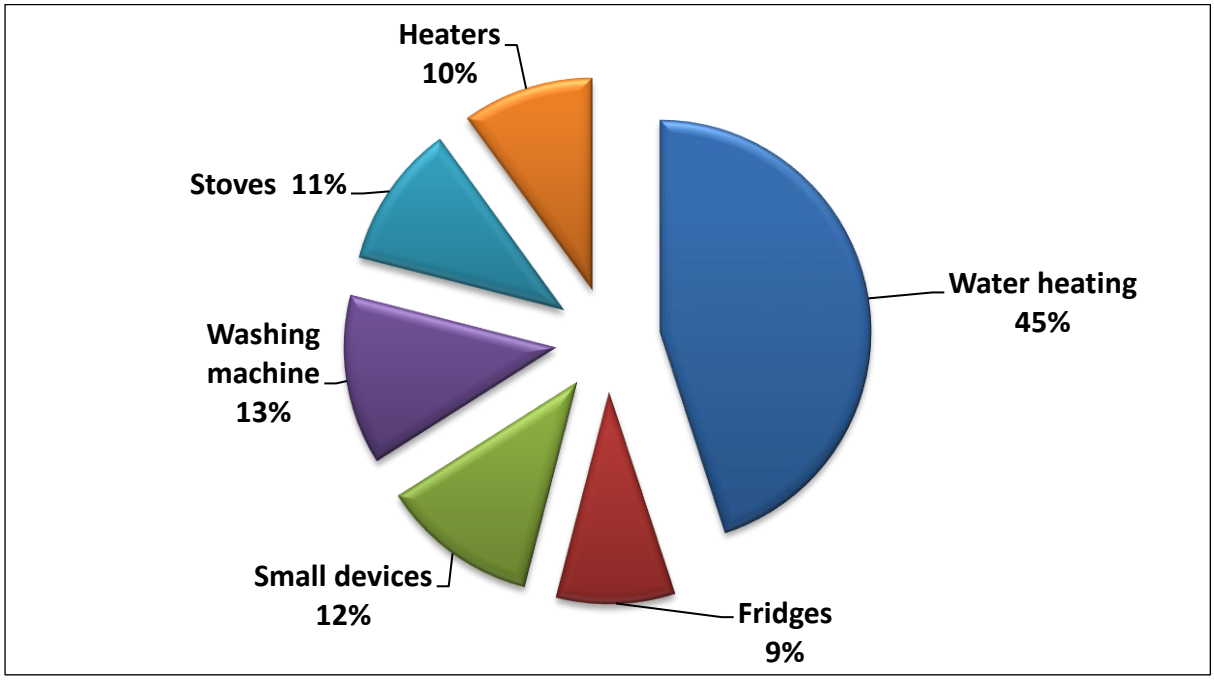

Figure 1.2: Residential sector energy demand share [Sustainable Energy Society South Africa, 2013].

Due to the abundance of coal in South Africa, the price of electricity has been relatively low compared to the global average [Edkins *et al*, 2010]. However, escalating production costs have resulted in a gradual price increase. To sustain primary energy production and operation costs the National Energy Regulator South Africa (NERSA) stipulated an annual electricity price increase of 8% [Department of Energy, 2013]. In addition, the Department of Energy projected an electricity consumption increase to 454 Terawatt hours in 2030 which is an increase of more than 75% from 260Twh in 2010 [Department of Energy, 2013]. This rise in energy demand coupled with environmental concerns has posed challenges in the energy sector.

1.1.1 Renewable energy in South Africa – Context for Solar water heaters

Although coal will remain the back born of the energy sector, it has become important to adopt an energy mix involving fossil fuels as well as cleaner and more sustainable renewable energy sources. The South African government is playing an important role in promoting the utilization of renewable energy in the country through research and development of solar, wind and biomass technologies. Following the Kyoto Protocol of 2010, the White Paper on Renewable Energy Policy was passed as a strategy to reduce greenhouse gas emissions. This created a resurgence of interest in solar water heater technology. The national utility in partnership with the Department of Energy implemented a national solar water heater demand side management program in the residential and commercial sector to reduce electricity demand. Demand Side Management (DSM) is the process whereby an electricity supplier influences the way electricity is utilized by the customer or end-user. DSM broadly entails the planning of activities of an initiative, the implementation thereof as well as the monitoring of activities which are designed to encourage consumers to modify patterns of electricity use. This process also includes the timing and level of electricity demand. The primary objective of DSM is to provide constant, efficient use of electricity thus resulting in lesser amounts of electricity being consumed during Eskom's peak periods, thus managing the demand effectively [Coetzee, 2009]. Several DSM projects have been implemented across South Africa and these include energy efficiency on lighting; energy efficiency on CFL distribution as well as load shifting on residential hot water systems. Energy service companies are responsible for implementation of such DSM project of which Eskom DSM is the primary financier of the projects.

For the national solar water heater DSM initiative in particular, the programme aims to increase the use of renewable energy for residential and commercial water heating and stall the rapid increase in electricity use for controlled and uncontrolled water heating purposes. The performance impact of this and other initiatives is quantified to an acceptable degree of accuracy by a process of measurement and verification (M AND V) whereby an independent auditing party, which are contracted by Eskom, determines the impact as a result of all DSM initiatives and give impartial feedback on the findings. From the inception of DSM the programs, demand reduction achieved between the 1st of April 2008 and 31 March 2009 was 916MW of which a contributions of 660MW and 240MW were made by the residential and the industrial sector respectively and 15MW was contributed by the commercial sector. It is evident that there is great potential for the residential sector to make substantial contribution to energy reduction and cost savings.

Incentives have been given in the form of rebates on the purchase of accredited solar water heating systems. Under this rebate system, up to 30% is granted after calculations by the South African Bureau of Standards (SABS) of the efficiency rating (Q – factor) of the systems. Tax credits and grants significantly reduce the high capital cost of solar heaters making them more competitive to fossil - fuel based systems. A cash rebate is also granted to consumers making them more affordable. The subsidies for solar water heating systems (SWHs) have resulted in a nationwide expansion of their market. Over 38 000 high pressure and 84 000 low pressure systems had been installed by 2011 in Reconstruction and Development Programme (RDP) households [Eskom Annual report, 2011] and by the first half of 2013, 350 000 systems had been installed across the country [Peters, 2013].

Solar water heaters (SWHs) have been in existence since the 1700s after the discovery that a black box with a glass cover can trap heat when placed in the sun. An estimated 40 million households made use of solar water geysers worldwide by 2004 [Gowda *et al*, 2014]. Small systems are normally used in residential applications while larger systems are employed in industrial applications such as in the food processing and textile industry [Khan *et al*, 2010]. SWH utilize the suns energy to produce hot water by capturing solar radiation, converting it to heat and transferring the heat to water. The primary components which make up a solar water heating system are a solar collector panel, an insulated storage tank, connecting pipes as well as safety and control valves. The solar collector is the main component in the system hence the need for its optimum performance and prediction of it performance [Luminuso and Fara, 2005].

This thesis evaluated the performance of a commercially available flat plate solar collector representative of collectors installed in South African households. The study focused on the prediction of collector outlet temperature (T_{co}), which is not usually estimated though this metric is important in the determination of system performance [Kalogirou *et al*, 1999]. The analysis considered the summer and winter variation of collector outlet temperature with climatic conditions and inlet temperature and used these operating parameters as inputs to a multi linear regression model.

1.2 PROBLEM STATEMENT

The collector outlet temperature is one important parameter to design engineers and researchers that requires accurate determination. Its prediction provides insight into the hot water temperature of the solar water heater system. White box modelling techniques have been widely used as a tool to predict collector performance. Research concerning dynamic modelling

is essential to adequately characterize the transient behavior of solar thermal collectors. However, the physical phenomena taking place in solar collectors are complex. The processes of heat transfer at the collector such as radiation, conduction and convection, and their dependence on long- wave irradiance results in a set of complex energy balance differential equations which are determined as functions of time and space coordinates. Simulation software such as TRYNSYS, WATSUN and Retscreen can be used for predicting solar collector performance; however they require sufficient expertise which may be tedious and difficult to perform. In addition, such software could be expensive for small research centres as well as to the general consumer. It would be desirable to have a modelling technique which is user friendly, less computational and has high accuracy. Multi linear regression provides such an alternative. Apart from its use in estimating parameters of physically-based collector models, multi linear regression has received limited attention in the field of solar thermal heating.

1.3 RESEARCH AIMS

The aim of the research is to investigate the performance of a flat plate collector under South African weather conditions, using the collector outlet temperature as the performance index; and use the measurements to model the collector outlet temperature using multi linear regression technique.

1.4 RESEARCH OBJECTIVES

The specific objectives are outlined below:

1. Analysis of collector parameters, solar radiation, ambient temperature and relative humidity variation logged concurrently from the measured data in Alice South Africa.
2. Development of .separate MLR-based models of performance and weather data for summer and winter seasons.
3. Validation of the derived multi linear regressions models using performance data.

1.5 RESEARCH QUESTIONS

The study endeavored to answer the following questions:

(i.) What are the performance differences of the solar collector relative to the summer and winter seasons?

(ii.) How do the modeled collector outlet temperatures compare with the experimentally measured values for summer and winter months?

(iii.) Can multi linear regression be used to accurately model the outlet temperature of a flat plate thermosiphon collector using solar radiation, ambient temperature, relative humidity and collector inlet temperature as predictor variables?

1.6 RESEARCH METHODOLOGY

The monitoring focused on obtaining sensor data from a flat plate solar collector installed at the University of Fort Hare Solar House, Alice Campus. The parameters measured were collector inlet temperature, collector outlet temperature, collector flow rate, solar radiation,

relative humidity and ambient temperature. The variations of collector outlet temperature, collector inlet temperature and flow rate with solar radiation and ambient temperature were subsequently determined.

Data was monitored during the summer months; over the period November 2013, December 2013, January 2014, and February 2014; and during the winter months over the period May 2014, June 2014, July 2014 and August 2014. A Hobo data acquisition system was used to measure all parameters in one minute intervals and averaged over 10minutes. Two multi linear regression models were formulated and validated using collector outlet temperature as the dependent variable and the solar radiation, ambient temperature, relative humidity and collector inlet temperature as the independent variables. Ordinary least square method was used to determine the model coefficients employing statistical analysis tool in OriginLab software.

1.7 DELINIATION

This study only considers the performance of a flat plate solar water heater located in the Eastern Cape Province; in Alice South Africa. South African climate is diverse and differs between the inland and the more coastal regions. However the results in this study are representative of typical collector performance in the South Eastern coast grassland region.

1.8 SIGNIFICANCE OF STUDY

This research has provided insight on the typical average collector outlet temperatures of a flat plate solar collector operating under real meteorological conditions for a location in South Africa which is important to local design engineers and researchers in the solar thermal

technologies field. An important contribution of this study is the development and validation of multi linear regression models to characterize the collector outlet temperature using easily measurable parameters namely solar radiation, ambient temperature, relative humidity and collector inlet temperature. The main significance of this method is its simplicity compared to numerical methods. Moreover, the derivation of the models was done with data collected from collectors operating normally with actual weather data. Multi linear regression is available in many affordable data analysis packages making it a viable alternative for developing predictive models for designers and researchers. Consumers can utilize this method with ease to assess and compare different collector performances and this may lead to production of good quality collectors by manufacturers.

1.9 HYPOTHESIS

As a predictor of the collector outlet temperature, the following model could be used for summer and winter season: The hot water temperature at the collector outlet can be predicted by a multi-linear regression in which the outlet temperature (T_{co}) is the dependent variable and solar radiation (I), ambient temperature (T_a), relative humidity (Rh), and collector inlet temperature (T_{ci}) are independent variables. The hypothesized model is therefore expressed as:

$$T_{co} = \alpha_0 + \alpha_1 I + \alpha_2 T_a + \alpha_3 Rh + \alpha_4 T_{ci} \quad (1.1)$$

1.10 DISSERTATION OUTLINE

This section summarizes the chapters of this dissertation and provides an overview of the scope of the study.

Chapter one presents the background to the study as well as the aims of the research which are to monitor the seasonal performance of a flat plate collector installed in Alice, South Africa and develop multi linear regression models for the collector outlet water temperature. The method employed in achieving the objectives is also discussed. Lastly the significance of the study and the model hypothesis are clearly stated.

Chapter two presents a synthesis of literature on the types of solar water heaters. The various configurations available are also discussed which include direct and indirect solar water heaters as well as active and thermosyphon solar water heaters. A summary of the parameters that influence the performance of solar thermal collectors is discussed. Lastly, a literature discussion of the experimental studies conducted in different locations is presented as well as discussion on the various modelling techniques and the relevant studies.

Chapter three presents a description of the system under study including the positioning of the sensors and their specifications. The modelling approach is discussed which includes the data collection and partitioning as well as the regression analysis. Lastly, a brief description of the statistical indictors and their mathematical relations is given.

Chapter four presents a discussion of the results obtained for the study. These are results of the performance monitoring which include hourly averages of solar radiation, ambient temperature and relative humidity values as well as collector outlet and collector inlet temperatures. The parameter estimation results are presented are presented including model validation plots. Lastly, the contribution by weight of the predictors is provided.

Chapter five presents the summary, conclusions and recommendations of the study. This is where major findings of the research are stated. The conclusion was based on the objectives of the study and research questions.

CHAPTER TWO

LITERATURE REVIEW

2.1 INTRODUCTION

There are mainly two types of solar collectors namely; concentrating and non-concentrating collectors. A non-concentrating collector 'has the same area for intercepting and for absorbing solar radiation, whereas a sun-tracking concentrating solar collector usually has concave reflecting surface to intercept and focus the sun's beam radiation to a smaller receiving area, thereby increasing the radiation flux' [Batabyal, 2013]. Concentrating collectors are used in applications in which very high temperatures are required (up to 400°C) such as industrial process heating and electricity generation from steam engines. Flat plate and evacuated tube collectors are examples of non-concentrating collectors. These are the main systems used in residential and commercial production of solar heated water.

2.2 TYPES OF SOLAR COLLECTORS

2.2.1 Flat plate collectors

Flat plate collectors (FPCs) are the most commonly installed systems for domestic solar water heating applications due to their relatively low cost and simple design [Duffie and Beckman, 2006]. Typically, a FPC is made up of a rectangular outer casing housing an absorber plate, with a transparent glass cover also known as a glazing. The absorber is usually made of copper,

galvanized steel or aluminium which are materials with high thermal conductivity. A selective coating such as black chrome is sprayed or painted over the absorber to enhance absorption of solar radiation. Selective coatings are generally made of mineral elements characterized by high absorptivity in the visible and infra-red range, and low emissivity. During heating solar energy intercepts the absorber plate where a portion of it is absorbed, converted into thermal energy and transferred to fluid in the pipes. The pipes are either embedded on the absorber plate or can be an integral part of the absorber; connected at the two ends by header pipes with a slightly larger diameter [Kalogirou, 2004]. The optical properties of the glass cover and absorber plate determine the fraction of absorbed radiation. Absorption at the plate gradually increases plate temperature which increases heat loss and results in reduced efficiency [Sekhar *et al*., 2009; Esen and Esen, 2005]. The glazing cover reduces convection and radiation heat loss between the cover and absorber cavity by allowing transmission of short wave length radiation and restricting long wave thermal radiation transmission. The choice of collector glazing material should therefore focus on reducing reflectance and absorbance and increasing transmittance. To reduce conduction heat losses, the bottom and edges of the collector casing are normally insulated. FPCs can heat water up to 100°C above ambient temperatures [Duffie and Beckman, 1991]. The performance of the system as a whole is largely dependent on the material used when constructing the SWH such as glazing, insulation and pipe material [Islam *et al*, 2013]. A typical flat plate collector is shown in Figure 2.1.

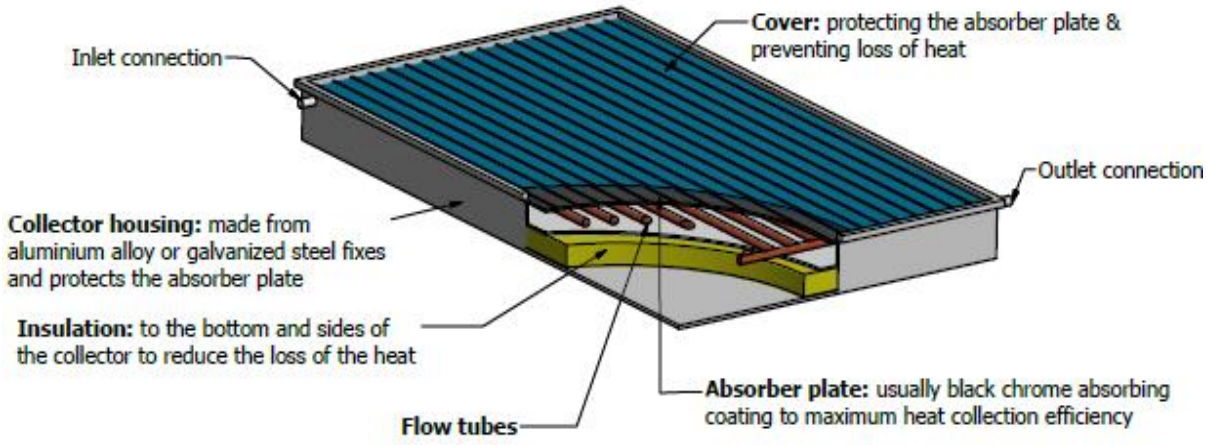

Figure 2.1: Single glazed Flat Plate Collector.

FPCs are capable of absorbing direct and diffuse radiation. This is important particularly during the winter season when solar radiation is low and the diffuse component of irradiance is higher. One generally identified limitation of FPCs is their inability to absorb solar radiation from large incidence angles encountered as the sun moves across the sky due to reflection from the glazing [Anderson and Furbo, 2009]. Flat plate collectors are mostly suited for warmer climates and for times when the intensity of the solar radiation is substantially high, their benefits are reduced when there are exposed to cold, cloudy and windy conditions [Arora *et al*, 2011].

2.2.2 Evacuated tube collectors

In evacuated tube type collector (ETC), the absorbing surface is enclosed in a vacuum-sealed tube which significantly reduces convection and conduction losses. This permits ETCs to achieve higher temperatures than FPCs. They have two methods of operation which generally give two types of ETCs; the glass-glass type and glass-metal type. The glass-glass collector

consists of two concentric glass tubes, a transparent inner tube that allows the passage of solar radiation and outer tube coated with selective coating, fused together at one end. These collectors are also called 'Sydney or Dewar tubes' [Caouris, 2012]. Between the tubes exists a vacuum that is constantly maintained by a barium getter positioned at the bottom of the tubes. Aluminium-based coating on the inner tube is used to greatly improve solar absorption.

The glass-metal type has only one tube with an aluminium plate on the inside which can be either curved or flat. A heat pipe made of copper is attached to the plate normally coated with $TiNOX^3$. A vacuum in the heat pipe enables the water to boil at lower temperatures than it would at normal atmospheric pressure [Sargsyan, 2010]. When solar radiation falls on the surface of the absorber, the liquid within the heat tube quickly turns to hot vapour and rises to the top of the pipe. Water flowing through the manifold is heated and stored in the tank, while the water in the heat pipe condenses, flows back to the base of the heat pipe and the process is repeated. The glass to metal seal can sometimes suffer loss of vacuum in these types of collectors. ETCs can easily attain temperatures between 80°C and 200°C depending on the solar radiation levels [Focus, 2012]. According to Kalogirou [2004], ETCs are capable of collecting direct and diffuse radiation like FPCs, however their efficiency is higher than FPCs at extreme incidence angles. A heat pipe solar collector is shown in Figure 2.2.

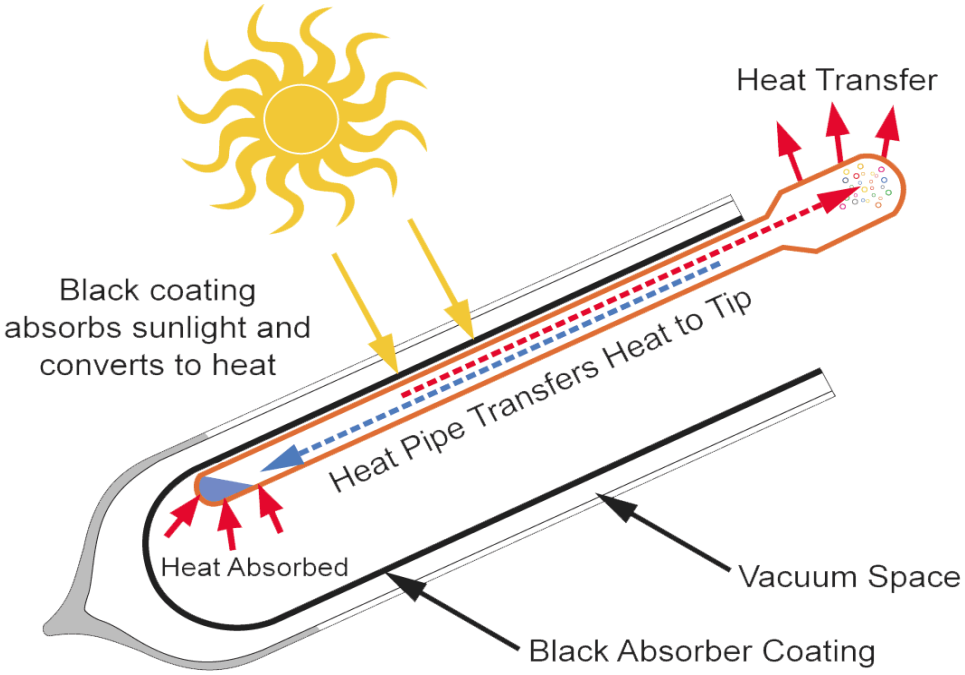

Figure 2.2: Evacuated tube collector showing operation of heat pipe.

Source: Surfine Renewable energy, 2014.

2.3 TYPES OF SYSTEM CONFIGURATIONS

There are generally four system layouts available for solar water heating systems which describe the relationship of the key components. They include active and thermosyphon configurations as well as direct and indirect configurations [Laughton, 2010].

2.3.1 Water circulation: Active and thermosyphon systems

Primary classification of SWHs is based on the way in which the fluid flows through the system and can be either active circulation or thermosiphon circulation. In active systems, the SWH incorporates a pump which can be electrically or solar powered to circulate fluid between the collector and storage tank. Thermosyphon systems do not employ any moving components.

Circulation is maintained by the density difference between the solar heated fluid and the cold water at the tank bottom. When there is sufficient solar radiation, water in the collector unit gets heated up, expands, and rises naturally to the top of the tank [Kalogirou, 2009]. Cold, heavier water falls by gravity from the bottom of the tank back to the collectors setting up a natural circulation loop which gradually heats the storage tank water. The thermosyphon effect is mainly influenced by the thermo-physical properties of liquid and the temperature of the surface in contact with liquid [Kishor *et al*, 2010]. Figure 2.4 shows basic operation of a thermosyphon system.

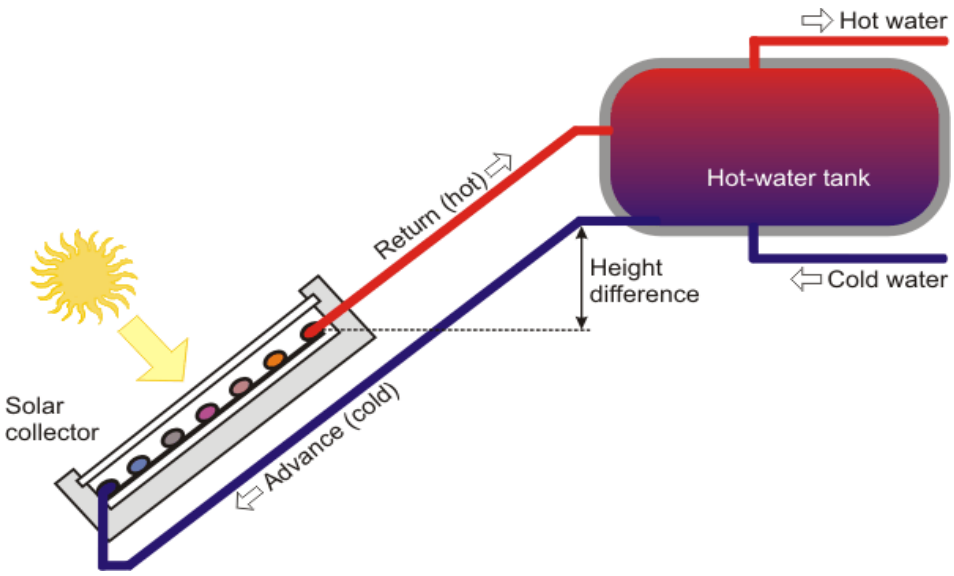

Figure 2.4: Thermosyphon solar water heater.

Source: Approdedia, 2014.

2.3.2 Heat transfer: Direct and indirect system

Solar water heaters can also be classified by how heat is transferred to the storage tank and this can either through direct or indirect means. In a direct solar water heating system, cold water

circulates directly from the storage tank to the collector, gets heated and circulates back to the tank again. Such systems are typically installed in climates where freezing rarely occurs. Although direct systems have simple and efficient design, they can be easily affected by scale and corrosion when water is acidic or hard [Riahi and Teharian, 2011]. Indirect solar water heaters are installed to address the installation challenges for very cold climates. This configuration has a solar and domestic circuit and incorporates a heat exchanger. In the solar circuit, a heat transfer fluid such as ethylene glycol or propylene glycol mixed with water circulates between the solar collector and the heat exchanger. Mixing propylene glycol with water lowers its freezing point making these systems suitable for use in freeze-prone areas. The fluid in the solar circuit transfers heat to water in the domestic circuit where water circulates from the storage tank to heat exchanger without mixing with the household water. A disadvantage of indirect systems is heat loss during the heat exchange process. Direct systems are common in tropical climates where freezing hardly occurs whereas indirect systems are commonly installed in temperate climates which are generally freeze prone regions [Amaobeng, 2012]. The typical configuration of an active indirect and active direct system is shown in Figure 2.5.

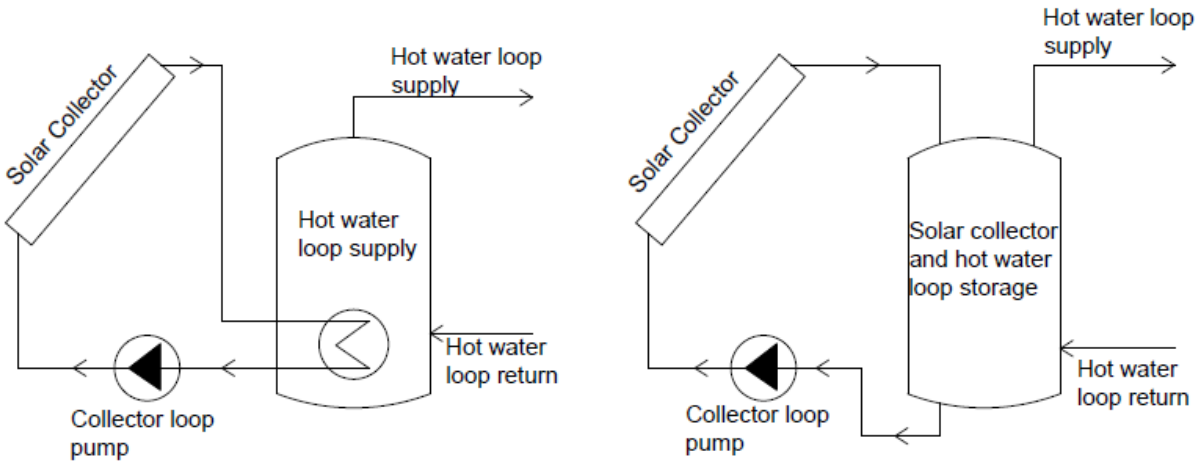

Figure 2.5: The diagrams above show left indirect active system and to the right direct active system.

2.4. FACTORS AFFECTING SOLAR COLLECTOR PERFORMANCE

2.4.1 Ambient conditions

The energy gained by a solar collector is impacted mainly by the ambient conditions of a location. The rate of energy absorption by a collector is determined by the incident solar radiation on the collector surface while ambient temperature affects the rate of heat loss on the collector surface. The closer the fluid temperature is to the ambient temperature, the lower the losses which in turn increases collector efficiency [Ramlow and Nusz, 2010]. Regarding wind speed, high wind speeds increase the rate of forced convection currents at the glass cover which results in heat loss from the collector surface to the surroundings.

High humidity has the effect of lowering the glazing surface temperature [Kishor *et al,* 2010]. Outside air humidity causes the formation of condensate inside the collector glazing and absorber. When the collectors' inside air humidity is higher than the outside air humidity, condensate may form which leads to corrosion and lowered collector efficiency [Nykanen, 2012].

2.4.2 Collector tilt and orientation

For optimum performance all year round, solar collectors should be installed at the same tilt angle as the latitude of the location [Duffie and Beckman, 1991]. Depending on the application however, collectors can be installed 10-15 degrees less or more than the latitude [Kalogirou, 2004]. With regards to orientation, solar collectors should be installed in such a way that the daily and seasonal solar radiation received is maximised. Generally, optimum orientation for collectors in the Southern hemisphere is due north while those in the Northern hemisphere should face due south. According to Kalogirou [2012], it is possible to install the collector such that it faces 90° East or West of North and not significantly reduce its performance.

2.4.3 Inlet temperature

The inlet temperature is the temperature of water entering the collector. Increasing inlet temperature decreases collector useful energy and system efficiency [Gowda *et al,* 2014; Teyeb *et al*, 2008]. When inlet temperature increases, the outlet temperature increases to the maximum attainable temperature. Continued increase in the inlet temperature reduces ΔT (T_{co}-T_{ci}) thereby decreasing Q_{use} from the equation $Q_{use} = \dot{m}C(T_{co}-T_{ci})$. Inlet temperature should therefore be kept as low as possible to improve thermal efficiency.

2.4.4 Collector layout

Collector layout can either be parallel or series, or a series-parallel combination. When collectors are connected in parallel, a single pipe divides into two and feeds into the inlet of both collectors. If the collectors are identical, water enters the collectors at the same temperature and exits with the same temperature. The performance of the collector array is the same as the performance of the individual collector [Kalogirou, 2012]. For series connection, the outlet of one collector becomes the inlet of the collector next in the array hence the performance of the collectors will not be equal [Duffie and Beckman, 1991].

2.4.5 Design parameters

Design parameters such as collector material, tube sizing and spacing and collector area have an effect on the performance of thermosyphon solar water heaters. Siebers and Viskanta (1979) studied the thermal analysis of some flat plate collector designs for improving their performance. Their results illustrated that a single surface selective on the absorber or the glass cover closest to the absorber to suppress thermal radiation heat loss is the most effective means of improving flat plate collector performance when only suppressing one mode of heat transfer. Khalifa (1999) investigated a thermosyphon domestic hot water system and results showed that temperature variation along the absorber fins, tubes and in the flow direction as well as the thermosyphonic mass flow rate greatly affected performance of the thermosyphon system. Agbo and Okeke investigated the effect of tube spacing as a design factor in the performance of a natural-circulation solar water heater for copper, zinc and galvanized steel absorber plates. The performance of the collector was determined in terms of the collector efficiency and the

collector fin efficiency both theoretically and by simulation based on the Hottel -Whiller model of the system. Their results showed that tube spacing varies inversely with collector efficiency and the fin efficiency for the three absorber plates. It was also seen that copper had the best performance followed by the zinc, while galvanized steel showed the least. They concluded that the performance optimized with a tube spacing not exceeding 10 cm irrespective of the absorber plate used. Amori and Jabouri (2010) studied a new design of solar collector whose risers were made of converging ducts whose exit area is half that of the entrance and compared it to a conventional absorber, with risers of the same cross sectional area along its length. Results show that a considerable enhancement of thermal performance (approximately 60%) of absorbed heat (useful gain) at solar noon was obtained for the new design which achieved an instantaneous efficiency was 31.5%, in comparison with the conventional type which achieved an instantaneous efficiency of 16.5%. Kulkarni and Deshmukh (2015) summarizes the effects that improve the collector efficiency by improving transparent covers, improve absorber plate to solar radiation and improve heat transfer coefficient. Kovács *et al* (2013) studied the performance of a new collector design with cylindrical absorber using the steady state method described in EN 12975-2. Their results showed that the performance is over estimated due to the specific characteristics of this collector type.

2.5 REVIEW OF RELATED WORK

Solar collectors are the main components of solar water heaters and over the years there has been an increasing interest in their performance around the world. This has led to extensive research to determine solar collector performance in various climatic conditions and ways to model and predict the performance. This section reviews studies related to performance of flat plate solar collectors in different geographical locations. In addition, the distinction between

white box and black box models is described together with a summary of fundamental and state of the art research conducted in the modeling of flat plate collectors.

2.5.1 Performance of flat plate collectors

The thermal capacity of a collector, the capacity and configuration of the storage tank, dimensions of the pipes as well as ambient conditions and flow rates are all important parameters in determining SWH performance. Evaluating the performance of a system is typically done by conducting experiments under specific operating conditions. Experimental research not only leads to better understanding of component behavior but also lends confidence to corresponding mathematical models [Riahi and Taherian, 2011]. Furthermore, differences in design, manufacturing materials and weather conditions result in differences in relative performance which are revealed during experimentation.

Samo *et al* [2012] studied the collector performances of an active and a thermosyphon SWH fabricated with locally available indigenous materials. The systems were monitored under moderate weather conditions encountered in Pakistan and the results obtained showed that the thermosyphon system performed better than the active system, recording an overall efficiency of 31% compared to 26.6% for the active system. The maximum temperatures obtained were 76.1° C and 95.5° C for the active system and thermosyphon system respectively.

Salas *et al* [2012] designed a thermosyphon solar water heating system for the purpose of experimentally evaluating its performance under Arequipa, Peru climatic conditions. The experimental set up consisted of ten flat plate collectors with two rows of five collectors each installed in parallel. They monitored the inlet and outlet temperature of each collector and the

storage tank, the pressure drop, heat absorbed and mass flow over several sunny days and the results indicated a pressure drop in the collectors at maximum solar radiation which was attributed to the 8mm diameter of the tubes. The results also showed that at noon the peak collector outlet temperature was 85°C and the peak flow rate was 0.0018kg/s, all corresponding to a maximum radiation of 1200Wm^2.

Riahi and Taherian [2011] carried out an experimental investigation of the dynamic response of a commercially available flat plate thermosyphon SWH to variations in solar radiation. The system which was installed in Babol, Iran (36E, 52N), was equipped with a mantle heat exchanger and incorporated a 180litre horizontal storage tank. Their collector was manufactured by sandwiching a copper tube between two aluminum plates which they perceived to be a more efficient design. They determined the mass flowrate using hydrogen bubble method to measure the flow rate from which they observed a peak flowrate of 0.0165kg/s at noon. They observed a maximum temperature of 90°C in the temperature of the liquid entering the mantle heat exchanger from the collector and concluded that the system performed well under the given climate even under cloudy conditions.

Belessiotis and Mathioulakis [2002] developed an efficient and simple simulation approach valid for solar-only systems for an indirect thermosyphon SWH and experimentally validated the model. The collector and the whole system were tested according to the ISO 9806 -1 and the ISO 9459 - 2 standards respectively. The experimental results indicated a peak flow rate of 0.018kg/s and collector outlet temperature of 58°C. A comparison between the model and measured values showed a maximum error in the instantaneous prediction of useful energy of approximately 10% and the standard error in the prediction of the daily useful energy did not exceed 2%. They concluded that their methodology could be used for the energy optimization

of the system at the design stage as well as to improve a system by using the methodology to analyse test results.

An experimental study was conducted in Yamoussoukro, Cote d'Voire (6.54°N) by Sako *et al* [2007] to determine the economic and technical viability of solar water heaters in the region, in relation to conventional sources of domestic hot water production. An indirect, thermosyphon prototype system consisting of a $2m^2$ flat plate collector and a 95litre storage tank was built and tested using locally available materials. The results obtained on a typical sunny day showed a collector peak temperature of approximately 85°C and an efficiency of 58.62% at 1pm for a maximum solar radiation of $1000W/m^2$ and they concluded that the systems were suitable for application in Cote d'Voire.

Another theoretical and experimental study was performed by Koffi *et al* [2008] on an indirect, thermosiphon solar water heater prototype in Yamoussoukro, Cote d'Ivoire 6.54°N. Detailed heat and mass transfer balance equations were formulated to calculate the collector inlet and outlet fluid temperatures, the heat exchanger inlet fluid temperature and the hot fluid mass flow rate with the system operating in quasi-stationary state. The experimental results obtained showed a maximum collector outlet temperature of 85.5°C at a heat flux of $989W/m^2$ and a collector thermal effectiveness in the range of 58%. The corresponding maximum fluid flow rate was 0.00856kg/s. A comparison between the experimental and simulated collector inlet and outlet and flow rate values showed good agreement during major insolation period with an error margin of +/-4%. The authors concluded that the model could be used as an efficient tool to predict and design solar systems operating under thermosiphon principle flow conditions.

Agbo [2011] evaluated the performance of a thermosyphon flat plate collector in Nsuka, Nigeria (7°N). He formulated collector models for optimization rather than prediction by evaluating the effect of number of glazing covers, thickness of glazing cover, tube spacing and nature of absorber plate material on the system's performance. The performance results indicated that the system had a maximum average daily collector efficiency of 0.658 and a mean system temperature of 81°C. The average seasonal value of efficiency was 0.54 over the dry, Harmattan and rainy seasons covered in the study. The simulation results showed that with a tube spacing not exceeding 10cm, the performance of the system was optimized irrespective of the absorber plate material.

Madan and Sirse [2015] performed an experimental investigation of a thermosiphon flat plate SWH during two winter months in Nagpur Maharashtra, India (21.15ºN, 79.09ºE). The tank was initially filled with 100lites of water in the morning and the collector left to heat up during the day while simultaneously measuring collector inlet, collector outlet, flowrate and solar radiation. Their results indicated a maximum collector outlet temperature of 73°C at an average solar radiation of 480W/m^2. They go on to state that the ideal maximum temperature should be 100°C but heat losses reduce the maximum temperature that can be attained and an increase in the number of riser tubes would likely improve the water outlet temperature.

Zerrouki *et al* [2002] undertook an experimental and theoretical study to analyse the natural circulation of a compact thermosyphon solar domestic hot water system produced and commercialized in Algeria. They performed measurements on mass flow rate, temperature rise and fluid and absorber temperatures inside the parallel tube design for a system of 1.8m^2 flat plate collector and 120L storage capacity. The maximum flowrate was observed to be 0.0085kg/s at 13:30. Furthermore a steady-state theoretical model was developed and

compared with measurements of basic physical parameters governing the natural circulation in a thermosyphon. Results obtained showed that the thermosyphonic flowrate calculated by the model agreed well with experimental values particularly during the main insolation period. However no information is provided on the maximum collector outlet temperature and average error between the modelled and measured values.

Chuawittayawuth and Kumar [2002] conducted an experimental and theoretical investigation to analyse the temperature profiles of the absorber plate, water temperature and water flow distribution in the riser tubes of a thermosyphon SWH. Their results showed that the temperature of riser tubes near the collector inlet were generally much higher than other subsequent risers on a clear day, while on cloudy days, the riser temperatures were uniform. The measured and modelled values revealed that the temperature of water near the riser outlets was fairly uniform particularly during cloudy and partly cloudy days at and that temperature of water in the riser depended on its flow rate.

2.5.2 Modeling

Calculating the performance of SWHs is essential for approximating the performance characteristics of the system and as a commercial argument [Andres and Lopez, 2002; Kalogirou, 2007]. Additionally, it also allows comparisons between different collector system designs. System optimization is simplified by developing models of different components. Numerous models have been formulated to predict the performance of solar water collectors and they all generally fall into three categories; namely white box models (also referred to as deterministic models) , black box models (also referred to as stochastic models) and grey box models.

2.5.2.1 White box models

The application of physical laws in formulating component models is known as white box modelling; hence there are also termed physically - based models. Solar water heater system operation is fundamentally based on thermodynamic laws [Duffie and Beckman, 1999] and these should be sufficiently understood to develop an accurate mathematical expression of the system. In solar thermal technology, white box models are generally formulated in continuous time using first principle energy and mass balance equations and expressed in terms of differential equations. The analytical solutions to the equations provide profiles of the characteristic performance index. White box models form the basis of simulation software such as TRYNSYS, MINSUN and Retscreen, and are especially efficient when users want to perform design modifications for optimization.

Researchers have modeled solar collectors since the 1950s. The initial modelling of collectors began with white box models and thermosyphon systems where of particular interest due to their simple design. Hottel and Woertz [1942], Hottel and Whillier [1955] and Bliss [1959] did the pioneer work on the modelling of solar collectors. They developed energy balance equations that enabled determination of collector temperatures as a function of the time and space coordinate [Kicsiny, 2014]. Their equations calculate useful heat from the heat loss coefficient which is dependent on parameters such as absorber plate temperatures, ambient temperature, flow rate and collector geometry but neglect thermal capacitance. The models form the basis of several model formulations and are still frequently used to date [Góngora-Gallardo *et al*, 2013]. For example, Duffie and Beckman [1991] used the assumptions developed by Hottel, Woertz and Whillier, considering one-dimensional heat transfer to

characterise the flat plate collector in steady state. They used electrical analogy to formulate energy balance equations for the the temperatures of absorber, back plate and glazing covers. Their equation is widely used for calculating thermal performance of solar collectors.

The first dynamic numerical model to describe a thermosyphon system was formulated by Close [1962]. This model determines average system temperature and flow rate, assuming ideal conditions of clear sky and no water draw off during the day. He formulated a one-node capacitance model were he assumed that the capacitances of the glass cover, fluid and plate are all lumped within the collector plate itself. The model represented by equation 2.1 is termed the 1-point lumped model and consists of a one energy balance differential equation based on the energy balance of solar thermal collector in steady state. A drawback of the Close model is its inaccurate profiling of the collector heat transfer fluid temperature.

$$C_p \frac{\partial T_p}{\partial \tau} = (\alpha\tau) A_p I_{p,n} - Q_{loss} - Q_{p,w} \tag{2.1}$$

Where C_p is the lumped thermal capacitance of the collector, T_p is the overall collector temperature, $(\alpha\tau)_p$ is the transmittance - absorbance product. The overall heat loss Q_{loss} and the useful heat transferred $Q_{p,w}$ are calculated using steady state formulation by [Hottel and Whillier,1955; Bliss,1959] and are given as;

$$Q_{p,w} = F_r A_p \left[\left(\alpha\tau_p \dot{I}_{p,n} - U\left(T_{f,in} - T_e\right) \right) \right] = \dot{m}_f C_f \left(T_{f,out} - T_{f,in}\right) \tag{2.2}$$

$$Q_{loss} = U A_p \left(T_p - T_e\right) \tag{2.3}$$

The terms F_r and U represent the heat removal factor and the overall heat loss coefficient between absorber plate and air of collector with area A_p respectively, while f,in and f,out are the fluid inlet and outlet temperatures respectively. T_e is the external temperatures surrounding the collector. Gupta and Garg [1968] further developed the Close model by incorporating the heat exchange plate efficiency factor. Experiments conducted to verify the model revealed that flowrate can be increased in thermosyphon systems by increasing the collector and tank height. Experimental investigations of the impact of tanker height from the top collector end showed that the efficiency and the mean tank temperature was not affected by the height of the tanker from the solar collector.

Ong [1974] applied the finite difference method of solution to predict the thermal performance of a flat plate thermosyphon solar water heater and found results that compared well the model with experiments measured under Malaysian weather conditions. The author verified the theoretical collector flowrate experimentally by measuring using dye trace inject.

Siddiqui [1997] studied the effect of solar radiation in heat transfer and fluid flow in an indirect thermosyphon solar water heater and found the average heat transfer coefficient increases with solar radiation due to the high temperature difference between the mean fluid temperature and ambient temperature.

A study was done by Morrison and Ranatunga [1980] to evaluate thermosyphon system response to step changes in insolation and found that there are long time delays before thermosyphon flowrate develops. Their results also indicated that the collection of energy is not affected by the thermosyphon time delays.

One of the most important collector models is contained in the EN 12975-2: Thermal solar systems and components - Solar collectors' standard [EN 12975, 2006]. This model was formulated to characterize the collector operation under quasi-dynamic test conditions and has several advantages. The testing conditions are less restrictive compared to the steady-state testing conditions which allow very little varying of operating conditions. However the inclusion of extended test conditions increases the number of parameters to be estimated which makes the model much more complex. Equation 2.4 shows the functional expression in which the normalization test results are given. As seen, the model requires determination of 7 parameters shown in bold in the equation. The model is also non-linear with respect to its inputs. Modelling the transient operation of a collector enables easier and less expensive testing, however the governing equations and computation of the models is made more complex. Facão *et al* [2004 also view that such models can sometimes result in non-convergence.

$$Q_{use}=A\left(\mathbf{F}'(\boldsymbol{\tau\alpha})_{\mathbf{en}}\right)K_{\theta B}(\theta_B)G_B+\mathbf{F}'(\boldsymbol{\tau\alpha})_{\mathbf{en}}\mathbf{K_{\theta D}}(\theta_D)G_D-\mathbf{c_6}uG-\mathbf{c_1}(T_m-T_a) \qquad (2.4)$$

$$-\mathbf{c_2}(T_m-T_a)^2-\mathbf{c_3}u(T_m-T_a)+\mathbf{c_4}\left(E_L-\delta T_a^4\right)-\mathbf{c_5}\frac{dT_m}{dt}$$

Another solar collector model along with the computational procedure was proposed by Muschaweck and Spirkl [1993] for quasi-dynamic collector testing. It can be regarded as a 'state of the art 'collector model according to Fischer *et al* [2012]. They extended the Hottel – Whillier – Bliss equations to a dynamic model with simple parameters which characterize collector physical phenomena including zero loss efficiency, slope of the characteristic curve and thermal mass using a multimode model. Their model considers the collector as split into n-segments in series configuration to determine the overall performance. The prediction of temperature difference across the collector averaged over a segment was found to be =<0.2 K.

Although the method is simple, the authors allude to difficulties in determining the heat thermal capacity. The method also requires the use of specific solvers to determine solutions for the ordinary differential equations [Amrizal, 2012].

Amrizal *et al* [2012] developed and experimentally verified a transient model for characterizing the dynamic thermal performance of a solar thermal collector. Their model was based on the piston flow collector concept were they divided the collector into n-segments of homogenous temperatures and each segment modelled by a linear ordinary differential equation. It simplifies the Muschaweck and Spirkl model in that it can be easily applied with any spreadsheet programs using simple expressions. It also considers less environmental variables in comparison to the EN 12975-2 collector model.

Teharian *et al* [2011] studied the dynamic simulation of a thermosyphon flat plate solar collector and experimentally validated it with weather conditions encountered in Iran. Their formulation included one segment models developed for the collector fluid, the absorber and the glass cover. Results obtained showed that the model accurately described the average collector temperature and efficiency on sunny days but showed variance on cloudy days. The authors attributed this behavior to the difference in the simulation time-step resolution and the climate data imported into the program.

Buzas *et al* [1998] proposed a simple linear ordinary differential equation to describe the time varying heat transfer process in a solar collector. The collector model describes the collector outlet temperature as a function of the collector inlet temperature, volumetric flowrate in the collector loop, irradiance on the collector plate, collector ambient air and overall heat loss coefficient. According to Kicsiny [2014], this is likely the simplest physically-based ODE

model of one dimension. A comparison of measured and modelled collector outlet temperature revealed an average temperature difference of 8.6 °C, a minimum difference of 3.7°C and a maximum difference of 72.1°C. The modelled collector outlet temperatures showed greater variance than the measured temperatures and they attributed this effect to the exclusion of the heat capacity of the collector structure in the model.

Hammadi [2009] formulated a first order linear differential equation to describe the temperature distribution in collector tubes. The collector flowrate was estimated by evaluating the heat and mass transfer balance between the buoyancy and pressure in the thermosyphon loop. His results focused on simulating the effect of wind velocity, collector area, and collector tilt angle on the storage temperature as well as the effect of collector tilt angle on the collector outlet temperature. The author concluded that performance of the solar water heater strongly depends on parameters such as the collector location, collector tilt, wind velocity, and the solar time.

While white box models may be effective and accurate, they have drawbacks which make them difficult to implement in practise. As shown from examples presented in the literature, white box models are generally nonlinear in nature making them complex and their application discouraging [Kishor *et al*, 2010]. The physical phenomena taking place in solar water heaters are complex and require expertise to develop [Andres and Lopez, 2002] and may require many input parameters. As a result the modelling process becomes cumbersome and time consuming. For these reasons some researchers propose simpler approaches to certain applications to model performance of solar collectors.

2.5.2.2 Black and grey box models

Black box models are developed when no prior information about a system or process is known. Typically, these models are data driven, requiring a set of output and one or more inputs in the form of historical performance data taken from experiments. They differ from white box models in that the model structure is not specified a priori, but instead determined from performance data. There are developed using parameter estimation methods such as regression based methods, dynamic parameter identification, generic optimization program and artificial neural networks [Budig *et al*, 2009]. Grey box models combine features of both white and black models, allowing incorporation of prior physical knowledge of a process as well as statistical techniques for parameter identification. According to Bohlin and Graebe [1995] grey box models 'provide a natural framework for modelling dynamic systems'.

Artificial neural networks (ANNs) consist of a black box model [Hagan *et al*, 1996] in which the relationship between inputs and outputs is learned from analysis of previous data. According to Haykin [1994] a neural network is 'a massively parallel distributed processor that has a natural propensity for storing experiential knowledge and making it available for use'. Typically, a neural network is made up of interconnected neurons which mimic the learning process of the human brain. ANN are highly dependent on available data and the modeler is generally unable to make any judgement on the statistical structure of the model. A network is generally comprised of an input layer, one or more hidden layers and an output layer [Cavallaro, 2013] as shown in Figure 2.6. The structure of an ANN includes the predictors which are fed as input signals from other sources into an input layer through nodes, which are used during neural network training. The inputs can either be outputs of other neurons or they can be external inputs [Fischer *et al*, 2012]. The hidden layer of the neural network is the

training location for the neural network. All outputs from the input layer are fed to each node, weighted by inter neuron connection strengths and are then assigned to non-linear functions that combine the inputs [Ahmadi – Nedushan *et al*, 2007]. The error between the training set and the ANN outputs is minimized by adjusting the network connection weights of each node using learning algorithms such as back propagation. Back propagation ensures that the rate and direction of learning is appropriate by implementing a gradient descent.

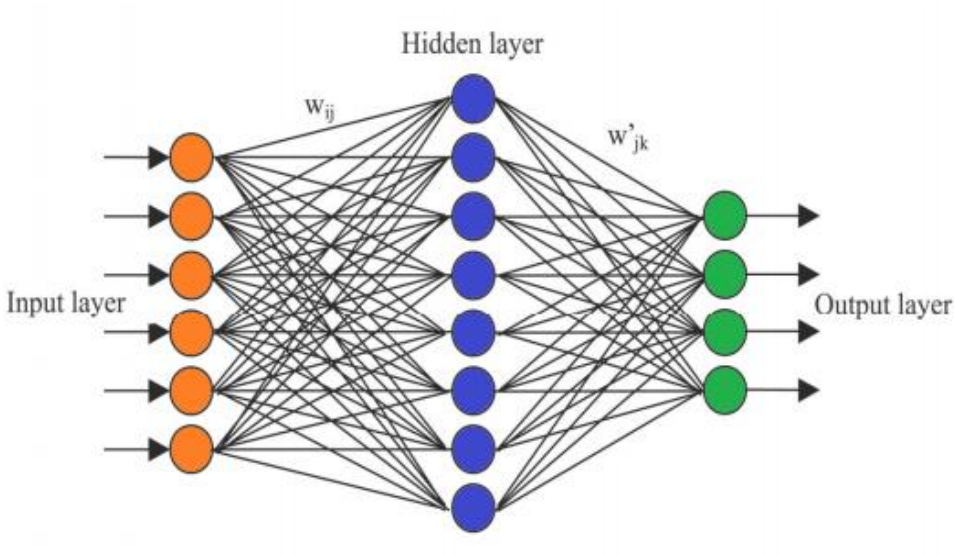

Figure 2.6: Typical Artificial Neural Network architecture [Batabyal, 2013].

ANNs have been widely used to model solar water heaters as well as in other application such as medicine, power systems, robotics, particularly when complex mapping and system identification are required. The ability of neural networks to estimate the performance of a solar domestic water heater was first investigated by Kalogirou e*t al* [1999]. They used a multilayer feed forward neural network which is a network consisting of an input layer (2 neurons), some hidden layers (8 neurons) and an output layer (2 neurons). They estimated the useful energy extracted and the temperature rise in the stored water from collector area 1.81 m^2 to 4.38 m^2, storage tank heat loss coefficient, tank type, total daily solar radiation, mean ambient air temperature, storage volume, water temperature in storage tank and type of system. Data from

33 sets were randomly collected out of which 30 sets were used for training and 3 sets to validate the model. The training data set yielded R^2 values of 0.9722 and 0.9751 for the useful energy extracted and the temperature rise in the stored water respectively. Unknown data considered for the training of the network at different weather conditions was used to investigate accuracy of the predictions. Predictions within 7.1% and 9.7% were obtained respectively for the two output parameters and they concluded that the performance of the ANN can be improved when the performance characteristics of the collector are known. The authors highlight the main drawback of using ANNs as the 'inability to understand the correlations among each different parameter, thus making the causes of a low reading of the thermal performance difficult to be understood'.

Kalogirou and Panteliou [1999] studied the suitability of neural networks as a tool to estimate the long term performance of a two flat plate, thermosyphon solar water heating system with a heat exchanger. The system was tested according to ISO/CD/9459.5 standard, under standard weather conditions encountered in Rome, Italy. The input data were leaned with adequate accuracy with correlation coefficients varying from 0.993 to 0.998, for the delivered power, fractional system gain, and mean load temperature difference and the average effective solar system area. Using unknown data on the network, a maximum percentage difference between the actual and predicted data of 6.3% was obtained.

Farkas and Géczy-Víg [2003] modelled the layer temperatures of the storage tank of a solar thermal system using ANNs. The identified model gave acceptable results inside the training interval showing average deviation of 0.22°C for the training and 0.24°C for the validation. They concluded that ANNs can be successfully applied for such type of predictions.

More specifically, neural networks have also been applied to solar collectors. Kalogirou [2006] developed 6 models to predict the performance parameters of flat plate solar air collector both in no-wind and wind conditions, taking into account the incidence angle modifier coefficients at longitudinal and transverse directions, the collector time constant, the collector stagnation temperature and the collector heat capacity. The input data for training, testing and validation of ANN were obtained from a database of 130 thermal solar collectors. Results obtained showed that the maximum differences in thermal performance for temperature difference of 10°C and 50°C at wind condition were 1.7 % and 1.9 %, and at no wind condition were 4.5 % and 4.9 %. The author concluded that more diverse design parameters and more training cases could improve the accuracy of the network.

Farkas and Géczy-Víg [2003] implemented ANNs to model three different types of solar collectors to forecast the outlet temperature of the solar collectors based on solar radiation, ambient temperature and inlet temperature. The parameter identification showed good agreement with measured values.

Lecoeuche and Lalot [2005] applied ANNs to predict the daily in-situ performance of solar air collectors using collector outlet temperature as the output and solar radiation and thermal heat loss coefficients as the input to the network and obtained satisfactory results with a variance lower than 0.5%. Facão *et al* [2004] made use of ANNs for the simulation of solar hybrid collectors and compared it to a white box model. They evaluated the results based on calculations of useful heat and thermal efficiency and concluded that ANNs have several advantages over energy balance based models such as high accuracy, insensitivity to uncertainty in the input parameters, instantaneous response as well as no convergence problem.

Zárate and Pereira [2006] applied ANNs on a thermosyphon SWH by considering parameters that influence the efficiency in the prediction of outlet water temperature. They considered the outlet temperature as the predicted output and the inlet water temperature, solar irradiance, ambient temperature, water flow rate, and two installation parameters; collector inclination and hot water tank height as input variables in ANN model. The results showed a correlation coefficient of 0.9942 and an average error in efficiency of 0.69847%.

Fischer *et al* [2012] demonstrated the superiority of ANNs over white box models using a conventional flat plate collector and an evacuated Sydney tube collector. The systems were tested according to the European Standard EN 12975-2 using collector energy output as the performance metric. Results showed that the ANN models yielded lower percentage differences in transferred energy in both clear sky and broken clouds conditions, for both collectors. The authors concluded that ANNs are more powerful in predicting collector output however special test sequences are required to cover a wide range of operating conditions. They further highlight that determining a very good ANN thermal performance model is highly dependent on the expertise of the user.

Kishor *et al* [2010] employed grey-box modelling approach to improve the prediction accuracy for a thermosyphon water heater. They predicted the collector outlet temperature using a fuzzy system based grey-box model, compared the results with neural network technique and found that the performance prediction was improved when a fuzzy system of 3 inputs (inlet water temperature, ambient temperature, solar irradiance) was used instead of two input (inlet water temperature, solar irradiance) or single input system (solar irradiance or inlet water temperature). The fuzzy model showed good level of accuracy compared to ANN technique and they concluded that the technique could be successfully used for prediction of solar water system performance.

Despite their advantages, ANNs present some difficulties during implementation. They are extremely complex and require large amounts of performance data. Due to their very 'black box' nature it is difficult to determine how the network solves the problem. In addition, the need for training makes the technique costly in terms of computational time. For example, Sözen *et al* developed a new formula based on neural networks to determine the efficiency of flat-plate solar collectors in Ankara, Turkey. They used data for three summer months in order to train the neural network [Sözen *et al*, 2008]. In another study by Kalogirou and Pentaloui [2000], 33 systems were tested and modelled using ANNs for three different locations in Greece. Of these systems, 30 were used for training and testing and only 3 for validation of the model. Another potential drawback of ANN is that they do not produce a parametric function of the model in which case any given condition not previously observed in the historic performance data cannot be predicted or simulated.

Gorni [2003] take the view that over training by which the network captures quantitative relationships generated by noise from the data could also be a problem and suggests that comparing networks with different training times could be a solution. However this would also lead to increased computational time. Another difficulty using ANN is that the contribution of individual input variables in determining the output within the network is unclear. In addition, the relative significance of each input parameter is unclear.

According to Kishor *et al* [2010], 'ANN approach slows down the estimation if the numbers of parameters are large and also there exists a danger of local minima convergence'. Facao *et al* [2004] however argue that convergence is not an issue in ANNs and the results are obtained almost simultaneously, which makes trained ANN more advantageous over physical models

while [Holcomb *et al*., 2009; Dodier and Henze, 2004] view that 'overfitting' is the main limitation of ANN. This occurs when the model fits in noise that is part of the input data.

Regression-based models are important particularly when the relationship between two or more variables should be understood. In the case of solar collectors, regression-based approach is applied in testing standards to determine thermal performance measurement of systems. Experiments are performed to obtain a valid data set and multi linear regression (MLR) is then used to determine collector efficiency coefficients of a general model derived within the framework of white box model approach [Belessiotis and Mathioulakis, 2002]. The simple linear regression used to determine collector efficiency is of the form;

$$\eta = \beta_0 - \beta_1 \left[\frac{T_i - T_a}{G}\right] + \varepsilon \qquad (2.5)$$

where β_0 and β_1 are the parameters to be estimated and ε is regression the error term. The parameters β_0 and β_1 represent $F_r(\tau\alpha)_e$ and F_rU_l where F_r corresponds to the heat removal factor, U_l is the collector overall loss efficiency, $(\tau\alpha)_e$ is the transmittance - absorbance product, T_i is the inlet temperature and T_a is the ambient temperature G is the solar irradiance.

Pereira *et al* [2005] compared two solar collector models; an ANN and a multi linear regression model to calculate the efficiency of a thermosyphon solar collector. The ANN training network was used to predict collector outlet temperature using solar radiation, ambient temperature and collector inlet temperature as independent variables. The structure of the ANN used to represent the thermosyphon system was represented as equation 2.6, and contained 7 hidden neurons (2n+1) and one neuron in the output layer from which the output water temperature was obtained.

$$f(T_{in}, T_{amb}, G) \rightarrow ANN \rightarrow T_{out} \quad (2.6)$$

The collector outlet temperature T_{out} predicted from the ANN was used to calculate collector efficiency using equation 2.7 while linear regression calculated efficiency using the physically-based model given in equation 2.5.

$$\eta = \frac{\dot{m}C_p(T_{out}-T_{in})}{GA_{ext}} \quad (2.7)$$

In the equation above, η is the thermal efficiency; $\dot{m}$ is the mass flow rate, C_p the specific heat capacity of water, T_{in} the input water temperature, G, the solar irradiance and A_{ext}, the area of the collector. Of these two models, their results indicated that the both models were equally good in predicting the efficiency. Linear regression model had a lower average error of 2.10 compared to 2.27 obtained in ANN. The linear regression technique had a slighter higher maximum error of 10.5 compared to 8.94 for ANN and a slightly higher standard deviation of 2.08 compared to 2.04 for ANN.

MLR is a non-iterative fast matrix method using the least-square fit to minimize an objective merit function [Fischer *et al*, 2012]. A MLR model expresses the relationship between a predictor variable *y* to one or more independent variables X by applying a method of least squares. The basic structure of a MLR model with response variable y and predictors $X_{1\text{-}i}$ is depicted as

$$y = \alpha_0 + \alpha_1 X_1 + \alpha_2 X_2 + \alpha_3 X_3 \ldots\ldots\ldots \alpha_i X + \varepsilon_i \quad (2.8)$$

The response y has a linear relation to the *ith* regressor variables and the parameters $\alpha_0 - \alpha_4$ are regression coefficients representing the expected change in response *y* per unit change in Xi and ε is an error term.

A recent study by Kicsiny [2014] proposed a black-box model in which he performed direct empirical correlations between collector input and output variables. The model relates collector outlet temperature with appropriately chosen values of solar radiation, ambient temperature, collector inlet temperature and collector outlet temperature measured in the weather conditions encountered in Godollo, Hungary. The experiments were performed on an active solar water heater by distinguishing three cases; permanently switched off pump, permanently switched on and frequent switch ons' and off . Results of the model validation indicated that the MLR method predicts the outlet collector temperatures significantly more accurately than the physically – based model with an average absolute error of 4.6% while the physically-based model had an error of 7.8%.

2.6 Summary

A review of literature on the types of solar collectors and types of configurations has been presented. Literature revealed that for domestic use, flat plate collectors and evacuated tubes are typically used, with flat plate collectors being the most widely installed. This is due to their simple design low cost and low maintenance. A review of literature also revealed that performance of solar water heaters is dependent on ambient conditions, collector tilt and orientation, Inlet temperature, collector layout as well as collector design. With a single, optimized collector design, the collector outlet temperature is strongly determined by ambient conditions of the location notable solar radiation, ambient temperature and wind speed. Solar

radiation received determines the rate of energy absorbed while ambient temperature and wind speed affects the heat loss process on the collector surface. Lastly a comprehensive review of literature has been presented on modelling solar water collectors using white box methods, and black box method. Literature revealed that white box physically- based methods are widely employed while black box - MLR methods have been limited to use in testing standards. As previously mentioned in section 1.8, the main advantages of regression - based models over physically - based models are their relative simplicity and minimal input data requirement. Through an understanding the factors that affect solar collector performance the hypothesis in section 1.9 was developed to model the collector outlet temperature by applying MLR. This study considered solar radiation, ambient temperature, relative humidity and inlet temperature as independent variables in the MLR model. In order to predict the collector outlet temperature in different seasons, two models were developed in Chapter 3 for summer and winter, which represent the main seasons in the region.

CHAPTER THREE

RESEARCH METHODOLOGY

3.1 OVERVIEW OF METHODOLOGY

This chapter introduces the methods employed in the research. The research methodology consisted of two parts namely, experimentation and mathematical modelling. A detailed description of the system being tested, the experimental setup and the various sensors used in the monitoring is provided. The methodology adopted for the monitoring is also described. Lastly, details of the multi linear regression analysis and the validation tests are outlined.

3.2 EXPERIMENTAL SETUP

As mentioned in section 2.5.1, experimental research is an essential element when seeking to understand and validate the performance of any solar water heater technology. A complete setup was designed to monitor and collect data. The experimental apparatus was located at Fort Hare University Solar House in Alice, South Africa. Geographically it is located 32° south, 26° east, at an altitude of 494m. The house has two bedrooms, a single shower and a living area connected to the kitchen. Two flat plate collectors of dimension 2 x1m^2 were installed side by side in a North facing, parallel configuration and used as the subject of investigation in this research. Figure 3.1 shows a photograph of the solar collectors.

Figure 3.1: Solar House University of Fort Hare. Roof showing solar collector panels.

The system was of direct, thermosiphon configuration and had a 200litre capacity stainless steel storage tank installed in the roof attic. The roof design only permitted the solar collectors to be tilted at an angle of 15°, an angle lower than the desired latitude angle of 32°. Photovoltaic panels occupied most of the roof area and the middle section was used to install the solar collectors as shown in the figure. This low tilt angle optimizes the collectors for winter operation, when the sun is lower in the sky. Table 3.1 lists the detailed specifications of the solar water heating system components with the schematic diagram of the experimental setup showing the position of the sensors shown in figure 3.2. The storage tank was equipped with a 2kW auxiliary heater which was deactivated during the monitoring period. Sensors T_{ci} and T_{co} measured the cold water inlet and the hot water outlet of the collectors respectively while flow meter F measured the thermosyphon water flow rate.

Table 3.1: System components specifications.

Description	Value/Type
Gross area	$4m^2$
Aperture area	$3.96m^2$
Absorber material and coating	Copper, Black chrome
Glazing material	Low iron, toughened hail resistant glass
Number of riser tubes (each collector)	10
Riser tube material	Copper
Thermal insulation material	Fibre glass
Storage tank capacity	200l

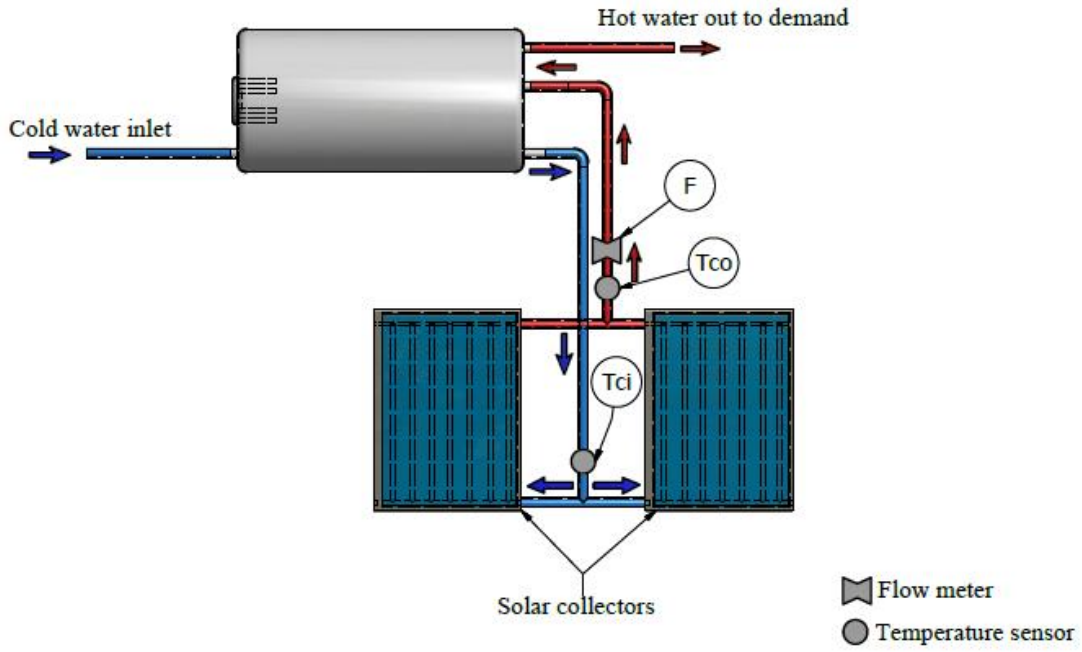

Figure 3.2: Schematic diagram of the solar water heater.

3.3 DATA COLLECTION SYSTEM

The data collection system was setup on the roof attic and comprised of a data logger, temperature sensors, a flow meter, an ambient temperature and relative humidity sensor as well as a pyranometer.

3.3.1 Temperature sensors

12Bit temperature sensors were used for measuring water temperature. The temperature sensors were made of a stainless steel waterproof sensor tip and weather proof polyvinylchloride housing and were installed on the surface of the pipe wire instead of directly in contact with the collector fluid. This prevents any obstruction of fluid flow and fluid leakage occurrences. The temperature sensors measured cold water entering both collectors and the temperature of water exiting both the collectors at the outlets.

3.3.2 Ambient temperature and relative humidity sensor

The ambient temperature and relative humidity in proximity to both collectors was measured using a Hobo temperature/RH smart sensor. This sensor was made of a single probe with a small circuit board containing the RH sensor and receptacle containing the temperature sensor. The RH sensor was protected by an ASA styrene polymer cap and a modified hydrophobic polyether sulfone fluid barrier membrane that allows vapour to penetrate while protecting the sensor from condensation [Onset Computer Corporation, 2007]. To protect the sensor from direct sunlight which can result in erroneous data readings, the sensors were covered with a

radiation shield. Two data channels from the single sensor measured both quantities simultaneously.

3.3.3 Pyranometer

A silicon pyronometer placed on the collectors' plane was used to measure global solar radiation incident on the collectors in W/m^2. The pyranometer was housed in anodized aluminium casing with acrylic diffuser. An array of silicon photodiodes on the inside of the casing measured power intensity of solar radiation when incident solar radiation lit the photodiodes.

3.3.4 Flow meter

Water flow measurements from the collectors into the storage tank were made with a Minol pulse flow meter. The measurements from the flow meter were measured as pulse signals at a rate of 3.785litres per pulse. A logging interval indicated the number of pulses that would have been outputted during the interval, which indicates the total volume of water that circulated from the collector to the tank during the interval.

3.3.4 Data logger

All measurements were logged in a Hobo U30 non remote sensing data logger. The Hobo U30 station logger monitors, records and saves all the data from the sensors according to the logging rate set by the user. Data was recorded every minute and sampled every second. After configuration the sensors automatically communicates configuration information to the logger without any need for calibration [Onset Computer Corporation, 2007]. Hoboware Pro software

installed in a personal computer allows communication between the logger and the personal computer for the purposes of retrieving and analysing data. The software also enables adjustments on sensor configuration to be performed. In addition, equipment malfunction can be spotted by analysing data on the software program. All sensors supported measurement averaging option; a function which enables data to be sampled at a faster rate than it is logged. The data is sampled as per set sampling rate and averaged according to the logging interval. The averaged value is recorded as the interval value. Measurement averaging is useful for reducing noise in the data and preventing aliasing, which can occur when the temperature varies more rapidly than it is being measured [Onset Computer Corporation, 2007]. Figure 3.3 shows the data logger and sensors installed while Figure 3.4 shows the data acquisition system on the roof attic.

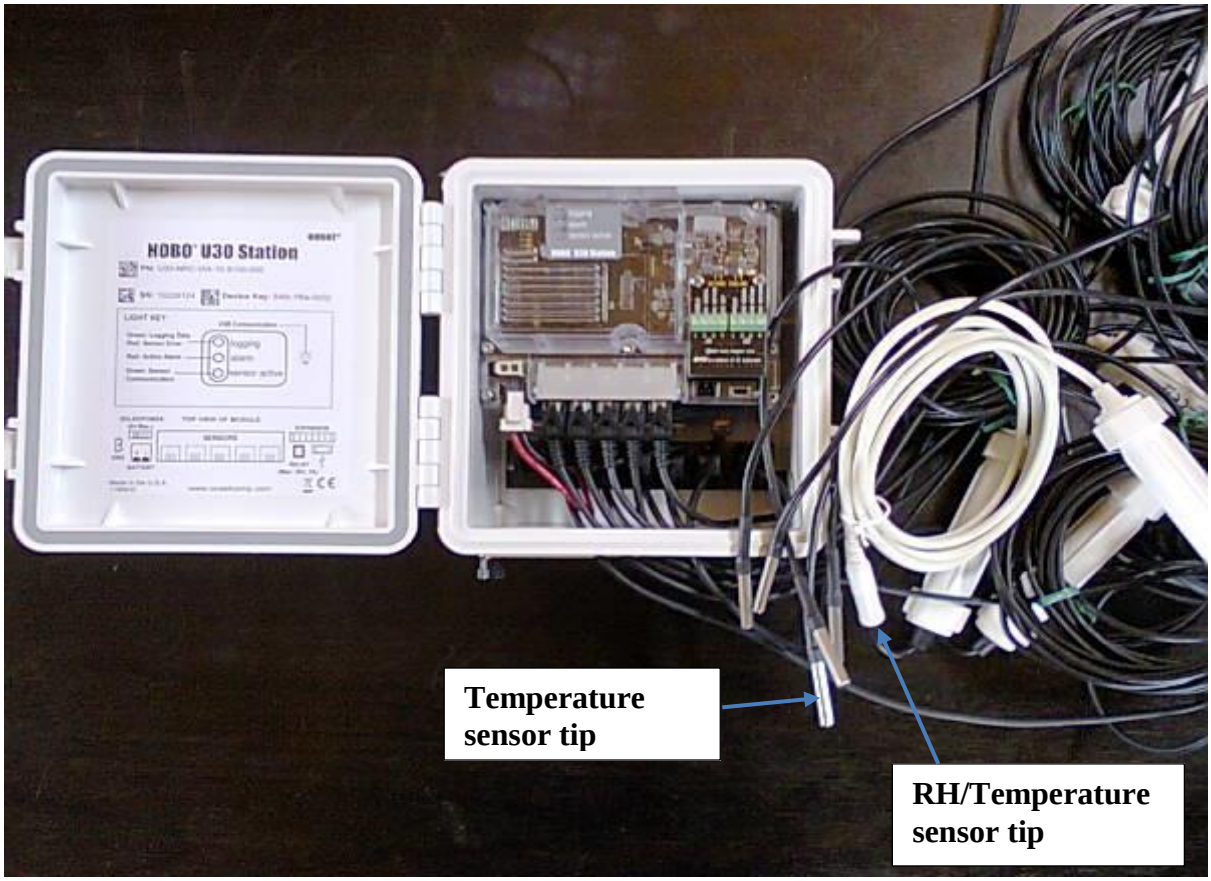

Figure 3.3: Hobo Data logger and sensors.

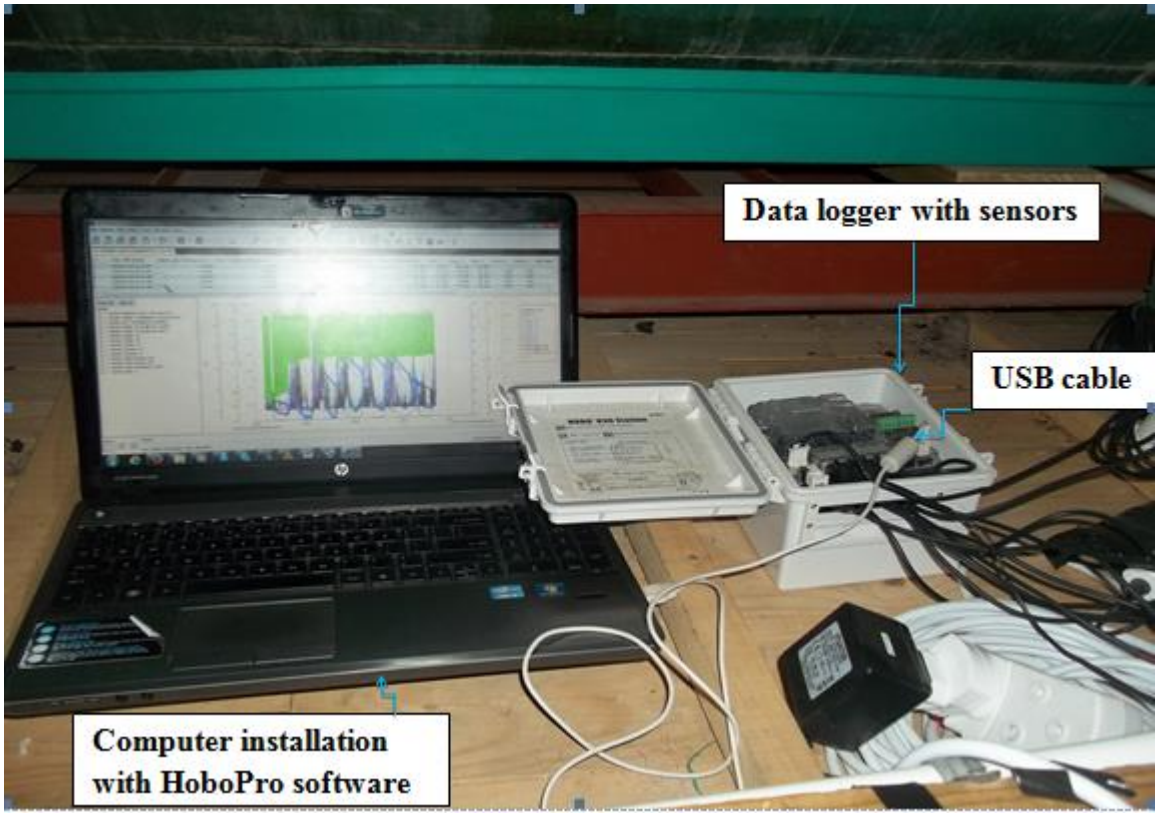

Figure 3.4: Data acquisition system on roof attic (sensor cables connected to data logger and USB cable connected to pc for data transfer).

A summary of the sensor specifications showing the sensor accuracies and measurement ranges is given in Table 3.2.

Table 3.2: Specifications of the measurement sensors.

Sensor	Type	Range	Accuracy
Water Temperature sensor	12 Bit TMB-M006	-40 -100°C	± 0.2 °C
Ambient temperature sensor	S-THB-M006	-40 - 75^{o}C	0.2^{o}C over 0 - 50^{o}C (± 0.2 m/s +3% of reading)
Relative humidity sensor	S-THB-M006	0-100% at -40 - 75^{o}C	+-2.5 from 10 - 90%
Pyranometer	Second Class S-LIB-M003	0 - 1280W/m^2	± 10W/m^2 or +- 5%
Flow meter	T-Minol-130 turbine flow meter	0.25Min- 22Max GPM	3.785litres/pulse

3.4 MODELLING APPROACH

The initial stage in MLR model development involves selecting output and input parameters necessary for describing the collector performance. MLR was proposed as opposed to single variate model due to their superiority over the single variate models. Various energy efficiency parameters such as water temperature at collector outlet, water temperature in storage tank, absorber plate mean temperature, overall heat loss coefficient; mass flow rate can be used as performance indices for solar water heaters [Chandavar *et al*, 2013]. The collector temperature rise is not usually estimated but its determination assists in the analysis of system performance

[Kishor *et al*, 2010]. This study uses the collector outlet temperature as the performance index to be determined. In addition, the prediction of collector outlet temperature enabled evaluation of the MLR model performance using direct correlations of the output, in this case the collector outlet temperature and a set of inputs.

Section 2.4 introduced variables that affect the performance of solar collectors. These factors can be classified as operating factors (which include interaction of weather parameters, collector inlet temperature and water withdraw pattern) and design factors (which include physical design of the system). It would be impossible to build a model comprising all factors affecting collector performance. Some are easily measurable such as climatic factors while some are unpredictable and difficult to model such as water withdraws. In view of this, the study considered weather parameters which have direct influence on the temperature rise of the water in the collector and include solar radiation and ambient temperature. Relative humidity which is a parameter not usually considered in collector model structures was also included as an input variable. The collector inlet temperature was factored in as an important operational factor influencing temperature rise and this is also highlighted by Rodríguez-Hidalgo *et al* [2011] who noted that actual meteorological data as well as collector inlet temperatures are required for predicting the collector outlet temperature. Mass flowrate varies with the level of insolation. It is therefore already accounted for in the changes of solar radiation during heat collection and was not added as a parameter that affects the collector outlet temperature.

Due to unavailability of readings caused by faulty sensor, wind speed was not used as an input variable. However it should be noted that collector output inherently includes wind speed and hence is indirectly taken into account. The solar collector system was therefore represented by a MLR equation in which the collector outlet temperature (T_{co}) was the predicted output and

solar radiation (I), ambient temperature (T_a), relative humidity (Rh) and collector inlet water temperature (T_{ci}) were the inputs to the model given as ;

$$T_{co}=\alpha_0+ \alpha_1 I+\alpha_2 T_a+ \alpha_3 Rh+\alpha_4 T_i \ + \ \varepsilon \qquad (3.1)$$

Equation 3.1 describes the average value of the collector outlet temperature for values of solar radiation, ambient temperature, relative humidity and inlet temperature in a time period while the error term ε describes the characteristics of the differences between individual values of collector outlet temperature and the expected values of outlet temperature.

The model coefficients together with their relative uncertainties are estimated by regression of the input and output experimental data. An important advantage of using this technique is the use of actual weather data encountered in the location. This gives more realistic results for estimation of collector performance as compared to other simulation software which rely on time series synthesizers such as Meteonorn, TMD, and TMY, whose data may not necessarily be similar to the actual environment in which a system operates [Kalogirou *et al*, 1999].

3.4.1 Monitoring and data collection period

The data was collected under actual operating conditions during summer and winter months. Extensive data is necessary to evaluate the day, week and monthly performance. This also enables evaluating the model precision for seasonal transient operation.

During a monitoring period, cold water was initially filled into the storage tank at the beginning of the experiment and the flat plate collectors left to heat the water continuously over several

days without any water draw off. The main experimental data were measured during the following periods;

Summer: 11 - 30 November 2013, 1 - 20 December 2013, 5 - 31 January 2013 and 1 - 28 February 2013.

Winter: 12 - 25 May 2014, 6 - 20 June 2014, 1 - 25 July 2014 and August 8 - 13 2014.

The data used for the parameter estimation during summer was taken from the period 23rd- 26th November 2013 while for the winter season it was taken from the 17th – 20th June 2014. These constitute days with varying solar radiation to take into account the variable nature of ambient conditions.

3.4.2 Data partitioning

Certain boundary conditions should be set before processing the data in order to consider only data points relevant for the analysis. In a solar collector, the outlet temperature rises gradually when there is sufficient excitation by solar radiation. The data was therefore partitioned according to the following criteria;

- When the difference between the collector inlet and collector was lower than 10^{o}C, and when the collector outlet temperature was less than 30^{o}C this data was excluded from the model. From observation of the dataset, there was no collector flow when temperatures were in this range and therefore no heat collection. Input parameter data in this range was also excluded in the analysis.

- Data averages between 4pm and 8am were excluded from the analysis as these corresponded to periods when collector was not in operation.

3.4.3 Data processing

Processing data before MLR can be applied is an essential step. The data was processed by averaging the instantaneous values over 10minute intervals. An important reason for averaging instantaneous values is to factor in time delay caused by collector thermal inertia effects. Averaging covers the variation introduced by time delay [Masic, 2009]. Weather variables are never constant; however the water temperature in the pipes does not change at the same rate as the changing variables. Heat is absorbed at the absorber surface and transferred to water through the absorber and pipe surface to the sensor tip. The time delay between weather changes and the corresponding temperature changes is determined by the thermal conductivity of the absorber and pipe surfaces. Its magnitude depends on this thermal conductivity and the magnitude of the outdoor temperature change. The high thermal conductivity of copper which is almost twice that of aluminum significantly reduces this time delay. Furthermore, the data is averaged to smooth the noise in the data due to random errors.

3.5 STATISTICAL ANALYSIS

When the data had been prepared statistical analysis was performed. OriginLab was chosen as the implementation language due to its simple data fitting and flexible graphic tools. OriginLab is an interactive graphic and data analysis program with an inbuilt statistical analysis tool. The criteria set in section 3.4.2 removed unwanted data from the complete data set and a separate

set of winter and summer values was obtained. The statistical procedures performed on the datasets are explained below.

3.5.1 Test of model assumptions

MLR models are built on the assumption that the independent variables have a linear relationship with the predictor variable and this judgement is made from the linearity tests results. X-Y scatter plot for each independent variable enable linearity to be determined. To judge linearity of independent variables a typical summer week (23 - 27January 2013) and winter week (6 - 10July 2014) was selected. This avoids the gathering of outliers in the collecting period. Results of the linearity tests are presented in the results chapter.

3.5.2 Parameter estimation

The aim of MLR is to estimate the coefficients of the hypothetical model. Parameter estimation methods of varying complexity are available such as ordinary least square method (OLS), weighted least square method (WLS used in MLR, dynamic parameter identification, artificial neural networks and generic optimization program (GOP). Fischer *et al* [2003] compared MLR based on least squares and a dynamic parameter identification method using the Levenberg Marquardt Algorithm and concluded that both methods lead to more or less the same results for the collector parameters. On the other hand, ANN and GOP are generally complex and time consuming. MLR using OLS was used as the methodology to determine the coefficients of the MLR model.

In all parameter estimation techniques the method to determine the coefficients is the same .A function L defined from the difference between the modelled and the experimentally determined values, is minimized with respect to the model coefficients as represented by equation 3.2 [Khaled, 2012].

$$L = \sum_{i=1}^{n}(T_{meas} - T_{mod}^{*})^2 \rightarrow \min \quad (3.2)$$

In this relation, T_{meas} is the measured value and T_{mod} * is the value calculated by the model (in this case temperature) and *n* is the number of observations. L is the sum of residual error squared for the measured data set used in model fitting [Khaled, 2012]. In OLS regression assumes constant variance and independence of errors. As previously stated in section 2.5.2, MLR uses a matrix method to minimize an objective function. The method is described below.

Equation 3.1 is derived from the general formula given as;

$$T_{meas}=\alpha_0+\alpha_1 x_{i,1}+\alpha_2 x_{i,2}+\dots\ \alpha_{p-1}x_{i,p-1}+\varepsilon_i \quad (3.3)$$

Where i refers to the ith unit. The α coefficients' estimates minimize the sum of squared errors in the data set. The formula that gives the predicted output value is therefore represented at;

$$\check{T}_i = \alpha_0 + \alpha_i x_{i,1} + \alpha_2 x_{i,2} \dots\dots\dots + \alpha_{p-1} x_{i,p-1} \quad (3.4)$$

In the above equation, the letter $x_{i,1}$ represents the estimate of the α_i coefficient; while $x_{i,2}$ is the sample estimate of α_2, and so on. The residual error term is calculated from the difference between an actual and predicted value of T. It is a random variable which is normally

distributed with mean zero and variance of ε same for all value of the predictor [Feelders, 2003] and is given by;

$$e_i = T_{mod} - \check{T}_{modi} \quad (3.5)$$

Ordinary least squares estimates of the α coefficients are calculated using the matrix formula;

$$a = \left(X^T X\right)^{-1} X^T y \quad (3.6)$$

Equation 3.6 is a minimization of the sum of squared errors given by;

$$\| e \|^2 = e^T e = (Y - \tilde{Y})^T (Y - \tilde{Y}) = Y - Xa^T (Y - Xa) \quad (3.7)$$

where $a = \left(a_0 a_1 \ldots . a_{p-1}\right)^T$ (3.8)

$$Y = \begin{pmatrix} Y_1 \\ Y_2 \\ Y_3 \\ Y_4 \end{pmatrix} \text{ (3.9)}, \quad X = \begin{pmatrix} 1 & X_{1,1} & X_{1,P-1} \\ : & X_{2,1} & X_{2,P-1} \\ : & : & : \\ 1 & X_{n,1} & X_{N-1} \end{pmatrix} \text{ (3.10)}; \quad \alpha = \begin{pmatrix} \alpha_0 \\ : \\ : \\ \alpha_{P-1} \end{pmatrix}; \quad \text{(3.11)}$$

and

$$\varepsilon = \begin{pmatrix} \epsilon_1 \\ : \\ : \\ \epsilon_I \end{pmatrix} \quad (3.12)$$

Matrix operations described by the above equations are used by spreadsheet programs such as OriginLab and Minitab to determine estimates of the coefficients.

3.5.3 Model validation

Validation assesses the reliability of the regression and its ability to predict the output. It typically involves the analysis of a model by comparison with a different set of experimental data used with the model. The data set used for model validation was taken from consecutive days taken over the eight month monitoring period. A total of 40 days were used for the validation. The data for the model validation was taken from the periods;

Summer: 11 – 25 November 2013, 6 – 10 December 2013, 22 - 26 January 2014, 13 - 17 February.

Winter: 18 - 22 May 2014, 12 - 16 June 2014, 7 - 11 July 2014 and 8 - 12 August 2013.

3.5.4 Coefficient of determination (R^2) and standard error (s_e)

Results of MLR produce the coefficient of determination (R^2) and standard errors (s_e) of the model. R^2 is the main criteria for evaluating the goodness of fit in linear regression calculations and selecting a proper linear regression model. It gives the extent to which the dependent variable is explained by the model and is given by equation 3.13. A value closer to unity indicates that the data are well explained by the model. A more appropriate measure for comparing models is the adjusted R^2. It is the coefficient R^2, adjusted for the number of independent variables and number of data points which are termed 'degrees of freedom'. The standard error estimate given by equation 3.14, measures the variability of the modelled values around the regression line. The larger the standard error estimate, the greater the scatter of the points around the regression line [Das *et al*, 2006].

$$R^2 = \frac{\sum(y_i^* - y_{ave})^2}{\sum(y_i - y_{ave})^2} \quad (3.13)$$

$$s_e = \sqrt{\frac{\sum(\eta - \acute{\eta})^2}{n-2}} \quad (3.14)$$

Where y_i^* is the computed value, y_{ave} is the average value, y_i is the measured value and n is the sample size.

3.5.5 Performance function- Percentage mean absolute error (PMAE)

The modeled and measured temperature values can be used to determine the capability of the developed model to predict actual measured experiment values. The performance function, percentage mean absolute error (PMAE), was used for this purpose. PMAE evaluates the percentage mean of the sum of errors of individual observations [Ayompe *et al*, 2011]. A negative value of PMAE indicates a net underestimation while a positive value indicates a net overestimation of the modeled values. PMAE is computed by the equation 15 below;

$$\text{PMAE} = \frac{100}{N}\sum_{i=1}^{N}\frac{y - y^*}{y^*} \quad (3.15)$$

Where N is the total number of observations, y_i and y_i* are the i^{th} measured and modeled values respectively.

CHAPTER FOUR

RESULTS AND DISCUSSION

4.1 INTRODUCTION

This chapter presents the experimental monitoring and model analysis results for the $4m^2$ flat plate collector system, operating under weather conditions encountered in Alice, South Africa. The first section presents results of the initial statistical analysis involving ascertaining linearity in the variables. The second section compares the collector performance in the different months by analysing the trend in collector inlet and outlet temperatures with the weather conditions. Lastly, the results of the multi linear regression are presented. The residual plots as well as the comparisons of the measured and modelled collector temperatures for average month week and average week day are also presented. Lastly, the contribution of each independent variable in determining collector outlet temperature is shown.

4.2 RESULTS OF STATISTICAL ANALYSIS: X - Y PLOTS

As previously mentioned in section 3.5, scatter diagrams indicate whether a linear relationship exists between an independent variable and an output. Figures 4.1 – 4.4 and figures 4.5 – 4.8 show the X-Y scatter plots for typical summer week from 23 - 27January 2013 and typical winter week from 6 – 10July 2014. As seen in the plots, the trends demonstrate that there was linearity in the dataset for all the independent variable therefore linear regression was a valid approach.

Summer X-Y scatter plots

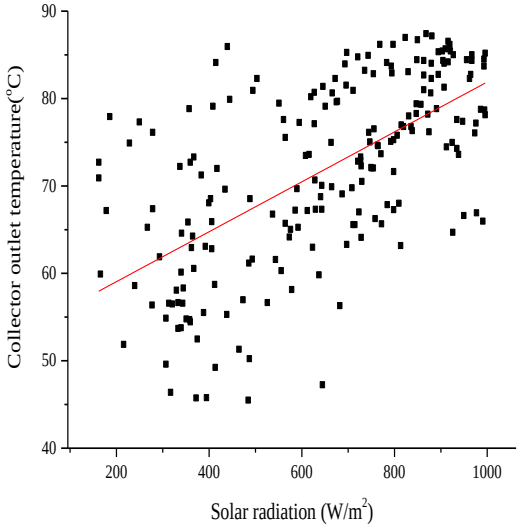

Figure 4.1: Solar radiation versus T_{co}

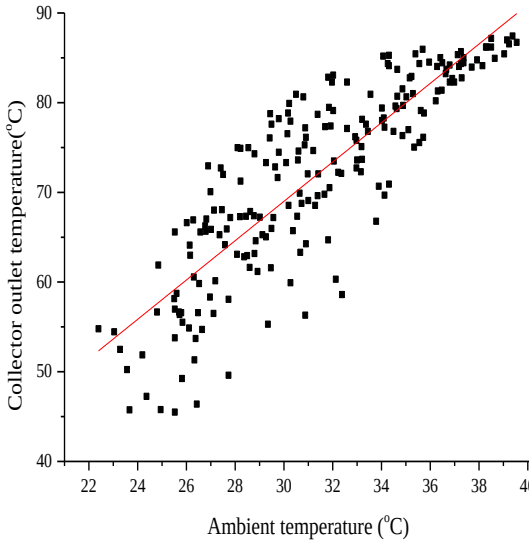

Figure 4.2: Ambient temperature versus T_{co}

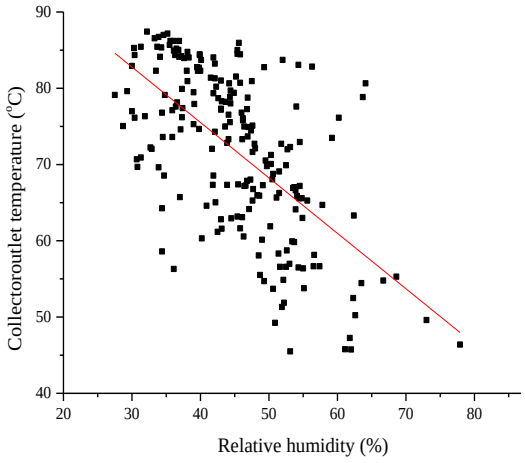

Figure 4.3: Relative humidity versus T_{co}

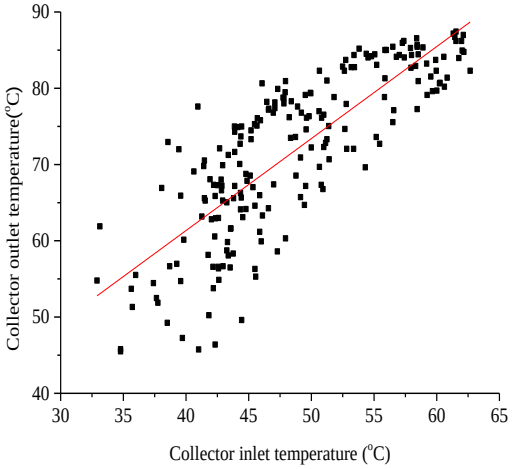

Figure 4.4: Collector inlet temperature versus T_{co}

Winter X-Y Scatter plots

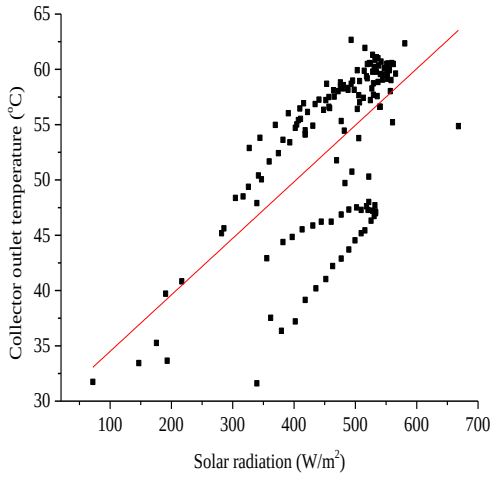

Figure 4.5: Solar radiation versus T_{co}

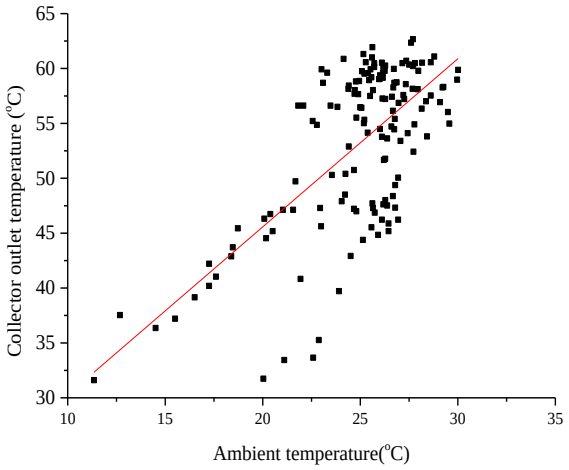

Figure 4.6: Ambient temperature versus T_{co}

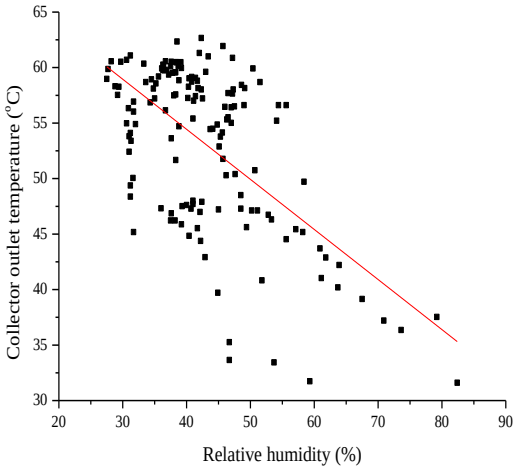

Figure 4.7: Relative humidity versus $T_{co.}$

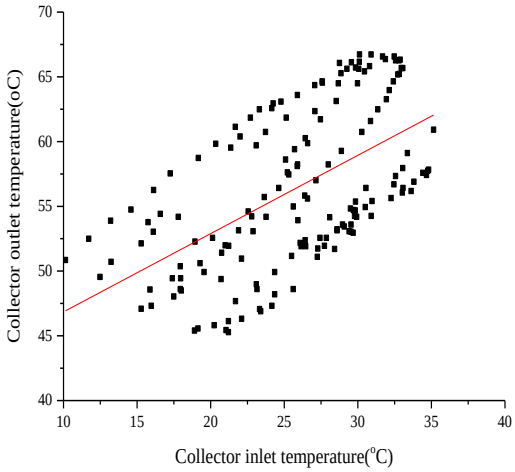

Figure 4.8: Collector inlet versus T_{co}

As expected ambient temperature, solar radiation and collector inlet temperature showed a positive correlation with the outlet temperature, indicating that when the individual variables increase, the water temperature increases. However, a negative correlation was observed between relative humidity and collector outlet temperature. It can also be noted in the plots that in the summer, the data points were more closely clustered along the line of best fit when there is generally higher impact of the independent variables on the collector outlet temperature, while in winter there were more dispersed. The formal correlations are presented in table 4.1.

Solar radiation and ambient temperature display a stronger correlation with water temperature in both seasons. The inter-correlations between independent variables were generally low, (below 5) which indicates that multicollinearity did not exist. Multicollinearity occurs when there are high correlations between two or more independent variables. This results in coefficients that are hard to interpret because they become sensitive to minor model changes.

Table 4.1: Correlations: T_{co}, Ta, Rh, T_{ci}, I (Summer).

	T_{co}	T_a	Rh	Tci
Ta	0.719			
	0.000			
Rh	-0.442	-0.433		
	0.000	0.000		
T_{ci}	-0.684	-0.314	-0.107	
	0.000	0.000	0.000	
I	0.889	0.282	-0.309	-0.135
	0.000	0.000	0.000	0.000

Table 4.2: Correlations: T_{co}, T_a, Rh, T_{ci}, I (Winter).

	T_{co}	T_a	Rh	T_{ci}
Ta	0.479			
	0.000			
Rh	-0.572	-0.413		
	0.000	0.000		
Tci	-0.584	-0.214	-0.107	
	0.000	0.000	0.000	
I	0.789	0.172	-0.109	-0.526
	0.000	0.000	0.000	0.000

4.3 ENVIRONMENTAL CONDITIONS AND COLLECTOR TEMPERATURES

Table 4.3 shows the average month day solar radiation, maximum daily ambient temperature as well as the minimum and maximum day relative humidity over the eight month period. The corresponding monthly average and daily maximum collector outlet (T_{co}) and inlet

temperatures (T_{ci}) are also shown in Table 4.4. Due to the earths tilt to the plane of orbit around the sun, average solar irradiance varies over the earths' surface during the course of the year. In November, December, January, and February, the sun is tilted towards the Southern hemisphere causing higher average solar radiation and ambient temperature during these months while in May, June, July and August the earth is tilted away from the Southern hemisphere causing lower average solar radiation and ambient temperature as shown in Table 4.3.

During the summer season the collector outlet temperatures were generally higher, ranging from an average maximum of 40.3°C in January and an average of 13.1°C in June. The maximum day collector outlet temperature ranged from a low of 64.2°C recorded in June to a high of 87.2°C recorded in January. This performance is comparable to the system monitored by Sako *et al* [2007] who obtained a maximum collector outlet temperature of ~85^{o}C at a maximum solar radiation just below 1000W/m^2 for a system installed in Yamoussoukro, Cote d'Voire and Salas *et al* [2012] who also obtained a maximum collector outlet temperature of 85^{o}C at maximum solar radiation of 1200W/m^2 for a system monitored in Aquirepa Peru. The high system performance in summer is due to high radiation intensity and its rate of absorptions as compared to winter season which has lower absorption rate [Aasi and Ajayi, 2012]. The highest maximum collector inlet temperature was 63.3°C in January while the lowest maximum was 40.1°C in June. Lower collector temperatures encountered particularly during the winter season reduce the monthly average collector outlet temperatures.

Table 4.3: Average daily solar radiation, maximum daily ambient temperature and average maximum and minimum relative humidity.

Month	**Solar radiation (kW/m^2)**	**Ambient temperature (°C)**	**Relative humidity (%)**	
	Ave/d	**Max/d**	**Ave/Max**	**Min**
November	6.5	37.0	94.4	62.4
December	7.2	37.2	95.2	63.7
January	7.6	43.8	96.7	67.2
February	6.9	35.2	93.9	60.3
May	6.5	32.6	93.5	52.3
June	5.7	22.6	89.5	44.7
July	6.1	26.4	88.9	38.4
August	6.8	32.6	90.6	49.4

Table 4.4: Monthly average and maximum daily collector outlet and inlet temperatures.

Month	**T_{co} (max)**	**T_{co} (ave)**	**T_{ci} (max)**	**T_{ci} (ave)**
November	84.1.	35.0	61.4	20.6
December	78.1	30.7	59.1	21.9
January	87.2	40.3	63.3	27.7
February	75.5	28.2	55.7	23.2
May	68.6	23.7	46.8	18.4
June	64.2	13.1	40.1	18.5
July	69.7	15.3	47.1	21.9
August	70.1	19.4	44.9	29.4

4.4 COLLECTOR MODEL ANALYSIS

4.4.1 Parameter Estimation

Multiple linear regression (MLR) was applied to find the coefficients of the collector models defined in equation 3.1, fitted to four days each in the month of November 2013 and June 2014. The estimated parameters are listed in Table 4.5. In parenthesis to the right of the estimates are the standard error deviations.

Table 4.5: Parameter estimates from MLR.

Coefficient	**Unit**	**Summer**	**Winter**
α_0	^oC	16.987 (1.15)	1.167 (2.064)
α_1	$^oC.m^2/W$	0.0279 ($8.2x10^{-4}$)	0.0443 ($1.13x10^{-3}$)
α_2	-	0.207 ($3.47x10^{-2}$)	0.669 ($6.22\ x10^{-2}$)
α_3	^oC	-0.015 ($1.08\ x10^{-2}$)	0.056 ($4.72x10^{-2}$)
α_4	-	0.654 ($2.3x10^{-2}$)	0.3300 ($1.39x10^{-2}$)
Adjusted R^2	-	0.98	0.93

$$T_{co}(\text{summer}) = 16.987 + 0.0279I + 0.207T_a - 0.015Rh + 0.654T_i \quad (4.1)$$

$$T_{co}(\text{winter}) = 1.167 + 0.0443I + 0.669T_a + 0.056Rh + 0.330T_i \quad (4.2)$$

The results obtained were very encouraging. The adjusted R^2 values were 0.98 and 0.93 for the summer and winter models respectively. These values are close to unity and show good model fit. The high values of adjusted R^2 from the four variable models also indicate that inclusion of these variables in the models is necessary for good model development. The very low standard

deviations indicate low dispersion of points around the regression line which also shows good estimation.

Ambient conditions during summer months are generally higher and this allows higher collector temperatures to be attained in the summer season. It can also be seen from the lower standard errors for the parameters having the same positive effect in T_{co} (α_1, α_2, and α_4) that the summer model estimation has lower uncertainty compared to winter. The high adjusted R^2 statistics demonstrate that the collector outlet temperature is strongly influenced by the four predictors therefore equations 4.1 and 4.2 can be applied to predict the collector outlet temperatures given a set of input variables.

The coefficients give the change in the collector output temperature for a unit change in the independent variable. The positive sign for the solar radiation (I), ambient temperature (Ta), and collector (T_{ci}) indicate that the collector outlet temperature will increase by a factor equal to the estimated coefficient. However the estimates for relative humidity show a different effect in the two seasons. The results show that a unit increase results in a decrease in the collector outlet temperature in summer. This can be attributed to the higher direct radiation in the summer season. Typically, humidity is higher in the mornings when solar radiation is low and decreases as direct radiation increases and collector outlet temperature increases. In winter there is more cloud cover and generally consistently high humidity throughout the day.

Figures 4.9 and 4.10 depict the measured temperature values against the modelled values.

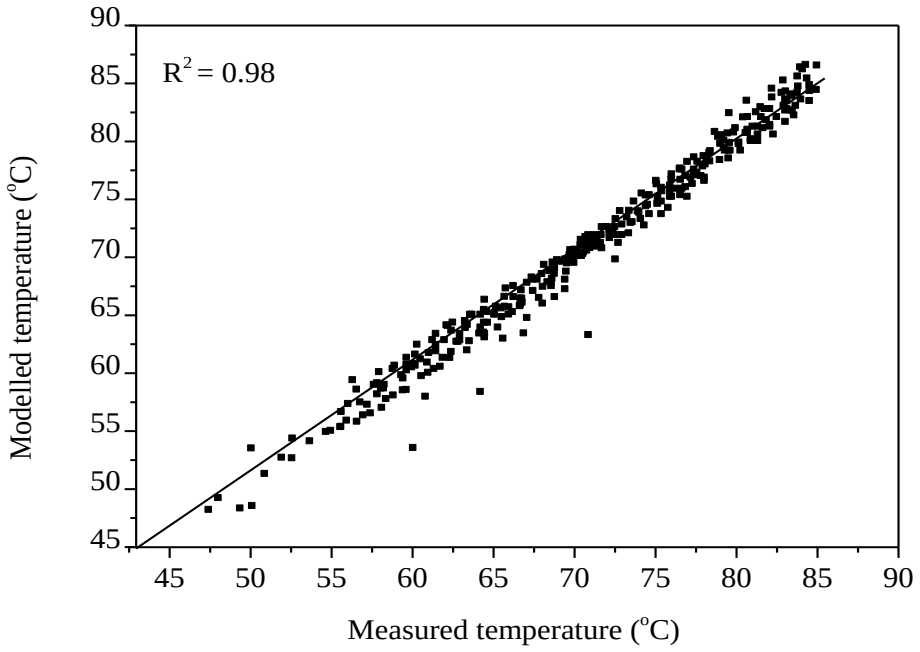

Figure 4.9: Correlation between modelled and measured outlet temperature: summer.

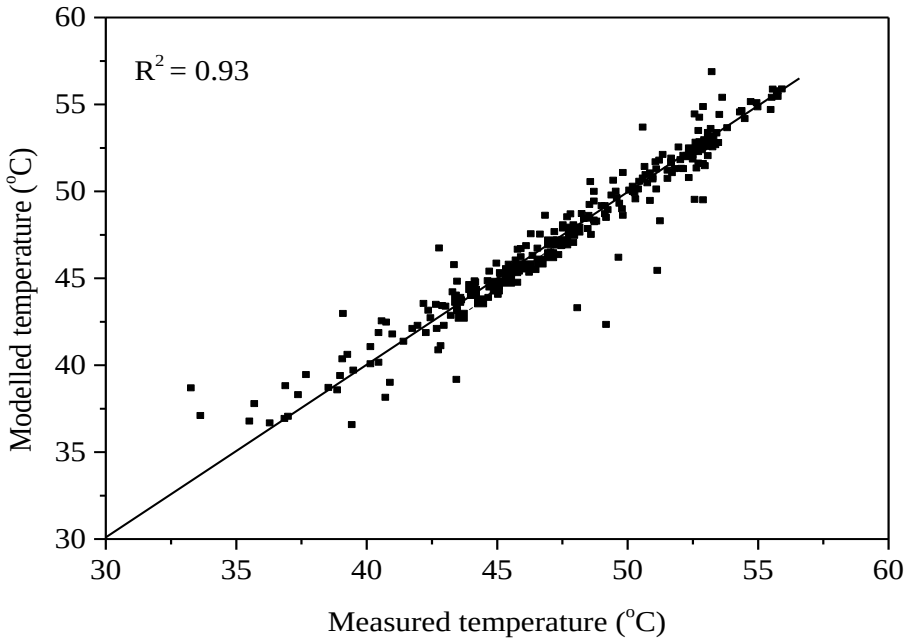

Figure 4.10: Correlation between modelled and measured outlet temperature: winter.

The figures confirm the high correlation coefficients obtained from the parameter estimation. A line with all points lying along the line of best fit would indicate a perfect fit. A great percentage of the data points scatter closely along the line of best fit in both graphs, tighter for the summer model compared to the winter model. The results indicate however that there was slightly greater variance with the lower temperatures in both the summer and winter estimation plot. This could be attributed to lower flow rates when the system initially heats up and is in unsteady state.

Representing the measured (Tmeas) and modelled (Tmod) collector outlet temperature values on the same graph can easily reveal discrepancies. This comparison is shown in figures 4.12 and 4.14. The ambient conditions are shown in figures 4.11 and 4.13.

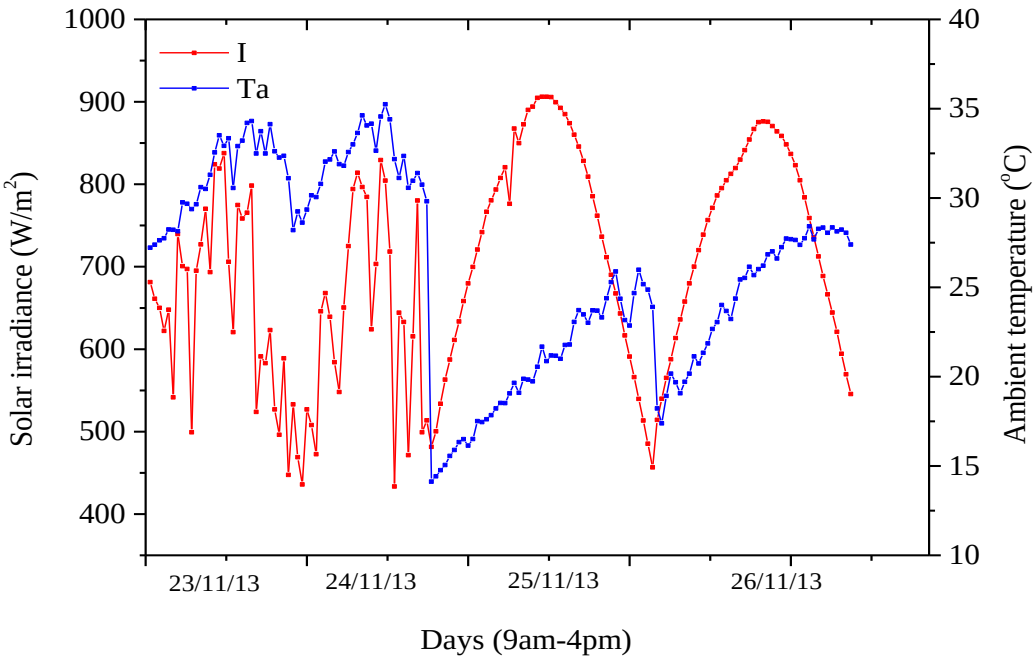

Figure 4.11: Solar radiation and ambient temperature for summer parameter estimation.

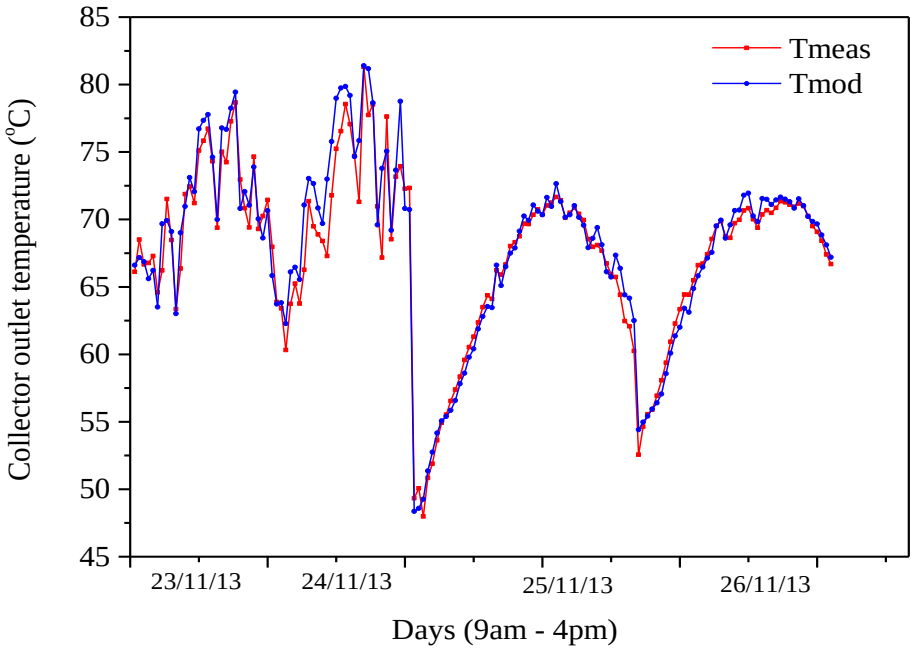

Figure 4.12: Measured and modeled temperature summer parameter estimation.

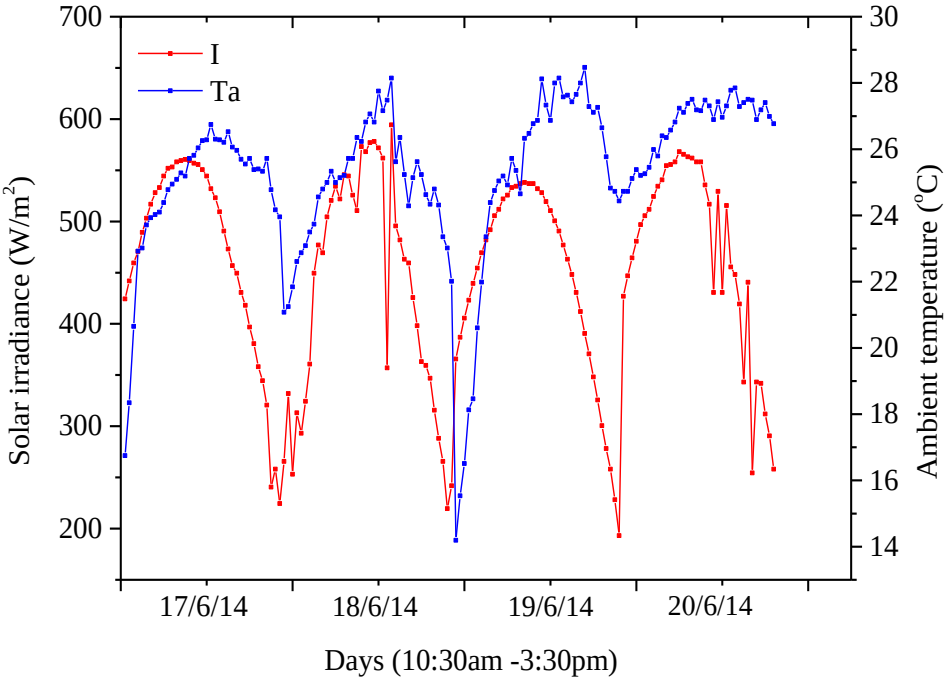

Figure 4.13: Solar radiation and ambient temperature for winter parameter estimation.

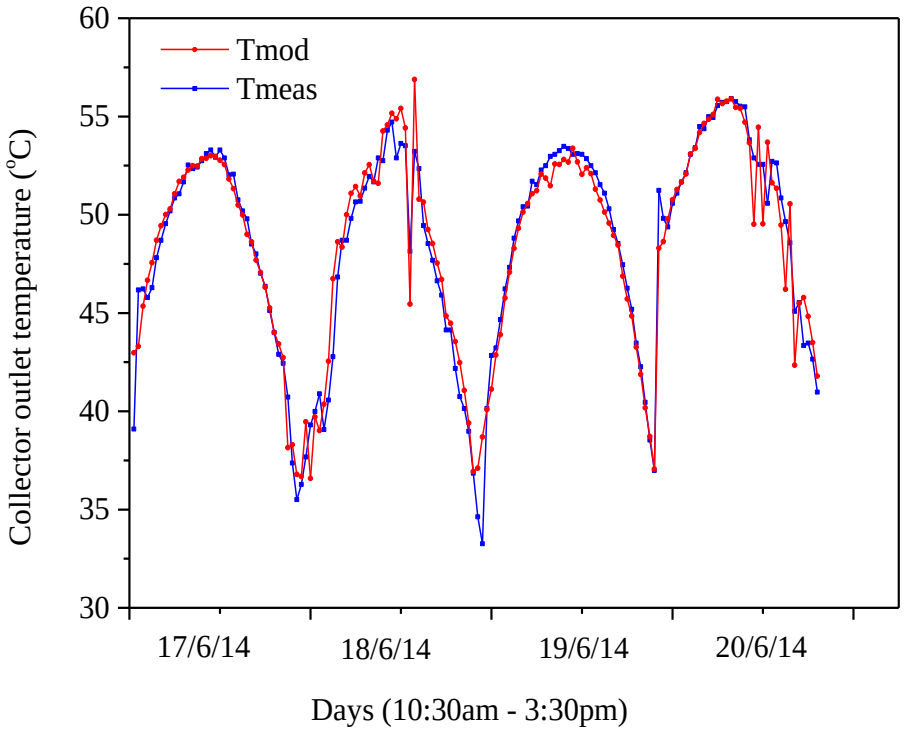

Figure 4.14: Measured and modeled temperature for winter parameter estimation.

It can be observed that agreement between measured and modelled temperatures is generally good in both seasons with very small variance. The models follow the same pattern as the measured temperature. Closer observation of figures 4.13 and 4.14 it can be noticed that on the second day, a sudden drop in solar radiation resulted in variance in the measured temperature and the model overestimated the outlet temperatures. This is also depicted in the residual error scatter plots illustrated in figures 4.15 and 4.16 were a clear large temperature difference of ~7^{o}C is seen. Residuals are important in indicating the appropriateness of the model used to fit the data [Catalina *et al*, 2013].

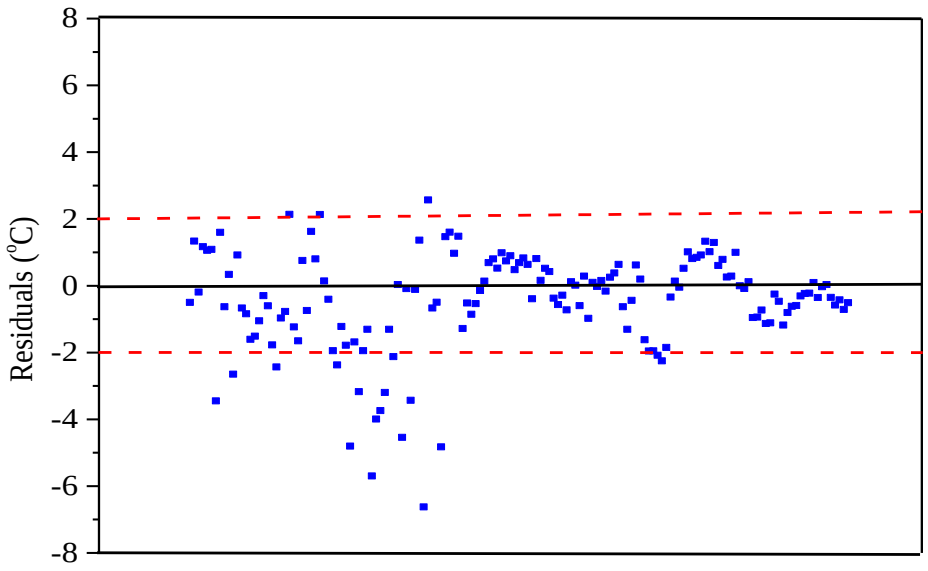

Figure 4.15: Winter model residual temperatures.

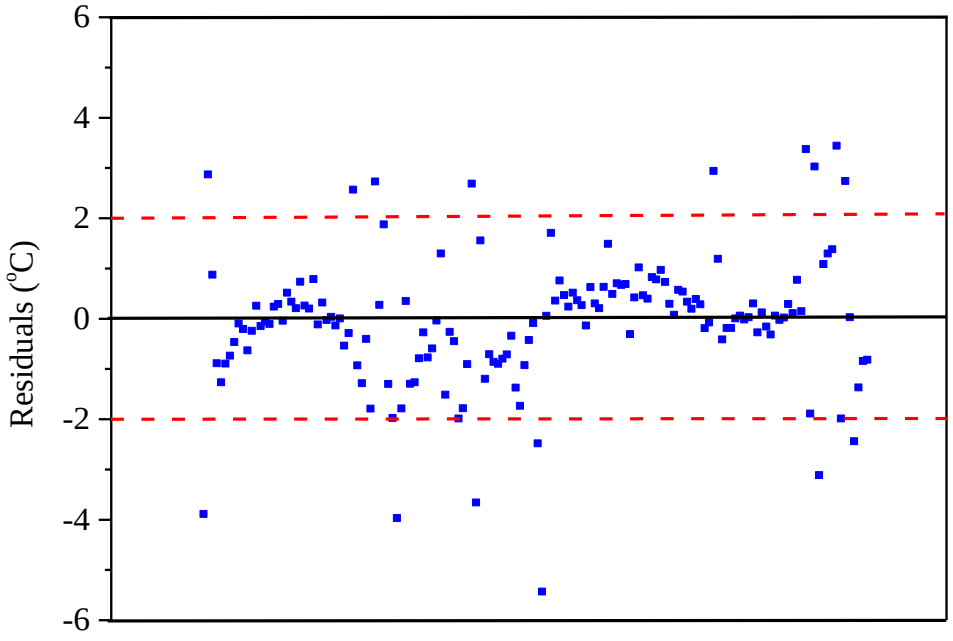

Figure 4.16: Summer model residual temperatures.

An appropriate residual plot should ideally be a horizontal random band. The graphs show that the residual distribution shows no noticeable pattern. This result indicates that the model prediction has no significant drift which would otherwise generate an overall drift in the prediction of the collector temperatures. It can also be observed that the range of errors was within +/- 8^{o}C for both models. In fact, a great percentage of the residuals lie within an error of +/-2^{o}C. This implies that the average percentage error is within 2% which is very satisfactory.

4.4.2 Model validation

This sections shows model validations by analysing 'typical weeks' and 'typical days' in different months of each season. The error values and plots of the measured and modelled collector outlet temperature are presented. Five days in each month during the monitoring period were selected to show the typical range of errors obtained. A summary of the daily minimum, maximum and absolute average error for the month days are shown in tables 4.6 and 4.8 respectively. It can be seen that in all expect on one day (12 August), the errors lie within that +/-10% range. According to [Saffaripour *et al*, 2013] errors that lie within a range of +/-10 % are acceptable in engineering applications. For the summer validation, errors range from 0.85 – 8.37% whereas for winter validation they range from 1.38 – 12.9%. It is can also be noted that the errors for the summer model are generally lower than that in winter. The greater precision in summer compared to winter can be explained by the more steady and higher solar radiation in this season. A PMAE of 4.07 and 6.2 was obtained for summer and winter respectively which is very satisfactory.

Table 4.6: Summary of daily PMAE for the collector outlet temperature (summer model).

Month	**Day**	**PMAE (%)**
November	11	2.72
	12	2.49
	13	7.97
	24	1.03
	25	1.97
December	6	6.55
	7	6.53
	8	5.94
	9	1.16
	10	1.58
January	23	1.34
	24	6.40
	25	7.13
	26	6.92
	27	8.37
February	13	1.83
	15	5.94
	16	0.85
	17	2.96
	18	1.71
Average PMAE	**4.07**	

Table 4.7: Summary of daily PMAE for the collector outlet temperature (winter model).

Month	**Day**	**PMAE (%)**
May	15	6.67
	16	7.60
	17	6.57
	18	1.87
	19	8.67
June	12	1.38
	13	8.95
	14	2.98
	15	4.63
	16	5.45
July	6	4.50
	7	8.03
	8	6.70
	9	4.87
	10	8.39
August	8	7.12
	9	5.99
	10	6.10
	11	4.55
	12	12.9
Average PMAE	**6.2**	

4.4.3 Typical week

One week in each season with typical weather conditions prevalent in South Africa was selected to show a more representative view of the collectors' long term performance and the capability of the model to predict the trend in the collector outlet temperatures. The profiles are shown for the collector performance between 9am and 4pm. Figure 4.17 and 4.20 show the comparison between the measured (Tmeas) and modelled (Tmod) collector outlet temperature during the week from 6 to 12 December 2013 and from 7 to 13 July 2014 while the figures 4.19 and 4.22 show the corresponding trend in solar radiation and ambient temperature.

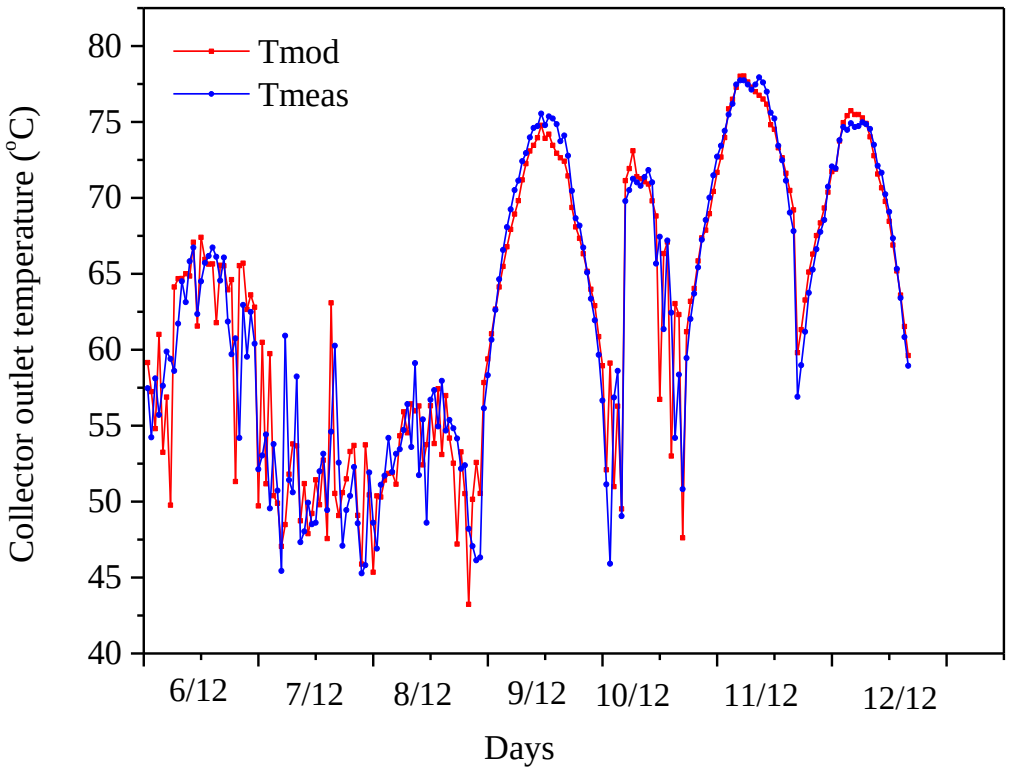

Figure 4.17: Measured and modelled temperature 6 – 12/12/13.

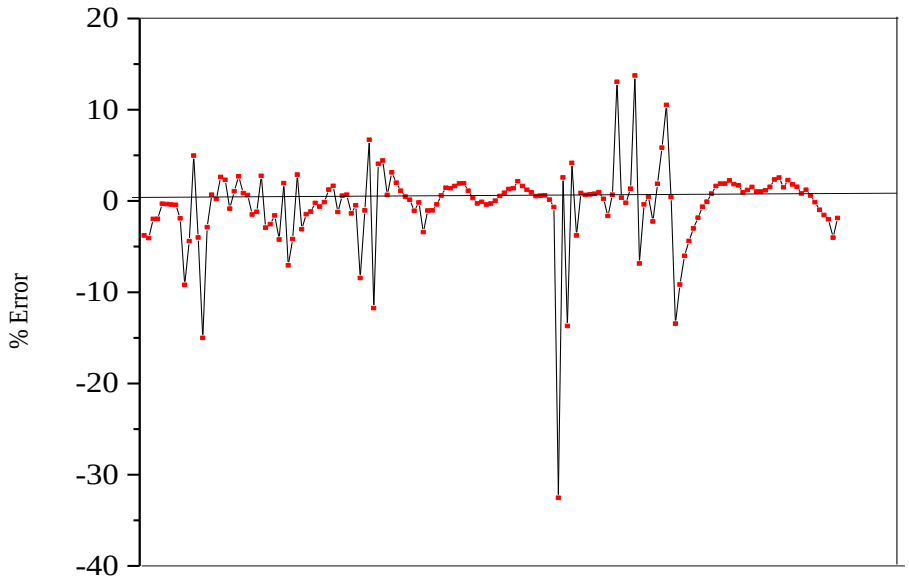

Figure 4.18 Residual percentage error of modelled temperatures 6 -12/12/13.

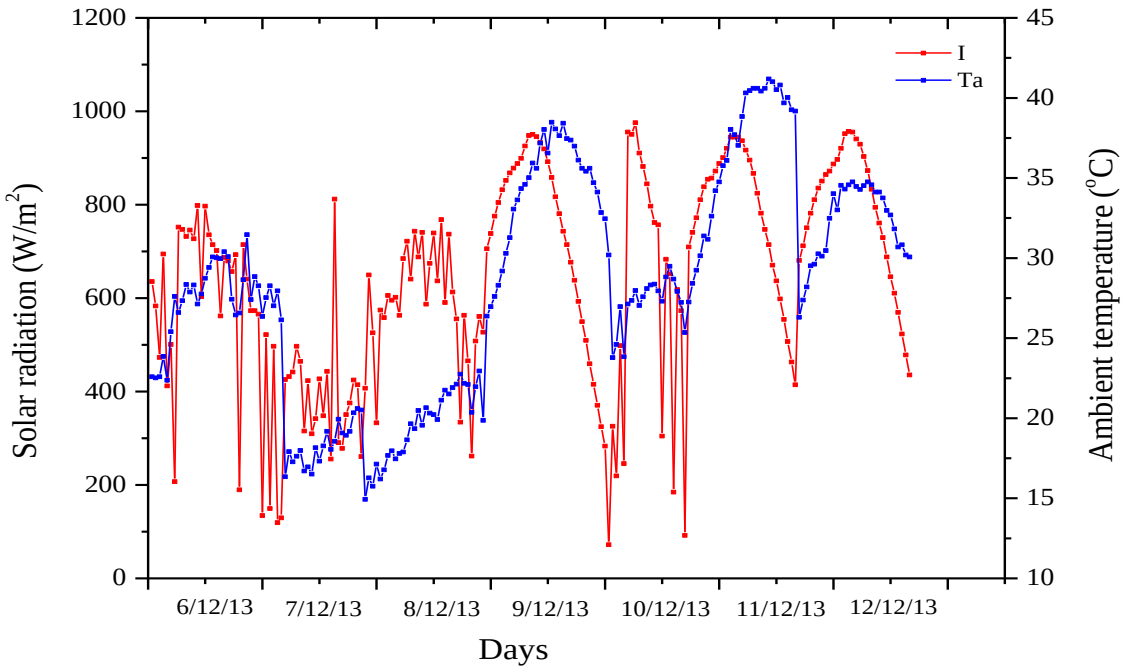

Figure 4.19: Solar radiation and ambient temperature 6 – 12/12/13.

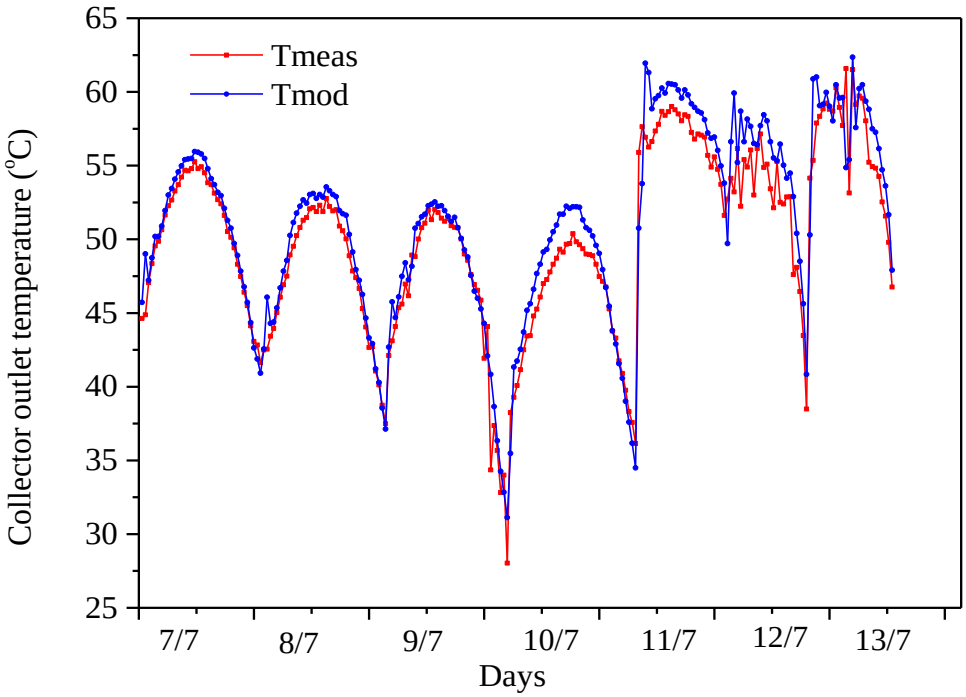

Figure 4.20: Measured and modelled temperature 7 – 13/07/14.

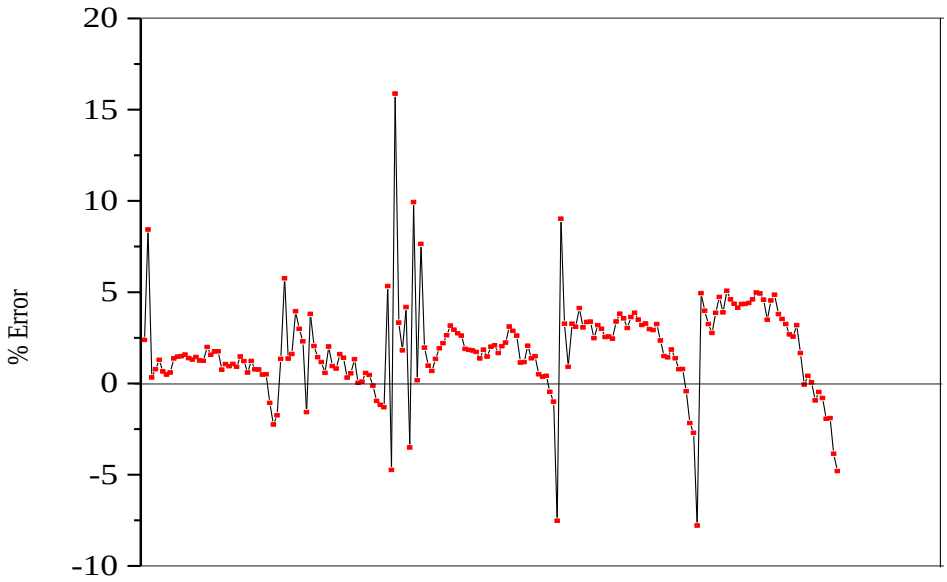

Figure 4.21 Residual percentage error of modelled temperature 7-13/07/14.

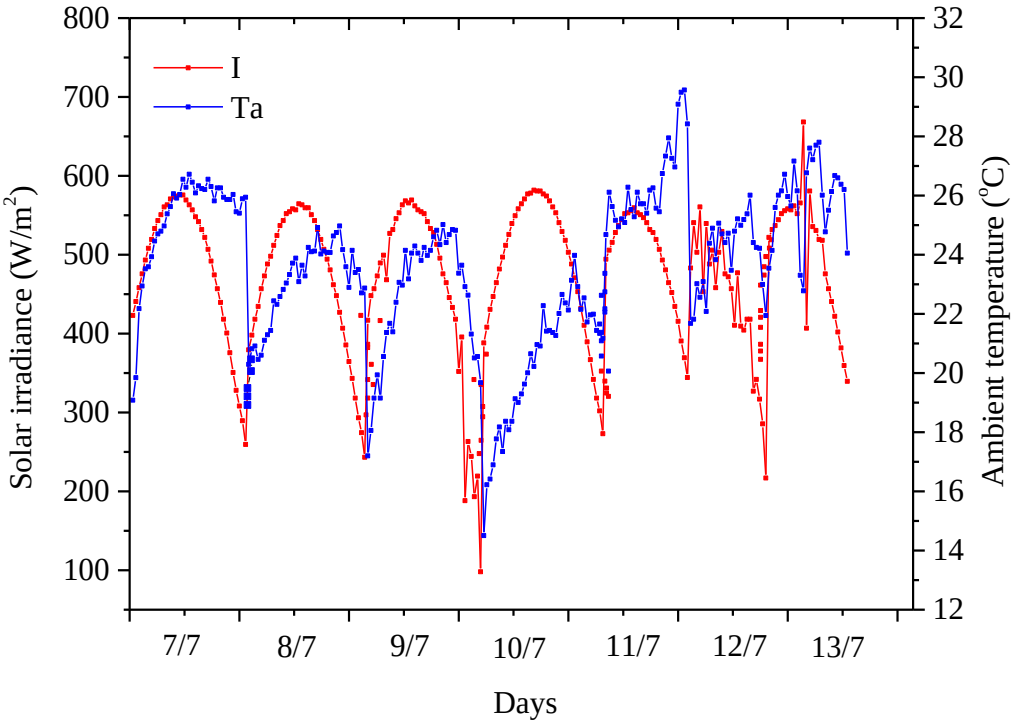

Figure 4.22: Solar radiation and ambient temperature 7 – 13/07/14.

As evidenced in figure 4.19 and 4.22 the two weeks were characterised by variable weather conditions and these were selected to show the models' performance in different ambient conditions. It can be seen from figures 4.17 and 4.20 that the models generally follow the same trend as the measured values. As observed in the parameter estimation, during days of intermittent cloud cover (12 and 13 July; 6 and 7 December) the models overestimate the outlet temperatures. The trend in the residual error of the modelled values ((Tmeas-Tmod)/Tmeas) % is illustrated in figures 4.18 and 4.21. Again it can be observed that the errors were mostly within +/-10%. It should be pointed out that water temperature measurements were made on the surface of the water pipes and not directly on the water and this is also a source of model uncertainty and results in errors.

4.4.4 Typical week days

To show a detailed analysis of the models and evaluate hourly behaviour of the collector models, two days in each season characterised by clear sky and intermittent cloud cover are presented. A clear sky day is a day without cloud cover and has a smooth intensity curve [Quaschning, 2005].

4.4.4.1 Summer days

The plots in figures 4.24 and 4.26 show the comparison between modelled and measured hourly averages of the collector outlet temperature taken from measurements from two summer days: 24/11/13 (clear sky) and 26/01/14 (heavy intermittent cloud cover). The incident solar radiation and ambient temperature on these two days is presented in Figures 4.23 and 4.25. The maximum solar radiation on these was 937W/m^2 and 1151W/m^2 while the maximum ambient temperatures were 34.3°C and 36.2°C respectively. It is seen that the collector outlet temperature increases significantly and is highest around midday when incident solar rays are perpendicular to collector surfaces. With single orientation of flat plate solar collector, the best performance occurs when the solar radiations are perpendicular to the collector surfaces, for this case at around noon [Bakari *et al,* 2014]. After midday the temperature reduces due to decline in solar radiation. The influence of solar radiation on collector temperatures is depicted from Figure 4.23 and 4.24 where high variations in solar radiation cause fluctuations in collector outlet temperatures.

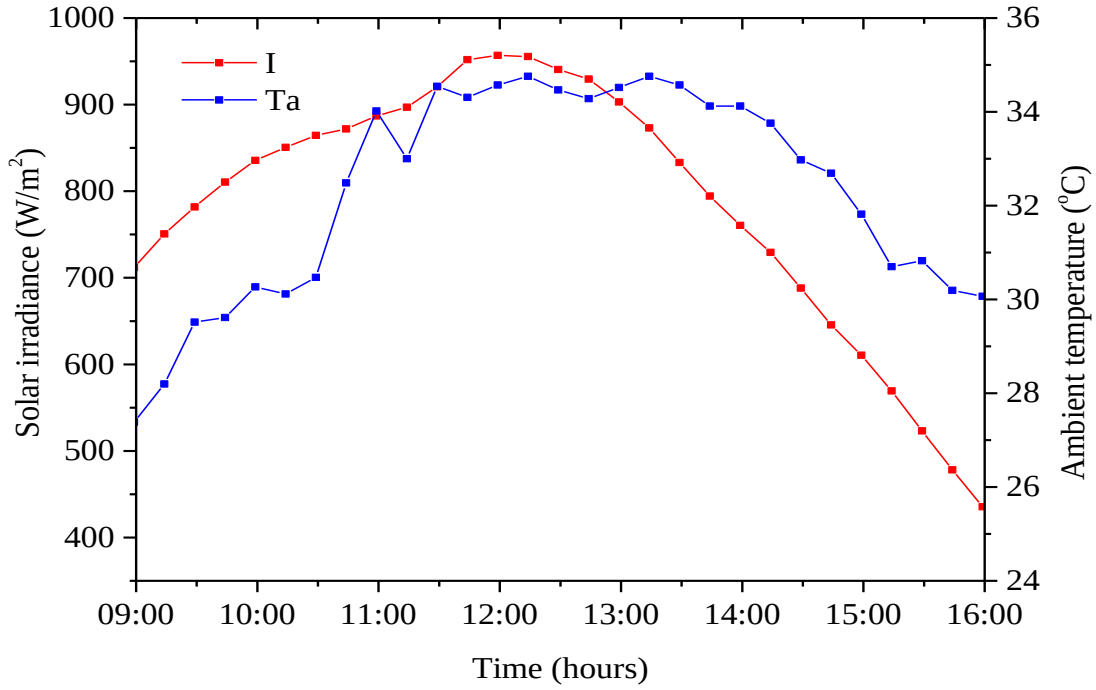

Figure 4.23: Solar radiation and ambient temperature 24/11/13.

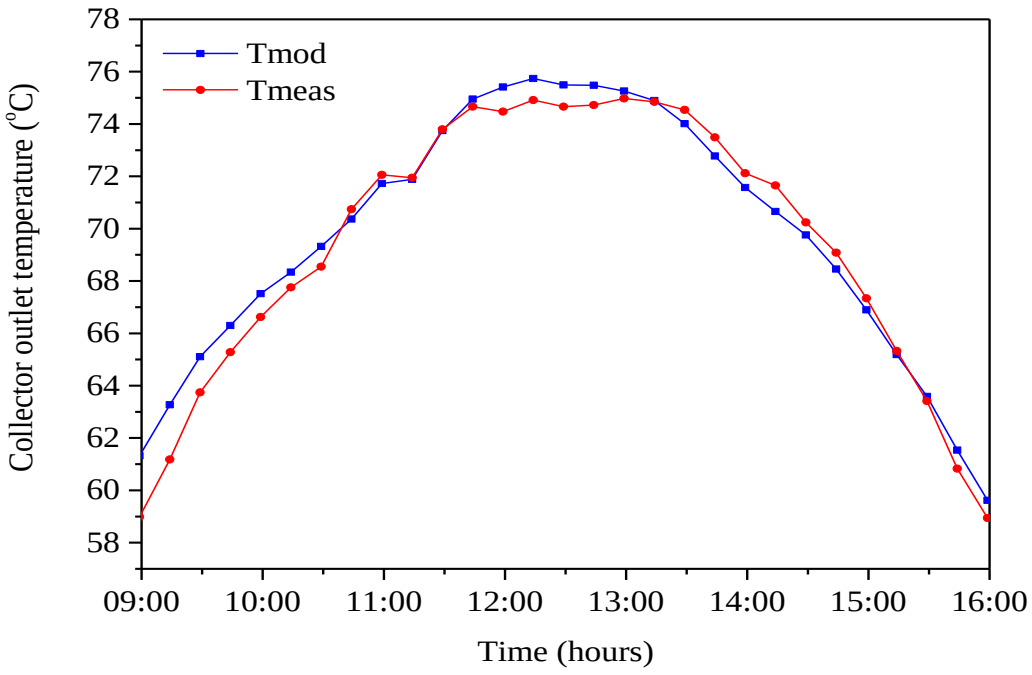

Figure 4.24: Measured and modelled temperature 24/11/13.

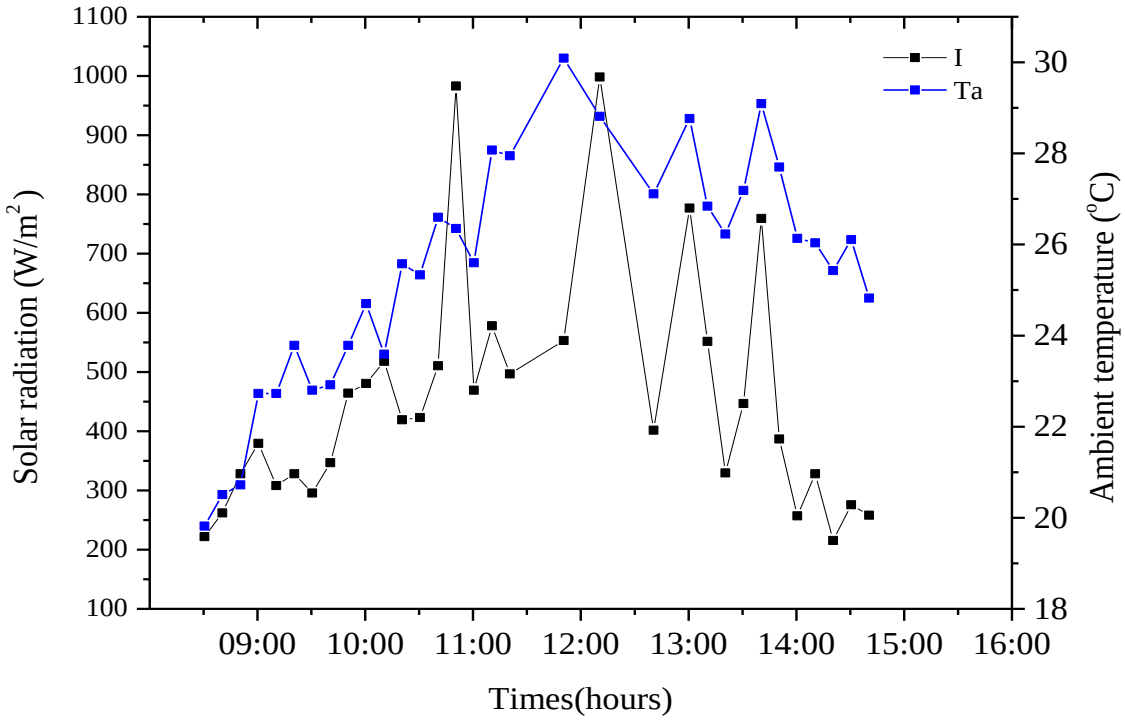

Figure 4.25: Solar radiation and ambient temperature 26/01/14.

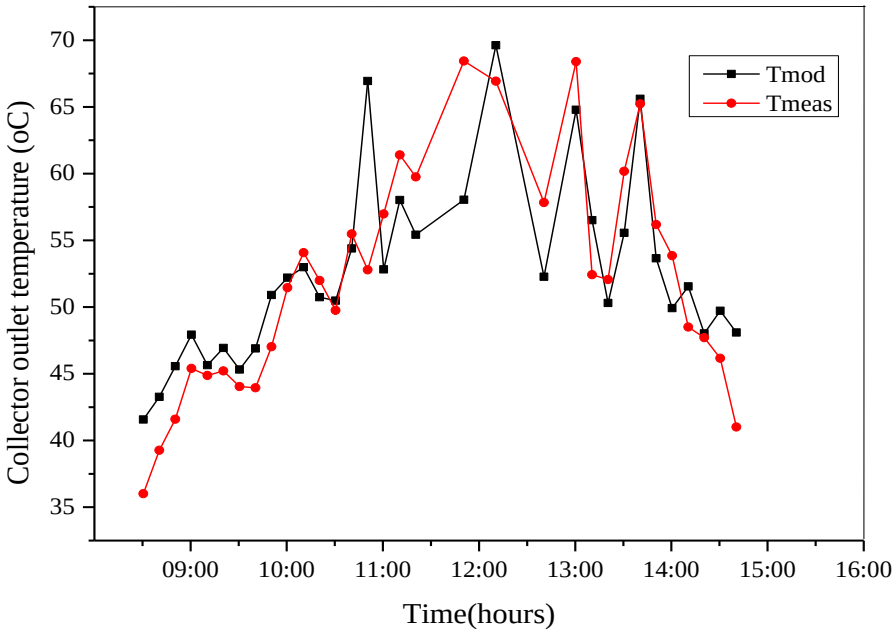

Figure 4.26: Measured and modelled temperatures 26/01/14.

4.4.4.2 Flow rate: summer clear sky day

The collector flow rate is an indication of the time varying response of the collector to changes in solar radiation. The hourly flow rate for the day characterised by clear sky (24/11/13) is depicted in figure 4.27. It is seen that the thermosyphon process begans at 08:30am, peaks at midday to a flow rate of 0.013kg/s and decreased until sunset. Our results are consistent with a study by Riahi and Teharian who recorded a maximum flow rate of 0.016kg/s for a maximum solar radiation of 1050W/m^2 [Riah and Teharian, 2011]. The probable reason for our slightly lower flow rate is the lower sensitivity of our flow meter to low flow rates. It can also be seen that increasing temperatures results in increase in flow rate, with maximum temperatures and maximum flow rate occurring in the same time range between 11am and 2pm. This increase is a result of the dependency of thermosyhon on water density variation.

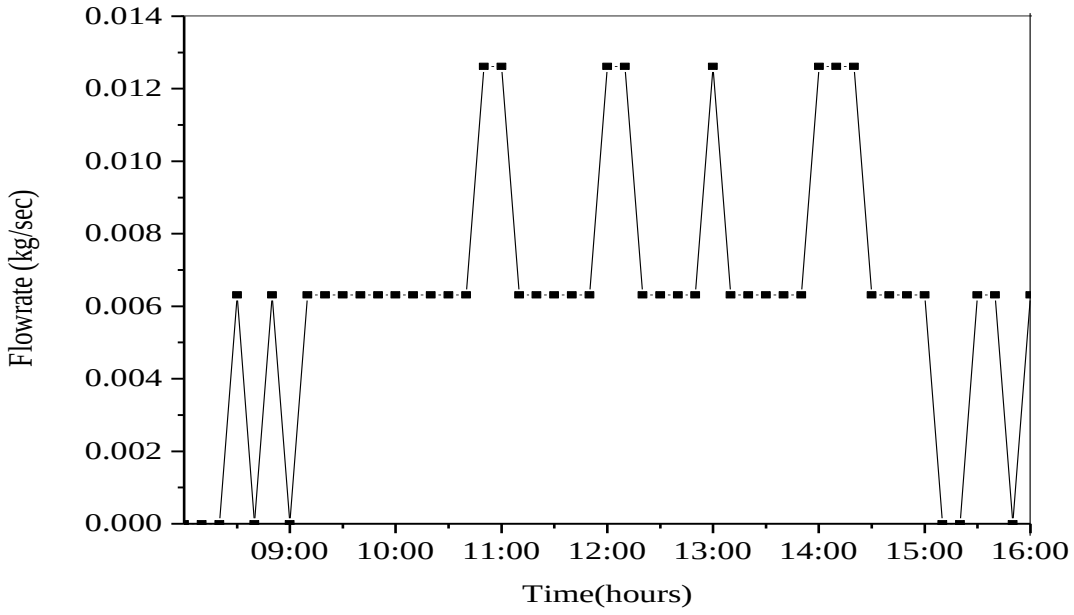

Figure 4.27: Collector flow rate: clear sky.

4.4.4.3 Winter days

Figure 4.29 and 4.31 presents the modelled and measured temperature taken from measurements on the 14/06/14 (clear sky) and 09/07/14 (intermittent cloud cover), representative of typical winter ambient conditions. The solar radiation and ambient temperature are shown in figures 4.26 and 4.28. The maximum solar radiation on these two winter days was 578W/m^2 and 610W/m^2 respectively while the maximum ambient temperatures were 22.3°C and 25.8°C respectively.

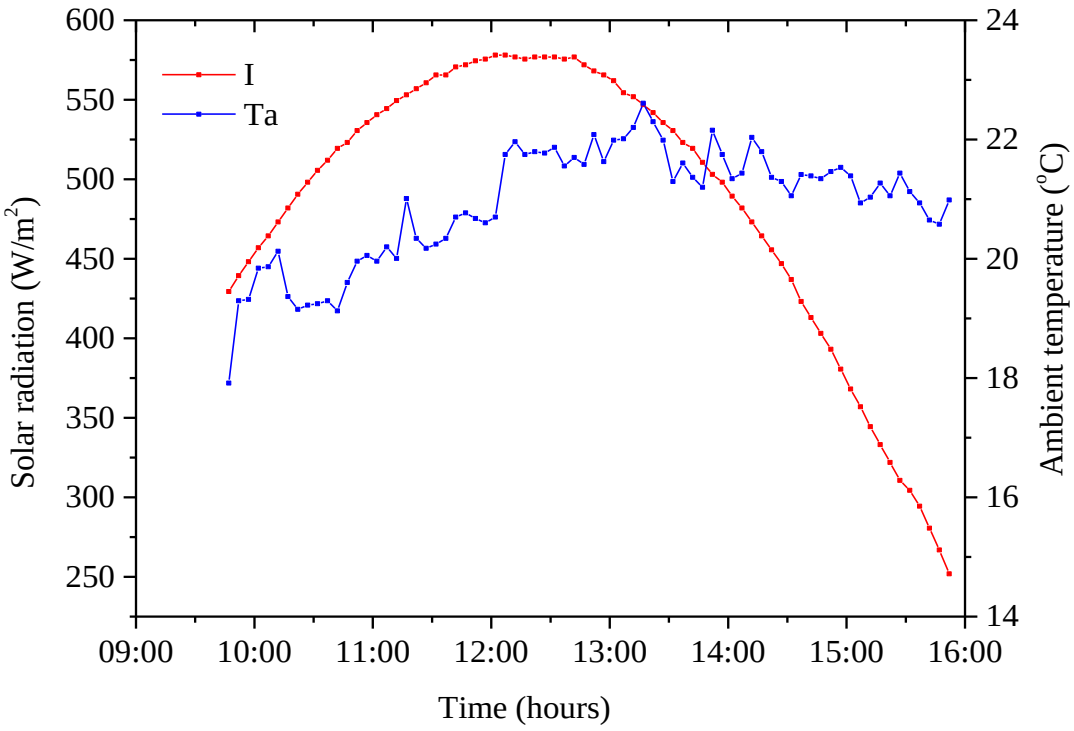

Figure 4.28: Solar radiation and ambient temperature 14/06/14.

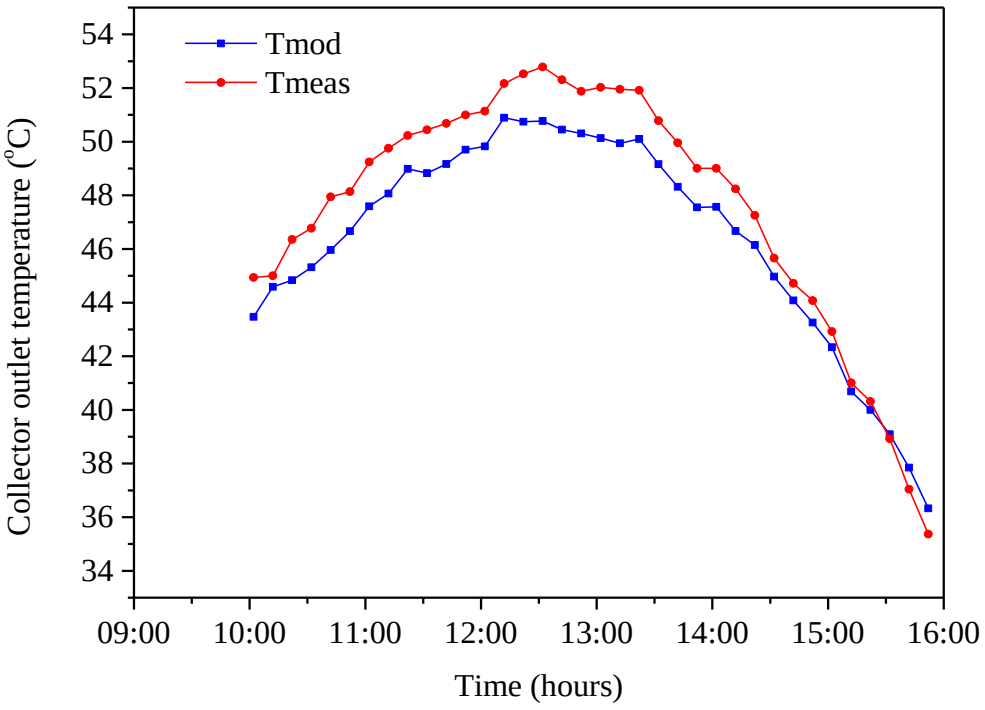

Figure 4.29: Measured and modelled temperatures 14/06/14.

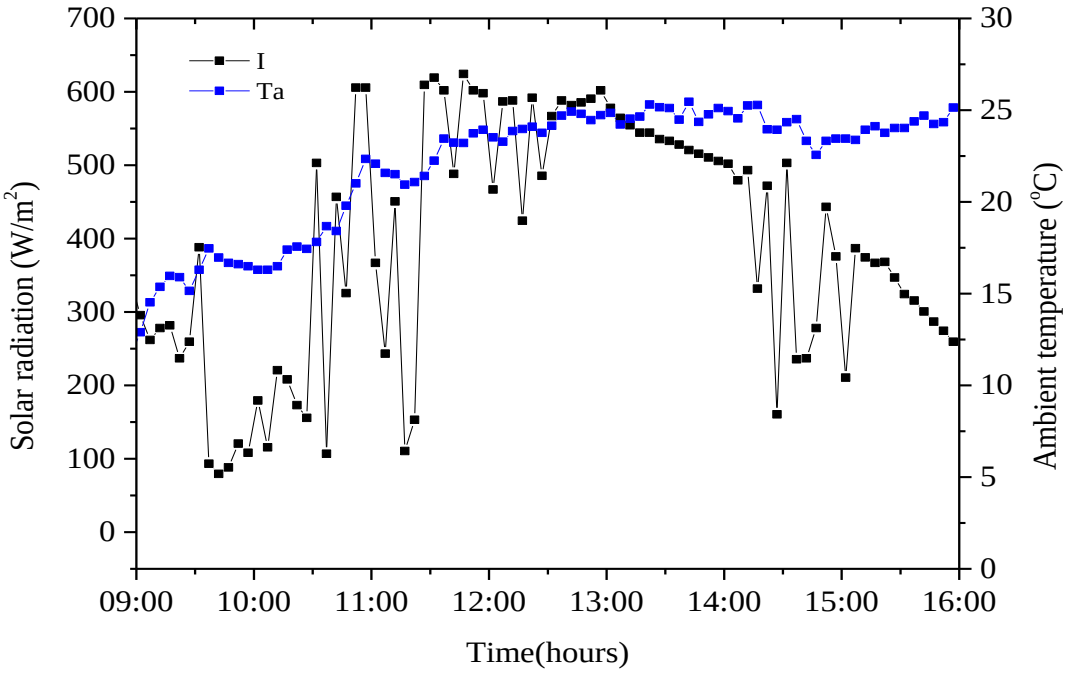

Figure 4.30: Solar radiation and ambient temperature 09/07/14.

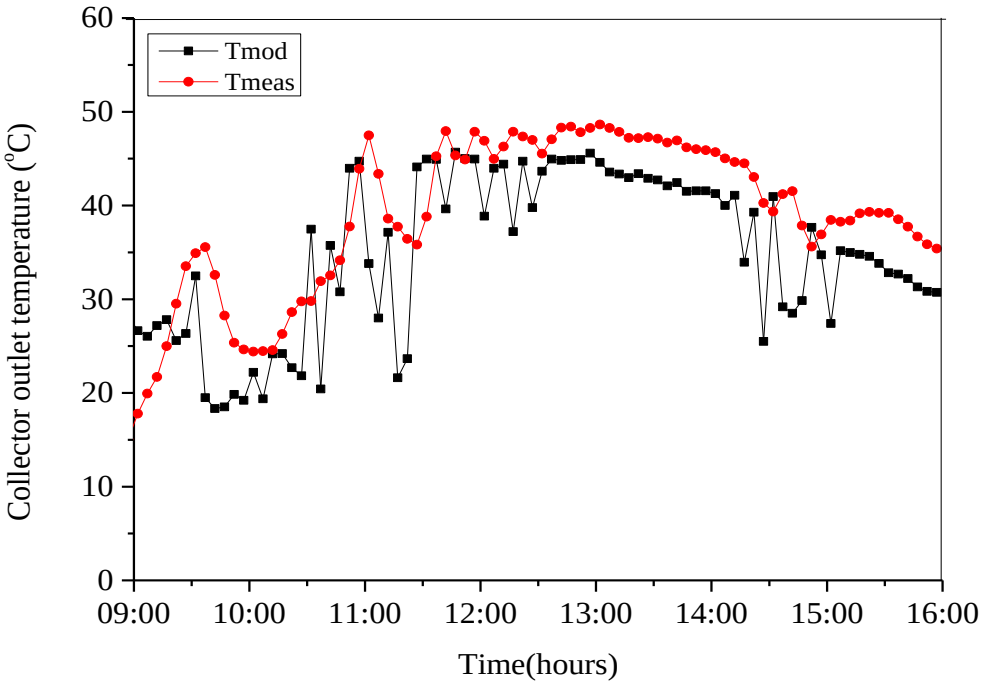

Figure 4.31: Measured and modelled temperatures 09/07/14.

4.4.4.4 Flow rate: Intermittent cloud cover

During the day with intermittent cloud cover it is seen that the flow rate shows an irregular pattern following solar radiation, and flow only occurs between 10 am and 2 pm. These fluctuations occur due to variations in solar intensity. The lower insolation results in lower flow rate of 0.0063kg/s. This clearly indicates how solar radiation affects system performance. In thermosyphon systems mass flow rate shows strong correlation with incident radiation, the greater the energy received the more vigorous the circulation [Bolaji, 2011].

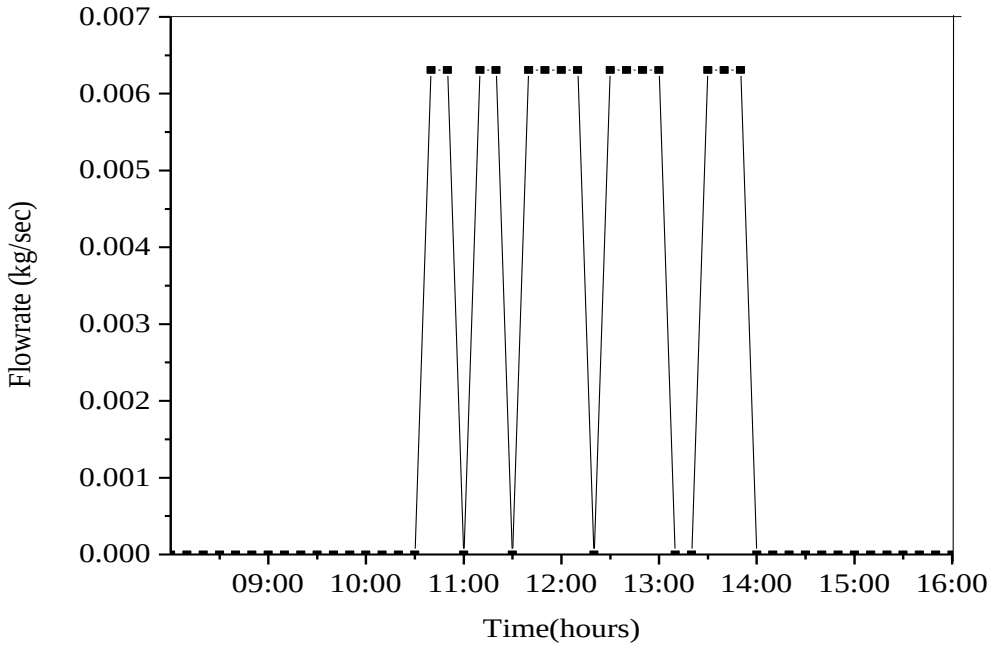

Figure 4.32: Collector flow rate: intermittent cloud cover.

Table 4.8 shows the maximum and minimum error of T_{com} with respect to $(T_{co}-T_{com})/T_{co}$, and the PMAE on the four days. A PMAE of T_{co} with respect to $(T_{co}-T_{com})/T_{co}$ of 1.025% and 2.97 % was found on the clear sky days the cloudy days had an error of 6.95% and 4.87%.

Table 4.8: Percentage mean absolute error for four characteristic days

Day	**Min % difference**	**Max % difference**	**PMAE (%)**
24/11/13	-3.96	1.40	1.025
26/01/14	-19.9	22.2	6.95
14/06/14	-7.53	9.02	2.97
09/07/14	-1.70	11.20	4.87

4.5 Model limitations

The results obtained show that the general model performance is satisfactory in both the summer and winter seasons. However, high discrepancies were observed particularly on days with intermittent cloud cover. Meteorological conditions do not necessarily vary with time in a regular pattern throughout the day. The weather pattern may also vary drastically on several days in a season. A temperate weather can have very changeable weather in summer and winter, one day having rainy conditions and the next sunny conditions [Ayompe and Duffy, 2013]. Real world collector performance is sensitive to collector thermal inertia and this inertia is disturbed by unsteady ambient conditions particularly when irradiance changes significantly over a few minutes. As a result, the models are restricted to specific circumstances to avoid inaccurate predictions. Nevertheless simplified regression based models can facilitate the performance prediction for solar collectors when they are applied for periods of high and smooth solar radiation.

4.6 Comparison with other studies

The ranges of errors obtained are consistent with those found by [Kicsiny, 2014]. In his model, he correlated collector outlet temperature with solar radiation, ambient temperature and collector inlet temperature using measurements from an active flat plat collector installed in Godollo, Hungry. Table 4.7 shows the current results and the results by Kicsiny comparing the average absolute percentage error for the whole validation period and the correlation coefficients he obtained for the different cases explained in section 2.5.2.2. The result from the

physically based model used to validate Kicsiny results is also provided. It is seen that the MLR model error differ by only 0.2%.

Table 4.9: Validity test results of the MLR models and physically based model.

Model	**Correlation coefficient**	**PMAE (%)**
Our model Summer	0.98	4.07
Winter	0.93	6.11
Kicsiny	0.999, 0.994, 0.791, 0.967	4.6
Physically based		7.8

It should be pointed out that with a system operating with thermosyphon, periods of significantly varying operating conditions, are difficult to model separately due to the nature of flow dynamics in the collector. For active systems, On an Off operation of the pump can be separated and modelled as different modes of operation as described in [Kicsiny, 2014]. For thermosyphon systems, the collector outlet temperature was modelled to reflect real time collector flow from periods of increasing flow (when T_{co} increases before solar noon) and when flow becomes more or less constant (at maximum flow approximately solar noon and when collector flow decrease (decreasing T_{co}). This is especially difficult during winter when the thermosyphon process takes place for a much shorter period of time. This can give contribution to variance in precision when comparing MLR modeling for an active and passive system such as the one under study. However, the results obtained above are considered acceptable and compare well with previous results. The comparison of modeled and experimental values from the whole monitoring period showed that periods of significantly varying solar radiation where the most difficult to predict accurately due to the effect of cloud cover.

4.7 Contribution of input variables to collector outlet temperature

The above results have shown the correlation of the collector outlet temperature with solar radiation, ambient temperature, relative humidity and inlet temperature in summer and winter seasons. The coefficient of each predictor shows the level of response of the collector outlet temperature to the each of the four independent variables.

In this section the significance of each parameter in terms of its weight contribution to the output is presented. To achieve this, the ReilifF test was performed using Matlab software. This test ranks the predictors according to their predictive strengths using the ReliefF algorithm by assigning a weight to each factor. The output of the Relief algorithm is a weight between −1 and 1 for each variable, a more positive weights indicating more predictive attributes [Mathsworks, 2015]. Figures 4.33 and 4.34 show the results of the weighting test for the summer and winter models respectively. The tabulated values are presented in Table 4.10. It can be seen that the contribution by weight of the predictors to the collector outlet temperature in summer were 0.036, 0.0177, 0.0213 and 0.019 for solar radiation, collector inlet, ambient temperature and relative humidity respectively. For the winter model the contribution of the predictors by weight was 0.03, 0.014, 0.0096 and 0.0113 for solar radiation, ambient temperature, relative humidity and collector in let temperature respectively.

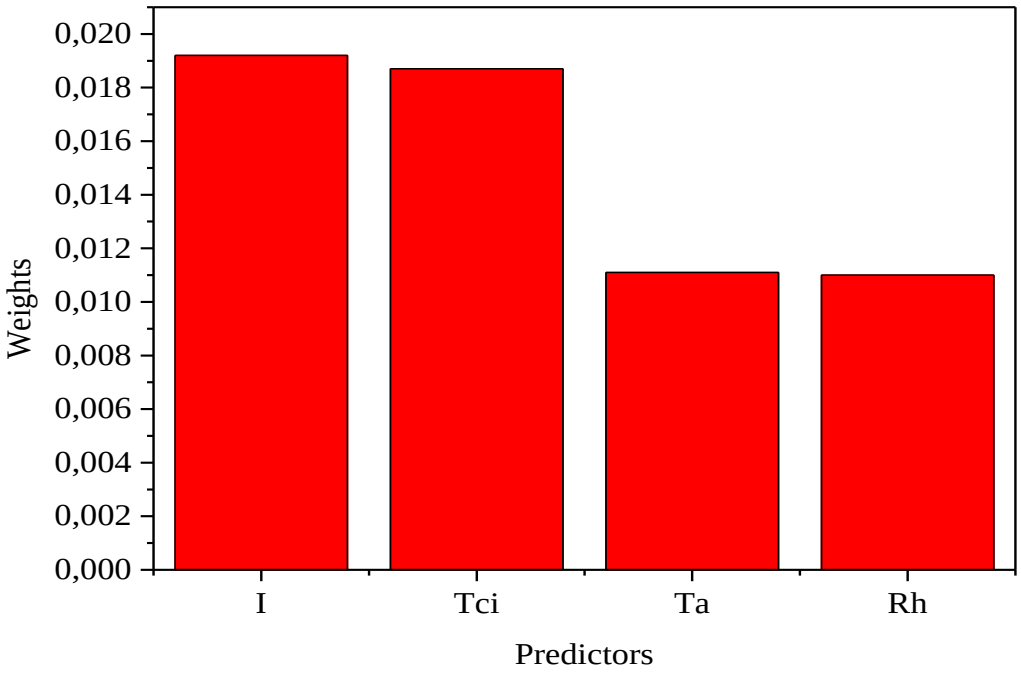

Figure 4.33: Summer model weighting factors.

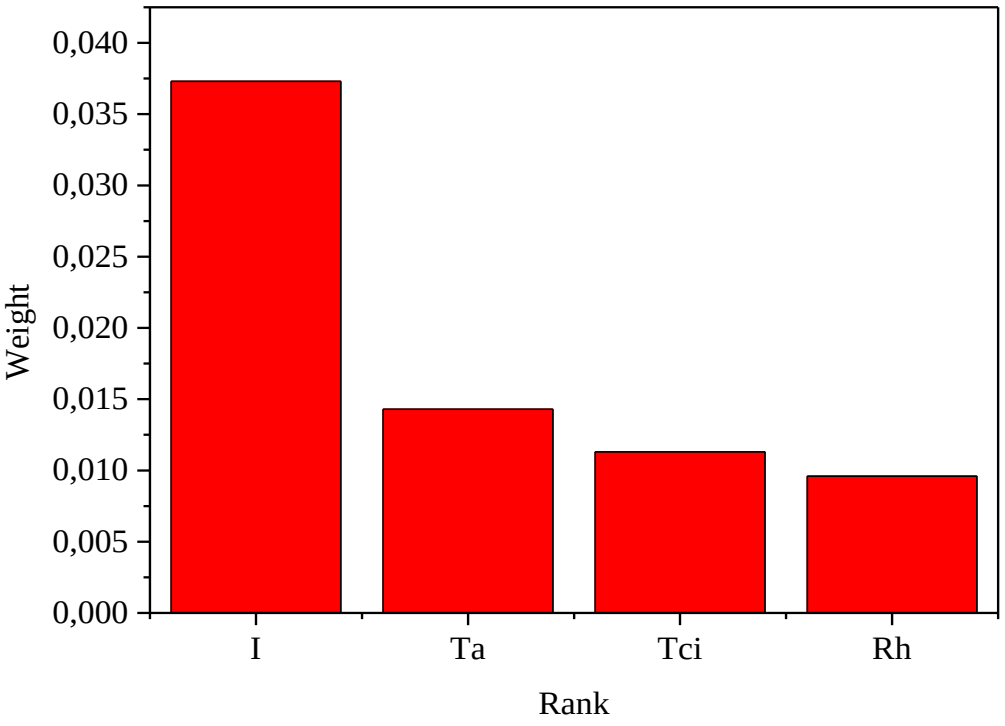

Figure 4.34: Winter model weighting factors.

Table 4.10: Weighting factors for predictors

Predictor	**Summer**		**Winter**	
	Weight	**Rank**	**Weight**	**Rank**
Solar radiation	0.0364	1	0.0373	1
Ambient temperature	0.0213	2	0.0143	2
Relative humidity	0.0177	4	0.0113	3
Collector inlet temperature	0.019	3	0.0096	4

In both seasons, solar radiation has the strongest influence on the predictors followed by ambient temperature. It is interesting to observe from the results that the collector inlet temperature has a stronger influence on the collector outlet temperature in the summer season. This can be attributed to the higher temperatures attained in the summer season. A greater temperature differential is attained when the collector outlet temperature is higher and this occurs in summer when rate of absorption in the collector is higher. This temperature differential is lower is winter. This is also important since a higher temperature difference results in higher collector efficiency [Abubakar and Egbo, 2014].

CHAPTER FIVE

CONCLUSION AND RECOMMENDATION

5.1 Study Finding and Deductions

Solar water heaters are an important technology and aid in reducing the use of fossil fuel based energy sources. The utilization of a free, clean and renewable energy source is among its most important advantages. This study investigated the performance of a solar water heater installed in Alice, South Africa by evaluating the variation in its collector outlet temperature over an eight month period. Data from the performance monitoring was used to develop and validate two multi linear regression (MLR) models. In these models, collector outlet temperature was correlated with solar radiation, ambient temperature, relative humidity and collector inlet temperature for summer and winter seasons.

Although several different configurations of solar water collectors exist, this research focused on a flat plate, thermosyphon system. The overall methodology consisted of installing weather, flow and temperature sensors around the collector system and using the measured data to performing statistical analysis. Analysis was done separately for summer and winter, and evaluated on a monthly, weekly and daily basis.

As was expected, the results showed that summer collector outlet temperatures were higher compared to winter season temperatures. Summer comprises mostly of clear sky days with high solar radiation and ambient temperatures compared to winter. The maximum collector

outlet temperatures in summer ranged between 70^{o}C and 90^{o}C whereas in winter collector outlet temperatures where typically between 50^{o}C and 70^{o}C.

The results of the MLR were very satisfactory. It was observed from the parameter estimation that modelled versus the measured temperature data points clustered very close to the line of origin, closer for summer compared to winter. This means that the error in the summer estimation was less than that for winter. This was also confirmed by the higher adjusted R-squared value of 0.98 for summer while for the winter model it was 0.93.

The predictability of the MLR models was verified by experiments performed on the flat plate collector for several selected days in summer and winter. The analysis comparing measured and modelled temperatures showed very good agreement particularly on clear sky days for both seasons. Results revealed a percentage mean absolute error in modelled temperature of 4.07% in summer and 6.2% in winter averaged for the entire monitoring period. Furthermore, the contribution by weight of each predictor was assessed. The results showed that solar radiation had the greatest significance in determining collector outlet temperature in both seasons followed by collector inlet temperature, ambient temperature and relative humidity in the summer season, while in the winter it was followed by ambient temperature, collector inlet temperature and relative humidity.

The comparison between the modeled and measured collector temperature for clear sky and cloudy days taken during the same season showed that the collector outlet temperature was highly sensitive to rapid changes in solar radiation intensity particularly when it took place in short time intervals. This resulted in inaccurate prediction of the collector outlet temperature. This indicates that MLR approach is season dependent and limits the models for use only under

specific conditions. In addition, MLR models do not perform well when the input data deviate from the set used to perform the estimation.

5.2 Summary of Contributions

Modelling is a very essential tool for determining the performance of solar water heaters. It allows prediction of various performance indices as well as manipulation of system components to achieve a desired optimized system. Over the years the complexity of physical-based models and simulation tools which use white-box approach has increased. However, employing such methods is cumbersome due to the use of many parameters and is generally complex. Although multi linear regression (MLR) is simple and easily applied prediction technique, there has been little research done on its use in solar thermal technology for determining direct correlations.

The major contribution of this work is the use of MLR approach to predict the collector outlet temperature in actual operating conditions. The study was done for a wide range of climatic conditions which is important in order to make meaningful predictions of collector temperatures. Model validation is an important step in studies involving modelling of a system so as to verify the extent to which the model represents the actual system. The results from the model validation in this study have shown that MLR produces accurate results and therefore this technique can be reliably used for collector performance prediction. From a designer and researcher's perspective, estimation of collector output temperature accurately is very crucial and it is important to have efficient assessment and modelling methods. MLR offers an easily applicable prediction method making it a desirable technique to solar thermal researcher and engineers. In addition, the proposed method allows modelling of the collector in transient state

by taking into account time-dependent solar radiation, ambient temperature and relative humidity. It also allows carrying out parametric studies on collectors and compare their performances under any set of environmental conditions. It is noteworthy to mention that proper maintenance of collector is important as this model does not take into account climatic effects such as accumulation of snow, dust, and sand particles which adversely affect the thermal performance of a collector. This study has provided information which can lead to development of better estimation tools.

Another important contribution of this study is the provision of much needed performance data for a collector installed in South African weather conditions. This information is not only important for designers and researchers in this field but also for potential investors. Knowledge of the actual system performance could be important in stimulating investments in solar water heaters and lead to further expansion of solar water heating rollout projects in the country. Lastly, this study provides basis for further research in alternative methodologies to test solar collectors in varying climatic conditions as opposed to the convectional strictly regulated testing methods.

5.3 Final Conclusions

Research has been conducted to model the collector outlet temperature of a thermosyphon flat plate solar water heater under actual operating conditions. Two MLR models were developed for summer and winter using solar radiation, ambient temperature, relative humidity and inlet temperature. Model coefficients were determined from ordinary list squares estimation implemented by OriginLab software. The results were validated using experimental data excluded from the model development and the models were found to have satisfactory

predictability. The findings were also compared with a similar model from literature tested for an active flat plate collector and were found to compare very well. The low errors particularly during clear sky days with very little cloud cover show that the collector outlet temperature can be predicted with high accuracy on such days. Multi linear regression is a simple technique available in many relatively affordable software packages that can be easily applied to model a typical flat plate collector outlet temperature. Though this technique can have low accuracy when applied for rapidly changing weather conditions, it is valuable in showing the applicability of statistical modelling to predict collector temperature compared to the more complex and cumbersome modelling techniques derived from numerical analysis. It must be noted that data-driven models such as MLR perform well when input data does not deviate much from the data used for the estimation. In addition, the models are limited to specific periods when solar radiation is high and cloud cover is not intermittent and this should be taken into consideration. Overall, the conclusion from the research work undertaken is that multi linear regression can be used to perform direct correlations of collector outlet temperature and varying independent parameters with very good accuracy. For prediction purposes it is better to select clear sky days with smooth profiles. These days also show better representation of the collector operation.

Mathematical modeling allows easy visualization of the performance of a system. As demonstrated by this study, empirical mathematical modeling is very accurate in the prediction of collector output temperature of solar water heater systems. Considering the growth of the solar thermal technology industry there is a need for fast and accurate prediction methods for solar collectors. In view of this it is recommendable for research centers and manufactures to include simple and easy to apply quality assurance procedures for the determination of the performance of their products. With the use of such methods as the one outlined, collector

characteristics of different systems can be compared with reasonable accuracy. The method can also be further developed into a testing standard for manufacturing companies with the requirement of only a few sensors. Its advantage would be ability to predict performance without the need for regulated conditions (meteorological, collector inlet, flow rate) such as those stipulated on standardized testing standards.

5.4 Recommendations and Further work

This research established a statistical relationship between collector outlet temperature and weather parameters for two seasons. In the two seasons it should be determined which of the input variables affect the prediction performance of the linear regression models significantly and lead to a more robust model. The performance of the system should be monitored for all four seasons of the year and comparison made on the most accurately predictive model for variations of ambient conditions in a year. Predictions in this study were made for a flat plate solar collector. Performance data for other system configurations should be made available and tested such as for evacuated tube collectors.

Lastly, more information should be obtained for a solar water heating system as a whole, including data on the tank temperatures, tank outlet flow rate and occupant hot water use. Other correlations should also be attempted between occupant hot water use and collector and tank temperatures.

REFERENCES

Aasa, S. A. and Ajayi, O. (2012) Evaluation of the temperature effect of a thermosyphon solar water heater, *Canadian Journal of Pure and Applied Sciences*,6, pp. 1855-1862.

Abubakar, G. B., and Egbo, G. (2014) Performance Evaluation of Flat Plate Solar Collector (Model Te39) In Bauchi, *American Journal of Engineering Research (AJER),* 3, pp. 34-40.

Agbo, S. (2011) Analysis of the performance profile of the NCERD thermosyphon solar water heater, *Journal of Energy in Southern Africa*, *22*, pp 22-26.

Agbo, S. N., and Okeke, C. E. (2007). Correlation between collector performance and the tube spacing for various absorber plate materials in a natural circulation solar water heater.*Trends in Applied Science Research,2* (3), 251-254.

Ahmadi-Nedushan, B., St-Hilaire, A., Ouarda, T. B., Bilodeau, L., Robichaud, E., Thiemonge, N., and Bobee, B. (2007) Predicting river water temperatures using stochastic models: case study of the Moisie River (Quebec, Canada), *Hydrological Processes, 21*, pp. 21-34.

Amrizal, N., Chemisana, D., Rosell, J. I., and Barrau, J. (2012) A dynamic model based on the piston flow concept for the thermal characterization of solar collectors, *Applied Energy,94*, pp. 244-250.

Amoabang, K.O. (2012) *On Assessing the feasibility of a solar water heating system based on performance and economic analysis*, A thesis submitted in partial fulfilment of the

requirements for the degree of Master of Science in Mechanical Energy, Kwame Nkrumah University of Science and Technology, Kumasi, Ghana.

Amori, K. E., and Jabouri, N. S. (2012). Thermal performance of solar hot water systems using a flat plate collector of accelerated risers, *The Journal of Engineering Research*, *9*(1), 1-10.

Andrés, A. C., and López, J. C. (2002) TRNSYS model of a thermosiphon solar domestic water heater with a horizontal store and mantle heat exchanger, *Solar Energy*, 72, pp 89-98.

Andersen, E., and Furbo, S. (2009) Theoretical variations of the thermal performance of different solar collectors and solar combi systems as function of the varying yearly weather conditions in Denmark, *Solar Energy*, 83, pp. 552-565.

Appropedia, (2014) Thermosiphon solar water heater http://www.appropedia.org/Thermosiphon Accessed 27 August 2014.

Arora, S., Chitkara, S., Udayakumar, R., and Ali, M. (2011) Thermal analysis of evacuated solar tube collectors, *Journal of Petroleum and Gas Engineering*, *2*, pp. 74-82.

Ayompe, L. M., Duffy, A., McCormack, S. J., and Conlon, M. (2011) Validated TRNSYS model for forced circulation solar water heating systems with flat plate and heat pipe evacuated tube collectors, *Applied Thermal Engineering*, 31, pp 1536-1542.

Ayompe, L.M. and Duffey, A. (2013) Analysis of the Thermal Performance of a Solar Water Heating System with Flat Plate Collector Temperate Climate. Dublin Institute of Technology. School of Civil and Building Services Engineering Articles.

Batabyal, K. (2013) *On the Performance prediction of solar water heating system using Artificial Neural Network,* A thesis submitted in partial fulfillment of the requirements for the degree of Master of Technology, Jadavpour University, West Bengal, India.

Bakari, R., Minja, R. J., and Njau, K. N. (2014) Effect of Glass Thickness on Performance of Flat Plate Solar Collectors for Fruits Drying, *Journal of Energy, 2014,* pp 1- 8.

Belessiotis,V. and Mathioulakis, E. (2002) Analytical Approach of Thermosyphon Solar Domestic Hot Water System Performance, *Solar Energy,* 72, pp 307-315.

Bliss, J. (1959) The derivations of several "plate-efficiency factors" useful in the design of flat plate heat collectors, *Solar Energy,* 3, pp. 55–64.

Budig, C., Orozaliev, J., de Keizer, A. C., Kusyy, O., and Vajen, K. (2009) Collector parameter identification methods and their uncertainties, In *Proc. ISES Solar World Congress, Johannesburg,* 11.

Buzás, J., Farkas, I., Biró, A., and Németh, R. (1998) Modelling and simulation aspects of a solar hot water system, *Mathematics and computers in simulation*, 48, pp. 33-46.

Bolaji, O.B. (2011) Mathematical Modelling and Experimental Investigation of Collector Efficiency of a Thermosyphonic Solar Water Heating System, *ANUL XVIII, NR*. 3, pp 1453 – 7397.

Bohlin, T. and Graebe, S. F. (1995) Issues in nonlinear stochastic grey-box identifcation. *International Journal of Adaptive Control and Signal Processing*, 9, pp. 465–490.

Catalina, T., Iordache, V. and Caracaleanu, B. (2013) Multiple regression model for fast prediction of the heating energy demand, *Energy and Buildings*, 57, pp 302-312.

Caouris, Y. G. (2012) Low Temperature Stationary Collectors. *Comprehensive Renewable Energy. 1st ed., Elsevier, Oxford, UK*, pp. 103-147.

Cavallaro, F. (2013). *Assessment and Simulation Tools for Sustainable Energy Systems: Theory and Applications* 129, Springer Science & Business Media.

Center for Climate and Energy solutions, Working Together for the Environment and the Economy 2015 http://www.c2es.org/energy/source/coal last accessed 25 August 2015.

Chandavar, A., Bhatt, S. and Krishnamurthy, S. (2013) Analytical and experimental investigation to determine the variation of H-B-W constants for a scaled forced circulation flat plate solar water heater, *ASME 2013 International Mechanical Engineering Congress and Exposition*, 6.

Chuawittayawuth, K., and Kumar, S. (2002) Experimental investigation of temperature and flow distribution in a thermosyphon solar water heating system, *Renewable Energy*, 26 pp. 431-448.

Close, D. J. (1962 The performance of solar water heaters with natural circulation, *Solar Energy*, 6, pp 33-40.

Coetzee, R.P. (2009) On *The development of a methodology to measure and verify the impact of a National Solar water heater programming* A thesis submitted in partial fulfillment of the degree of Master in Mechanical Engineering at North West University, South Africa.

Das, S., Bandyopadhyay, B., and Saha, S. K. (2006) Sensitivity Analysis of the Test Parameters of a Solar Flat Plate Collector for Performance Studies, *Advances in Energy Research*, pp 515-520.

Department of Energy (2013) A survey of energy related behavior and perceptions in South Africa The Residential sector 2013 http://www.energy.gov.za/files/media/Pub/DoE-2013-Survey-of-EnergyRelated-Behaviour-and-Perception-in-SA.pdf last accessed February 2014.

Dodier, R. H., and Henze, G. P. (2004) Statistical Analysis of Neural Networks as Applied to Building Energy Prediction, *Journal of Solar Energy Engineering*, 126, pp 592-600.

Duffie, J. A., and Beckman, W. A. (2006) *Solar Engineering of Thermal 1 Processes*: John Wiley and Sons.

Duffie,J and Beckman W. (1991) *Solar engineering of thermal processes.* John Wiley and Sons, NY.

Duffie J.A. and Beckman W.A., (1999) *Solar Engineering of Thermal Processes*, 2a. Ed. John Wyley&Sons, Inc., USA.

Edkins, M., Marquard A., and Winkler, H (2010) South Africa Renewable Energy Policy Roadmap. University of Cape Town Energy Research Center Final Report.

EN 12975,2006. EN 12975-2:2:2006. Thermal Solar Systems and Components – Solar Collectors – Part 2: Test Methods.European Standard EN 12975:2006, CEN, European Committee for Standardisation; 2006.

Esen, M. and Esen, H. (2005) Experimental investigation of a two-phase closed thermosyphon solar water heater, *Solar Energy*, 79, pp 459 – 468.

Eskom, (2009) Demand-side Management Implementation in South Africa. Presentation prepared by Matlala, T. Eskom Holdings Ltd. Sandton. [Online] Available: www.eskomdsm.co.za/sites/default/files/u1/DSMImplementationinSAp.pdf Accessed: 16 June 2012.

Facão, J., Varga, S. and Oliveira, A. C. (2004) Evaluation of the use of artificial neural networks for the simulation of hybrid solar collectors, *International Journal of green energy*,1, pp. 337-352.

Feelders., A. (2003) Introduction to Intelligent Data Analysis http://www.cs.uu.nl/docs/vakken/ida/idadict2004.pdf last accessed 7 August 015.

Fischer, S., Heidemann, W., Müller-Steinhagen, H. and Perers, B. (2003) Collector parameter identification -- iterative methods versus multiple linear regression, Proceedings of ISES Solar World Congress, Gothenburg. http://www.itw.uni-stuttgart.de/dokumente/Publikationen/publikationen_solarpaces06_sf.pdf Accessed 4 April 2014.

Fischer, S., Frey, P. and Drück, H. (2012) A comparison between state-of-the-art and neural network modelling of solar collectors, *Solar Energy, 86* pp. 3268-3277.

Farkas, I. and Géczy-Víg P (2003) Neural network modelling of flat-plate solar collectors, *Computers and electronics in Agriculture*, 40, pp. 87-102.

Focus Technology Company Ltd, China (2012) Evacuated Tube Collector focussolar.en.made-in-china.com/China-Solar-Water-Heater Last accessed 4 September 2014.

Góngora-Gallardo, G., Castro-Gil, M., Colmenar-Santos, A. and Tawfik, M. (2013) Efficiency factors of solar collectors of parallel plates for water, *Solar Energy,94*, pp. 335-343.

Gowda, N., Gowda, B.P. and Chandrashekar, R. (2014) Investigation of Mathematical Modelling to Assess the Performance of Solar Flat Plate Collector, *International Journal of Renewable Energy Research (IJRER),4*, pp. 255-260.

Gupta, C. L., and Garg, H. P. (1968) System design in solar water heaters with natural circulation, *Solar Energy*, *12*, pp. 163-182.

Haykin, S., (1994) Neural Networks: A Comprehensive Foundation, Macmillan, New York.

Hagan, M., Demuth, H, and Beale M, (1996) Neural network design. Boston: PWS Publishing Company.1996.

Hammadi, H.S. (2009) Study of solar water heater system with natural circulation in Basrah, *Al-Qadisiya Journal For Engineering Sciences*, 2,pp 1-12.

Holcomb, D., Li, W., and Seshia, S. (2009) Algorithms for Green Buildings: Learning-Based Techniques for Energy Prediction and Fault Diagnosis (No. Technical Report No. UCB/EECS-2009-138). University of California at Berkeley.

Hottel, H. and Woertz, B. (1942) The performance of flat plate solar heat collector. *Trans ASME* , 64, pp 91–104.

Hottel, H. and Whillier. A. (1955) Evaluation of flat-plate solar collector performance. *Transactions of the conference on the use of solar energy thermal processes. Tucson, AZ(USA*); pp. 74–104.

International Energy Agency, Climate Reviews (2011), http://www.globalization101.org/fossil-fuels/. last accessed 20 November 2015

International Energy Agency, World Energy Outlook (2013), www.iea.org/Textbase/npsum/WEO2013SUM.pdf last accessed 21 June 2014.

Islam, M., Raisal, K Sumathy, K., and Khan, U. S. (2013) Solar water heating systems and their market trends, *Renewable and Sustainable Energy Reviews*, 17, pp. 1 -25.

Kalogirou, S. A., and Panteliou, S. (1999) Dynamic system testing method and artificial neural networks for solar water heater long-term performance prediction, In *Proceedings of the European symposium on intelligent techniques ESIT*, 99, pp 1-6.

Kalogirou, S. A., Panteliou, S., and Dentsoras, A. (1999) Modeling of solar domestic water heating systems using artificial neural networks, *Solar Energy*,65, pp. 335-342.

Kalogirou, S. A. and Panteliou, S. (2000) Thermosiphon solar domestic water heating systems: long-term performance prediction using artificial neural networks. *Solar Energy*, 69, pp. 163-174.

Kalogirou, S. (2004) Solar thermal collectors and applications, *Progress in Energy and Combustion Science*, 30, pp. 231-295.

Kalogirou, S.A. (2006) Prediction of flat-plate collector performance parameters using artificial neural networks, *Solar Energy*, 80, pp. 248-259.

Kalogirou, S. (2007) Solar Energy for Domestic Heating and Cooling and Hot Water Production, *International Journal of Energy, Environment and Economics*, 14, pp. 289-339.

Kalogirou, S.A. (2009) Chapter five: Solar water heating systems. Solar Energy Engineering, Process and systems, pp 251-354.

Kalogirou,S.A. (2012) A detailed thermal model of a parabolic trough collector. *Energy* 48, pp. 298-306.

Kicsiny, R. (2014) Multiple linear regression based model for solar collector, *Solar Energy* 110, pp. 496-506.

Khaled, A. (2012) On the *Technical and economic performance of parabolic trough in Jordan*, A thesis submitted in fulfilment of the degree Doctoral dissertation, University of Kassel.

Khan, M. M. A., Abdul Malek, A. B. M., Mithu, M. A. H., and Das, D. K. (2010) Design, fabrication and performance evaluation of natural circulation rectangular box-type solar domestic water heating system, *International Journal of Sustainable Energy*, *29* pp. 164-177.

Kishor, N., Das, M. K., Narain, A., and Ranjan, V. P. (2010) Fuzzy model representation of thermosyphon solar water heating system *Solar Energy*, 84, pp. 948-955.

Koffi, P. M. E., Andoh, H. Y., Gbaha, P., Toure, S., and Ado, G. (2008) Theoretical and experimental study of solar water heater with internal exchanger using thermosiphon system, *Energy Conversion and Management*,49, pp. 2279-2290.

Kovács, P., Pettersson, U., Persson, M., Perers, B., & Fischer, S. (2013)Improving the accuracy in performance prediction for new collector designs. http://www.estif.org/solarkeymark/Links/Internal_links/network/sknwebdoclist/SKN_N0172R0.pdf Accessed 3 April 2016 .

Kulkarni, M. M., and Deshmukh, D. S.(2015) Design of Experiment for Solar Water Heater Performance Analysis, *International Journal of Science, Spirituality, Business and Technology*.(3) pp 55 – 60).

Laughton, C. (2010) Solar Domestic Water Heating: The Earthscan Expert Handbook for Planning, Design and Installation. Routledge.

Lecoeuche,S. and Lalot, S. (2005) Prediction of the daily performance of solar collectors, *International Community Heat Mass Transfer*, 32, pp 603–11.

Luminosu, I. and Fara, L. (2005) Determination of the optimal operation mode of a flat solar collector by exergetic analysis and numerical simulation, *Energy*, 30 pp 731-747.

Madan, J. V., and Sirse, O. M. (2015) Experimental Study on Efficiency Of Solar Collector At Nagpur (India) During Winter, *International Journal of Scientific and Technology Research*, 4, 231-234.

Masic, M. (2009) On *Using Building Energy Monitoring to Verify Building Energy Performance,* submitted in fulfilment of the Doctor of Philosophy , Norwegian University of Science and Technology, Norway.

The Mathsworks Inc. 2015. http://www.mathworks.com/help/stats/relieff.html last accessed June 2015.

Morrison, G. L., and Ranatunga, D. B. J. (1980) Transient response of thermosyphon solar collectors, *Solar Energy*, 24, pp. 55-61.

Muschaweck, J., and Spirkl, W. (1993) Dynamic solar collector performance testing, *Solar Energy Materials and solar cells*, 30, 2, pp. 95-105.

Morrison, G. L., and Ranatunga, D. B. J. (1980) Transient response of thermosyphon solar collectors. *Solar Energy*, 24, pp. 55-61.

Nykanen, A. (2012) On the *Thermal performance and microclimate test methods for Flate plate solar thermal collectors*, A thesis submitted in partial fulfilment of the degree of Master in Renewable Energy, University of Jyvaskyla.

Ong K.S. (1974.) A finite difference method for the evaluation of the thermal performance of a solar water heater, *Solar Energy*, 16, pp. 137-147.

Onset Computer Corporation (2007) Hobo U30 Station. Non Remote Communication Manual (NRC).Users guide. http://www.onsetcomp.com/files/manual_pdfs/11866-H-U30-NRC-Manual.pdf. last Accessed 12th November 20124.

Pereira, E. M. D., Zárate, L. E., and Vimieiro, R. (2005) Representation of solar collectors via neural networks with reduction of the training set number, 18th International Congress of Mechanical Engineering, Ouro Preto, pp 1-8.

Peters, D. (2013) Minister of Energy Budget Vote Speech. http://www.pmg.org.za/ last accessed 7 June, 2013.

Quaschning, V. (2005) Understanding renewable energy systems. London: Earthscan., pp 1-267

Ramlow, B. and Nusz B (2010) Solar water heating, Revised and expanded edition: A comprehensive guide to solar water and space heating systems. New Society Printers, Gabrila Island,BC, Canada.

Riahi, A., and Taherian, H. (2011) Experimental investigation on the performance of thermosyphon solar water heater in the South Caspian Sea, *Thermal Science*,15, pp. 447-456.

Rodríguez-Hidalgo, M. C., Rodríguez-Aumente, P. A., Lecuona, A., Gutiérrez-Urueta, G. L., and Ventas, R. (2011) Flat plate thermal solar collector efficiency: Transient behavior under working conditions. Part I: Model description and experimental validation, *Applied Thermal Engineering*, 31, pp. 2394 - 2404.

Saffaripour, M.H, Mehrabian, M.H. and Bazargan, H. (2013) Predicting solar radiation fluxes for solar energy system applications, *International Journal of Environmental Science Technologies*, 10, pp. 761–768.

Samo, R.Z, Siyal A.A, Siyal, Z.A, and Jatoi A.R., (2012) An analysis of an active and passive solar water heating system, *Sixteenth International Water Technology Conference, IWTC 16 2012, Istanbul, Turkey* pp *1-10.*

Sargsyan, A, (2010) Use of Renewable energy sources in the world and Armenia Through innovations to clear technologies. Lusabats Publishing house, pp 1-86.

Salas, Y. C., Aguilar, J. A., Milón, J. J., and Braga, S. L. (2012) Experimental study on the performance of thermosyphon solar water heater in Arequipa, Peru, *International conference on Heat transfer, Fluid Mechanics and Thermodynamics*, pp 141-145.

Sako, M. K., NGuessan, Y., Andoh, H. Y., Koffi, P. M. E., Gbaha, P., and Sangaré, M. K. (2007) Economical and Technical Viability of a Thermosyphon Solar Water Heater in Cote DIvoire, *Journal of Applied Sciences*,*7*, 3977-3982.

Sekhar, Y.R, Shamer, V. and Basaveswara, R.M. 2009 Evaluation of heat loss coefficients in solar flat plate collectors, *ARPN Journal of Engineering and Applied Sciences*, 4, pp. 15–19.

Siddiqui, M. A., (1997) Heat transfer and fluid flow studies in the collector tubes of a closed-loop natural circulation solar water heater, *Energy Conversion and Management*, 38, pp. 799-812.

Siebers D.L and Viskanta, R. (1979). Thermal Analysis of Some Flat-Plate Solar Collector Designs for Improving Performance, *Journal of Energy*,3, No.1 pp. 8-15.

Sözen, A., Menlik, T., & Ünvar, S. (2008) Determination of efficiency of flat-plate solar collectors using neural network approach, *Expert Systems with Applications, 35*, pp. 1533-1539.

Surfine Renewable energy Heat pipe evacuated tube solar collector http://www.ecosurefine.com/solar-water-heaters/pressurized-heat-pipe-solar-water-heater/ last accessed 5May 2015

Sustainable Energy Society South Africa (2013) http://www.swkong.com/company/ energy/ solar_recycling_energy, 1082448.html. Accessed June 11, 2013

Teyeb, A., Dehmani. .L., Kerkeni C and Kaabi L. (2008) Parametrical study of the influence of the climatic data and the construction properties on the efficiency of a collector/storage solar water heater, *Renewable Energies*, 11, pp. 87-94.

Zárate, L. E. and Pereira, E. (2006) Parametric Analysis of Solar Collectors Through Sensitivity Factors Via Artificial Neural Networks, In *Neural Networks, 2006. IJCNN'06. International Joint Conference on Neural Networks*, pp. 2742-2748.

Zerrouki, A., Boumedien, A., and Bouhadef, K. (2002) The natural circulation solar water heater model with linear temperature distribution, *Renewable Energy*, 26, pp. 549-559.

APPENDIX A

Research Output - Publications

1. South African Institute of Physics Presentation Ndlovu, N., Michael, S., Tangwe S. (2015) .Evaluation of an empirical model for a flat plate solar collector,

2. South African Institute of Physics Presentation Ndlovu, N., Michael, S., Tangwe S. (2014). Geyser heating cycle of a 2kW flat plate sola water heater.

3. South African Institute of Physics Presentation Ndlovu, N., Michael, S., Tangwe S.,E.L Meyer (2012). Performance monitoring of a flat plate solar water heater.

APPENDIX B

Results of parameter estimation from OriginLab:

Summer

Summer MLR (Tco)(2014/12/17 23:29:16)

Notes

Input Data

Masked Data - Values Excluded from Computations

Bad Data (missing values) -- Values that are invalid and thus not used in computations

Parameters

		Value	Standard Error	t-Value
Co	Intercept	16.98707	1.18113	14.38207
	"I"	0.02792	8.53702E-4	32.6991
	"Ta"	0.20731	0.04214	4.91968
	"Rh"	-0.01505	0.01156	-1.30202
	"Ci"	0.65444	0.03131	20.90176

Statistics

	Co
Number of Points	192
Degrees of Freedom	187
Residual Sum of Squares	364.21944
Adj. R-Square	0.97568

Winter model

Winter MLR (2014/12/18 15:21:23)

Notes

Input Data

Masked Data - Values Excluded from Computations

Bad Data (missing values) -- Values that are invalid and thus not used in computations

Parameters

		Value	Standard Error	t-Value
Co	Intercept	1.16783	2.06355	0.56593
	"I"	0.0443	0.00113	39.33405
	"Ta"	0.66933	0.06216	10.76791
	"Rh"	0.33073	0.04722	7.00437
	"Ci"	0.05579	0.0139	4.01354

Statistics

	Co
Number of Points	191
Degrees of Freedom	186
Residual Sum of Squares	389.59096
Adj. R-Square	0.92541

APPENDIX C

Data collected on the 24th November 2013

Table C1: Measured input variables, Tmod and PMAE

Time	I	Ta	RH	Tci	Tmeas	Tmod	Error	PAE
08:59	711,9	27,382	45,8	30,748	58,985	61,31918	-3,95724	3,957243
09:14	750,6	28,196	44,5	31,842	61,182	63,26824	-3,40988	3,409885
09:29	781,9	29,515	43,7	32,924	63,739	65,10683	-2,14598	2,145978
09:44	810,6	29,615	41,1	33,469	65,277	66,2981	-1,56426	1,564262
09:59	835,6	30,268	39	34,045	66,623	67,5169	-1,34174	1,341735
10:14	850,6	30,117	38,9	34,73	67,755	68,34037	-0,86395	0,863945
10:29	864,4	30,469	39,1	35,555	68,546	69,32282	-1,13328	1,133276
10:44	871,9	32,484	38,9	36,2	70,739	70,36811	0,524303	0,524303
10:59	886,9	34,019	37,1	37,124	72,06	71,72298	0,467688	0,467688
11:14	896,9	33,001	37,2	37,288	71,944	71,88777	0,078152	0,078152
11:29	920,6	34,545	36,4	38,644	73,795	73,74711	0,064893	0,064893
11:44	951,9	34,308	35,1	39,234	74,662	74,94868	-0,38397	0,383968
11:59	956,9	34,572	35,5	39,658	74,474	75,40987	-1,25664	1,256641
12:14	955,6	34,757	35,1	40,142	74,914	75,73585	-1,09706	1,097059
12:29	940,6	34,466	35,5	40,487	74,662	75,49029	-1,10939	1,109392
12:44	929,4	34,281	34,8	40,978	74,725	75,48135	-1,01218	1,012184
12:59	903,1	34,519	34,9	41,648	74,977	75,25754	-0,37417	0,374168
13:14	873,1	34,757	33,9	42,238	74,85	74,89797	-0,06409	0,064093
13:29	833,1	34,572	33,8	42,594	74,537	74,01409	0,701545	0,701545
13:44	794,4	34,124	33,8	42,445	73,49	72,77881	0,967733	0,967733
13:59	760,6	34,124	34,1	42,001	72,119	71,57116	0,759634	0,759634
14:14	729,4	33,757	35,3	42,031	71,653	70,65431	1,393783	1,393783
14:29	688,1	32,975	35,8	42,624	70,235	69,75766	0,679628	0,679628
14:44	645,6	32,691	38,2	42,535	69,082	68,45705	0,904652	0,904652
14:59	610,6	31,816	41,5	41,942	67,339	66,8931	0,66217	0,66217
15:14	569,4	30,697	43,9	41,443	65,326	65,18619	0,214023	0,214023
15:29	523,1	30,824	45,9	40,92	63,411	63,59016	-0,28254	0,282543
15:44	478,1	30,192	46,8	39,857	60,83	61,53502	-1,159	1,159004
15:59	435,6	30,066	47,2	38,728	58,943	59,61659	-1,14277	1,142774
							PMAE	**1,024702**

APPENDIX D

Data collected on the 26th January 2014

Table D1: Measured input variables, Tmod and PMAE

Time	I	Ta	RH	Tci	Co	Com	Error	PAE
09:00	354,4	27,014	54,1	42,327	65,869	59,04319	10,3627	10,3627
09:15	798,1	28,196	49,1	42,505	67,287	71,4596	-6,2012	6,201202
09:30	798,1	29,74	47,6	43,89	71,653	72,70852	-1,4731	1,473097
09:45	911,9	29,79	47,4	45,186	74,474	76,64259	-2,91187	2,911869
10:00	399,4	27,456	50,5	41,913	68,069	60,1329	11,65891	11,65891
10:15	383,1	28,221	50,3	43,374	71,251	60,81046	14,65319	14,65319
10:30	359,4	27,407	51,8	44,319	72,709	60,59772	16,65719	16,65719
10:45	990,6	29,49	48,3	45,877	65,969	79,14399	-19,9715	19,97148
11:00	249,4	31,689	43	46,609	77,325	60,14596	22,21667	22,21667
11:15	975,6	30,874	43	46,577	77,19	79,56347	-3,07484	3,07484
11:30	994,4	31,382	42,6	47,81	78,697	80,98925	-2,91276	2,912757
11:45	985,6	29,439	46,9	47,744	78,767	80,24118	-1,87157	1,871568
12:00	961,9	31,97	40	50,647	82,295	82,12918	0,201497	0,201497
12:15	966,9	34,255	36,3	53,405	84,359	84,59819	-0,28354	0,283542
12:30	995,6	34,071	36,5	53,813	85,186	85,59895	-0,48476	0,484757
12:45	185,6	30,268	39,1	52,782	77,936	62,2269	20,15641	20,15641
13:00	938,1	33,001	35,9	55,174	73,612	84,72427	-15,0957	15,09574
13:15	414,4	34,308	34,1	56,778	84,115	71,93197	14,48378	14,48378
13:30	904,4	35,555	30,4	57,018	84,359	85,63303	-1,51025	1,510249
13:45	903,1	35,395	31,3	58,443	85,438	86,48378	-1,22403	1,224025
14:00	794,4	35,235	30	58,319	82,918	83,45407	-0,64651	0,646505
14:15	503,1	32,587	33,5	59,962	82,295	76,06272	7,573099	7,573099
14:30	434,4	31,382	33,9	54,3	69,627	70,24681	-0,89018	0,890184
14:45	750,6	31,408	32,9	53,368	72,06	78,1947	-8,51332	8,513319
15:15	696,9	34,308	30,3	57,908	85,27	80,35594	5,762937	5,762937
15:30	674,4	34,572	29,3	59,662	79,618	80,96599	-1,69307	1,69307
15:45	650,6	35,609	27,5	59,238	79,119	80,28789	-1,47739	1,477386
16:00	626,9	32,587	35,9	56,579	77,123	77,15548	-0,04212	0,042118
							PMAE	**6,928717**

APPENDIX E

Data collected on the 14 June 2014

Table D1: Measured input variables, Tmod and PMAE

Time	Co	I	Ta	RH	Tci	Tmeas	Tmod	Error	PAE
09:42	39,29	409,4	16,272	57,8	26,695	39,29	42,24835	-7,52951	7,529514
09:52	46,067	429,4	17,915	52	20,65	46,067	41,91128	9,021025	9,021025
10:02	44,936	448,1	19,318	49,5	20,436	44,936	43,46845	3,265861	3,265861
10:12	44,999	464,4	19,865	47,3	20,913	44,999	44,59163	0,905279	0,905279
10:22	46,353	481,9	19,365	41,1	21,366	46,353	44,83608	3,272537	3,272537
10:32	46,77	498,1	19,222	37,3	21,581	46,77	45,31709	3,106497	3,106497
10:42	47,941	511,9	19,294	35,8	21,795	47,941	45,96369	4,124464	4,124464
10:52	48,139	523,1	19,603	35,3	21,867	48,139	46,66257	3,067004	3,067004
11:02	49,242	535,6	20,055	35,1	22,106	49,242	47,58673	3,361509	3,361509
11:12	49,751	544,4	20,198	33,9	22,298	49,751	48,06881	3,381218	3,381218
11:22	50,231	553,1	21,008	34,1	22,226	50,231	48,9837	2,483123	2,483123
11:32	50,439	560,6	20,174	33,8	22,489	50,439	48,82799	3,193976	3,193976
11:42	50,682	565,6	20,341	33,9	22,489	50,682	49,16684	2,989536	2,989536
11:52	50,996	571,9	20,77	32,9	22,561	50,996	49,70107	2,53927	2,53927
12:02	51,137	575,6	20,603	32,6	22,824	51,137	49,82344	2,568698	2,568698
12:12	52,167	578,1	21,748	33	23,328	52,167	50,88954	2,448797	2,448797
12:22	52,528	575,6	21,748	31,4	23,497	52,528	50,74539	3,393629	3,393629
12:32	52,782	576,9	21,772	30,1	23,569	52,782	50,77032	3,811303	3,811303
12:42	52,311	575,6	21,557	27,9	23,569	52,311	50,44607	3,565085	3,565085
12:52	51,88	571,9	21,581	27,6	23,641	51,88	50,30529	3,035289	3,035289
13:02	52,024	565,6	21,628	26,7	24,026	52,024	50,13476	3,63148	3,63148
13:12	51,952	554,4	22,011	26,4	24,219	51,952	49,94203	3,868907	3,868907
13:22	51,916	546,9	22,609	26,6	24,46	51,916	50,10088	3,496271	3,496271
13:32	50,786	535,6	21,987	26,5	24,412	50,786	49,16253	3,196693	3,196693
13:42	49,956	523,1	21,604	26,6	24,291	49,956	48,318	3,278884	3,278884
13:52	49,006	510,6	21,199	27	24,388	49,006	47,54758	2,975998	2,975998
14:02	49,006	498,1	21,748	27,2	24,992	49,006	47,57218	2,925803	2,925803
14:12	48,238	481,9	21,437	27,9	24,944	48,238	46,66955	3,251472	3,251472
14:22	47,255	464,4	21,795	27,8	24,992	47,255	46,14421	2,350634	2,350634
14:32	45,656	446,9	21,294	28,1	24,75	45,656	44,97035	1,501776	1,501776
14:42	44,719	423,1	21,413	28	25,016	44,719	44,07804	1,433301	1,433301
14:52	44,073	403,1	21,342	27,7	25,404	44,073	43,25609	1,853531	1,853531
15:02	42,923	380,6	21,533	27,6	25,258	42,923	42,33332	1,373815	1,373815
15:12	41,007	356,9	20,936	27,1	24,75	41,007	40,68794	0,778063	0,778063
15:22	40,314	333,1	21,27	27,3	25,137	40,314	39,99629	0,788096	0,788096
15:32	38,924	310,6	21,437	27,5	25,04	38,924	39,09039	-0,42748	0,427479
15:42	37,042	294,4	20,936	27,4	24,484	37,042	37,84796	-2,17581	2,17581
15:52	35,368	266,9	20,579	27,1	24,339	35,368	36,32608	-2,7089	2,708895
								PMAE	**2,975803**

APPENDIX F

Data collected on the 9th July 2014

Table D1: Measured input variables, Tmod and PMAE

Time	I	Ta	RH	Tci	Tmod	Tmeas	Error	PAE
11:32	483,1	21,676	58,4	37,48	52,73023	49,717	-6,06077	6,06077
11:42	540,6	21,819	55,6	34,202	54,13292	56,619	4,390897	4,390897
11:52	503,1	23,016	50,4	34,889	53,20985	59,919	11,19703	11,19703
12:02	560,6	22,561	54,1	36,389	56,15508	55,213	-1,70626	1,706264
12:12	453,1	23,088	51,5	38,309	52,23541	58,693	11,00231	11,00231
12:22	539,4	22,082	54,4	37,866	55,40051	56,619	2,152089	2,152089
12:32	488,1	24,388	49,1	39,431	54,89313	58,154	5,607301	5,607301
12:42	505,6	24,895	47,2	39,914	56,06142	57,664	2,779163	2,779163
12:52	458,1	23,833	47,5	39,121	53,00087	56,5	6,193148	6,193148
13:02	503,1	25,065	47	40,228	56,15713	56,421	0,467673	0,467673
13:12	529,4	24,702	46,5	40,516	57,14661	57,704	0,965947	0,965947
13:22	475,6	24,412	48,6	41,094	54,8775	58,443	6,100821	6,100821
13:32	471,9	24,726	47,3	41,825	55,09295	58,031	5,062899	5,062899
13:42	456,9	23,472	49	41,036	53,42308	56,619	5,644598	5,644598
13:52	410,6	24,798	46,5	41,094	52,13917	55,521	6,091088	6,091088
14:02	476,9	25,21	46,3	40,92	55,28331	55,328	0,080778	0,080778
14:12	409,4	24,992	46	42,06	52,50741	56,46	7,000695	7,000695
14:22	404,4	25,186	47	41,825	52,39384	55,021	4,774836	4,774836
14:32	418,1	25,38	45,6	41,268	52,86827	54,15	2,366996	2,366996
14:42	418,1	26,012	44,1	40,286	52,88282	54,489	2,947711	2,947711
14:52	326,9	24,412	45,1	39,601	47,60105	52,891	10,0016	10,0016
15:02	341,9	24,243	47,6	39,008	48,09584	50,404	4,579328	4,579328
15:12	316,9	24,219	48,5	37,315	46,46262	48,504	4,20869	4,20869
15:22	285,6	22,992	49,4	34,783	43,46768	45,624	4,726276	4,726276
15:32	216,9	21,939	51,8	30,646	38,48531	40,833	5,74948	5,74948
							PMAE	**4,874336**